

## II Workshop on Photon Physics and Simulation at Hadron Colliders

May 18th, 2015

# SM (non-Higgs) photon measurements at the LHC

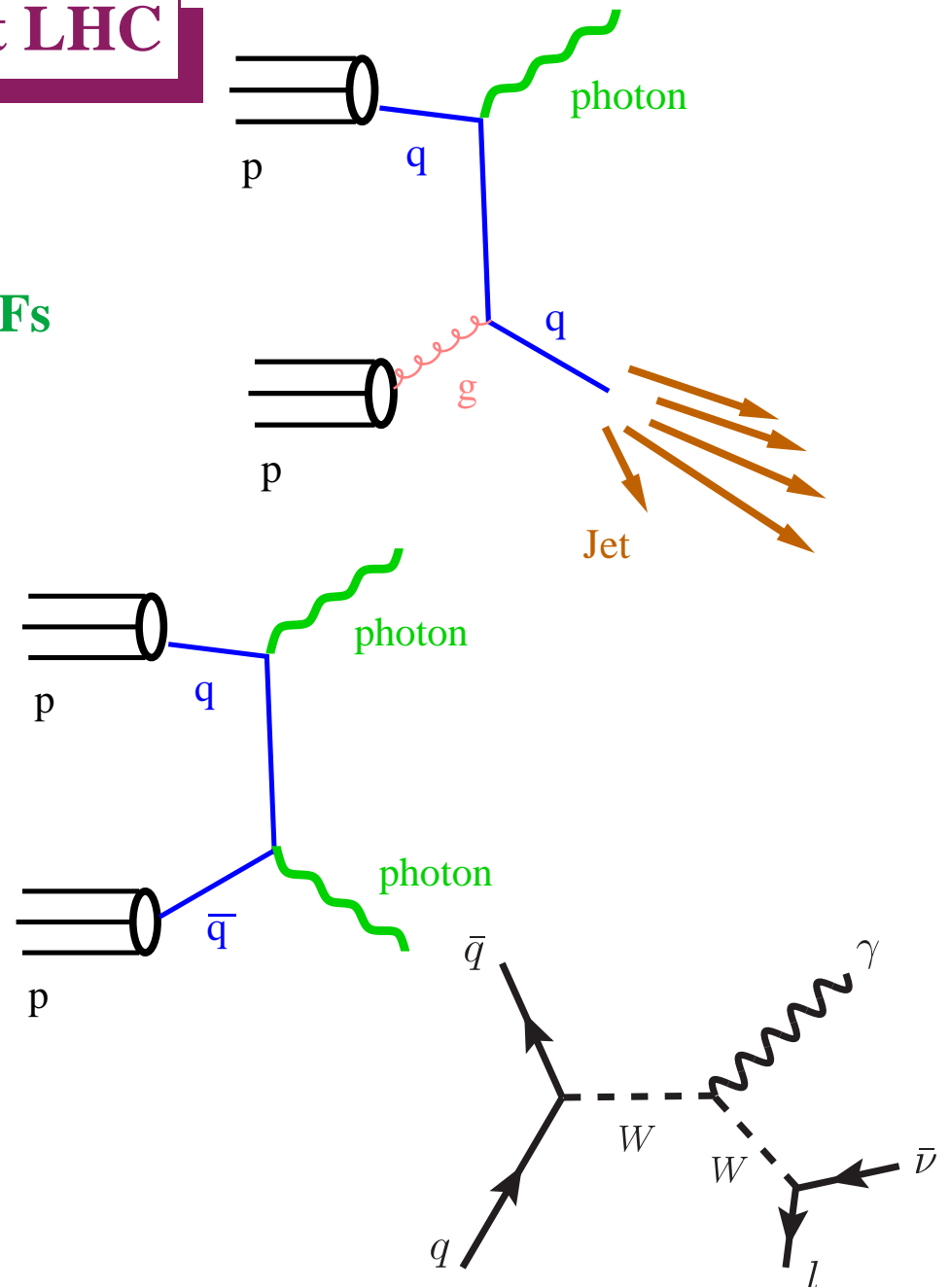
J. Terrón (Universidad Autónoma de Madrid)

### • Outline

- Introduction
- Inclusive photon production
- Photon + jet production
- Photon pair production
- $V\gamma$  and  $V\gamma\gamma$  production
- Summary

## Photon production in $pp$ collisions at LHC

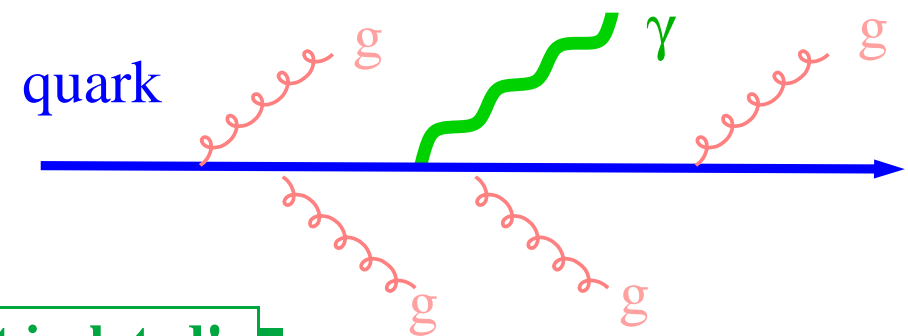
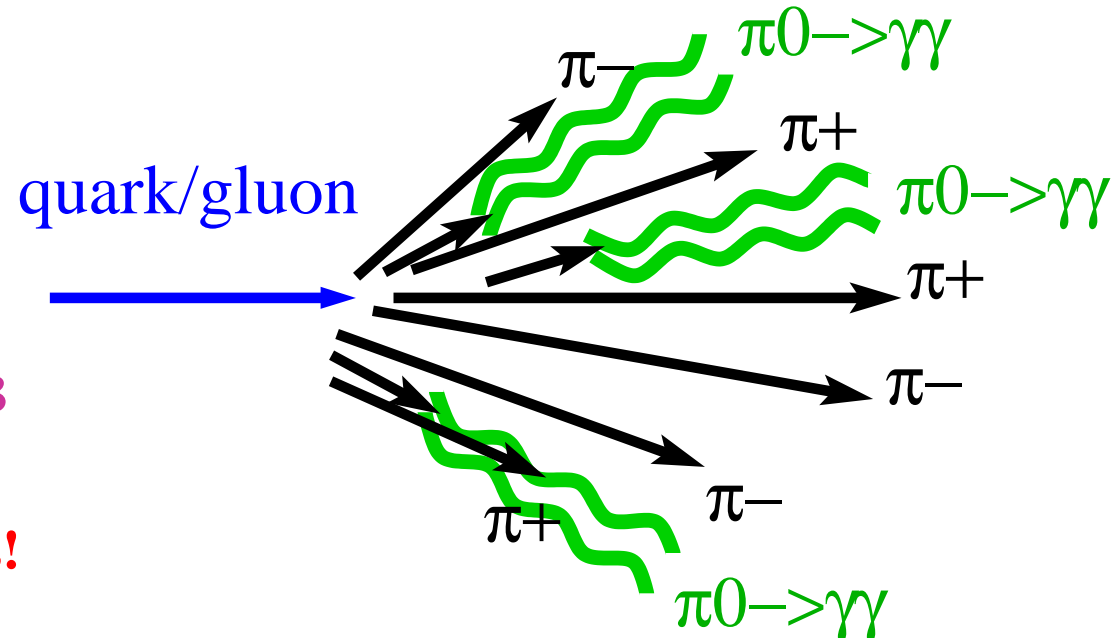
- Photon production in  $pp$  collisions allows
  - tests of perturbative QCD
  - experimental information on the proton PDFs
- Possibilities to study inclusive production of photons or in association with jets
- Prompt photons represent a cleaner probe of the hard interaction
- Diphoton production is of special interest as the major background to  $H \rightarrow \gamma\gamma$
- $V\gamma$  and  $V\gamma\gamma$  production ( $V = W, Z$ ) probe the electroweak sector of the SM



## Other sources of photons

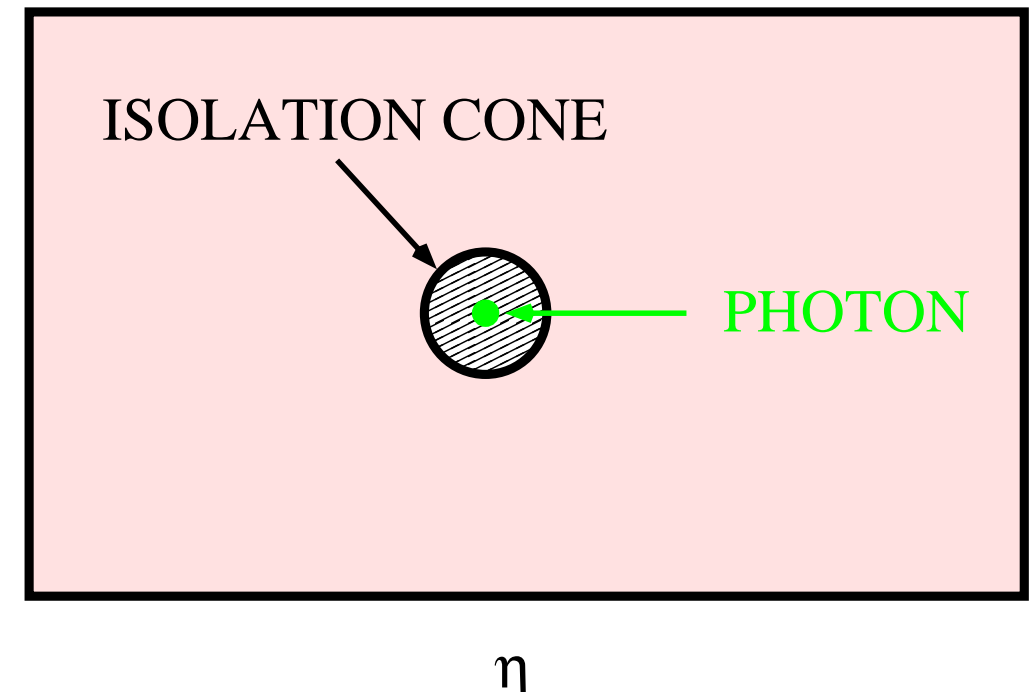
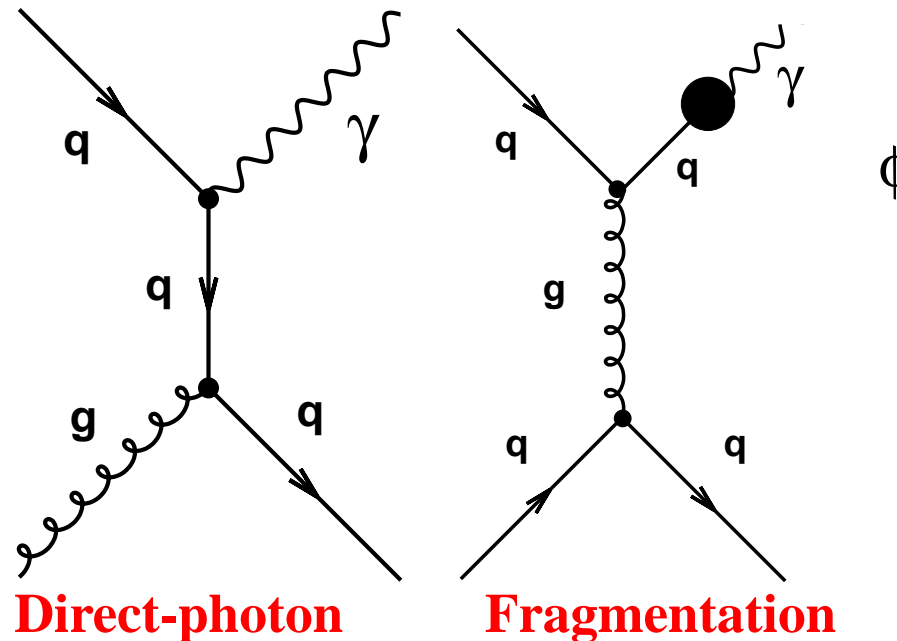
- Quarks and gluons are sources of photons
  - Quarks and gluons fragment mostly into pions and, by isospin symmetry, 1/3 are  $\pi^0$ 's, which decay into two photons
  - ⇒  $\gamma$ 's are produced copiously inside jets!

- Quarks have electric charge and radiate photons
  - ⇒ fragmentation function  $D_{q/g}^\gamma(z, \mu_f)$



⇒ Distinct feature: photons inside jets, i.e. not isolated!

## Photon isolation

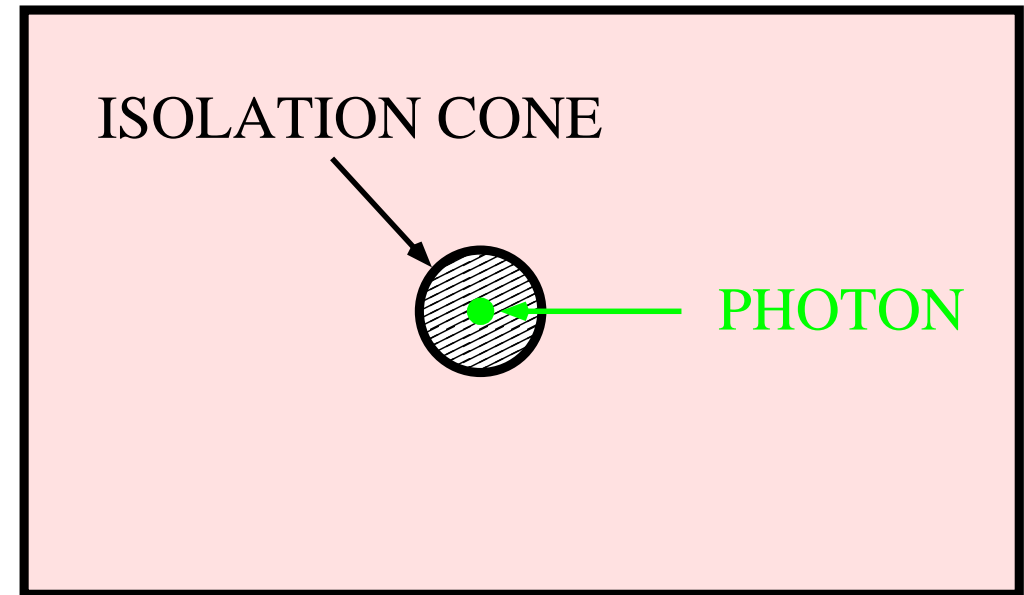


- It is essential to require the photon to be isolated. It is achieved by requiring  $E_T^{iso} \equiv \sum_i E_T^i < E_T^{max}$  with the sum over the particles (except the photon!) inside a cone of radius  $R$  centered on the photon in the  $\eta - \phi$  plane
- The isolation requirement suppresses the contribution of photons inside jets:  
 $\pi^0$  (as well as other neutral mesons) decays and the fragmentation contribution

## Corrections for non-perturbative effects; photon isolation

- The measurements are corrected for detector effects to the “particle” level  
→ to isolated photons, where  $E_T^{iso}$  is calculated using all the final-state particles and the jet-area method is also applied ( $\Rightarrow E_T^{iso*}$ )

This is performed using MC simulations



- Corrections for non-perturbative effects (hadronisation and underlying event)  
→ Applied to fixed-order pQCD calculations
- $$C_{NP} = \frac{\sigma_{\gamma+x}(\text{MC, particle-level, UE})}{\sigma_{\gamma+x}(\text{MC, parton-level, no UE})}$$
- Less dependence on the modelling of the final state by having used the jet-area method to subtract the “extra” transverse energy contribution to  $E_T^{iso}$

# Inclusive photon production

# Inclusive isolated photon production in $pp$ collisions at $\sqrt{s} = 7 \text{ TeV}$

- Measurement of  $d\sigma/dE_T^\gamma$  in the phase-space region defined by:

$\rightarrow 45 < E_T^\gamma < 400 \text{ GeV}$

$\rightarrow$  four regions in  $|\eta^\gamma|$ : [0,0.6], [0.6,1.37],  
[1.52,1.81] and [1.81,2.37],

using  $\mathcal{L} = 35 \text{ pb}^{-1}$

- Data-driven signal extraction using two-dimensional sideband method:

$\rightarrow E_T^{iso}$  (corrected for pileup+underlying event)

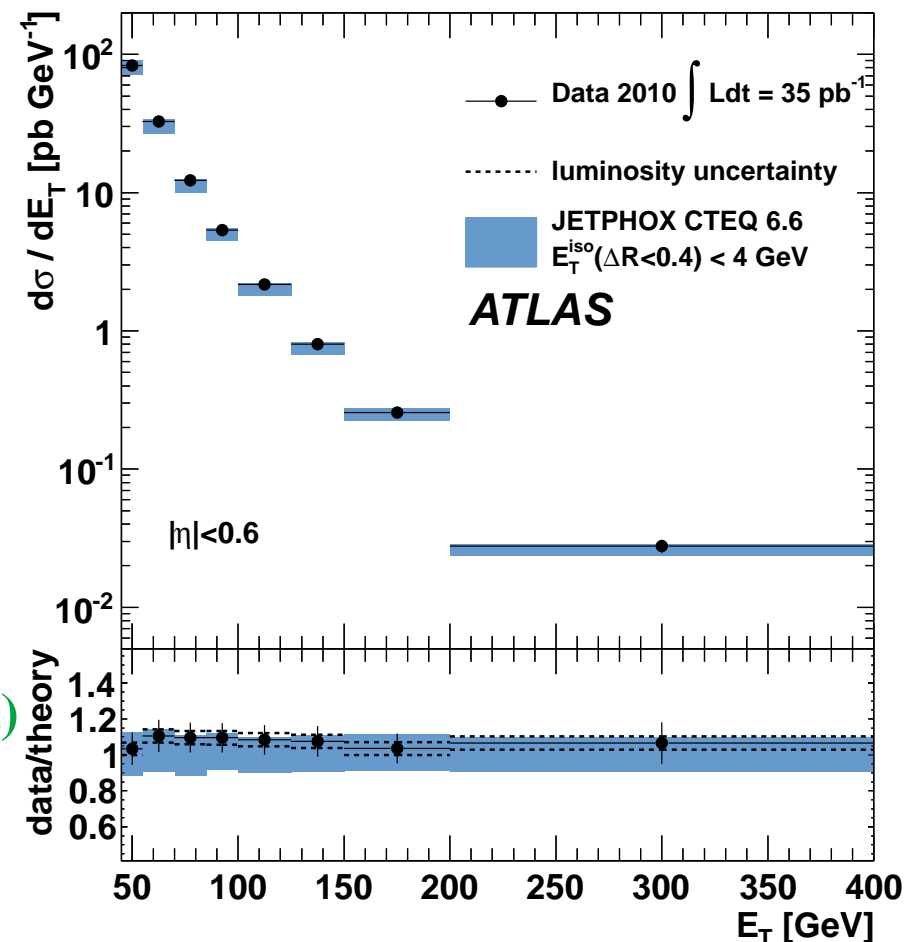
$\rightarrow$  photon quality (shower shape ID criteria)

- Cross sections for isolated prompt photons

$\rightarrow$  photons not coming from hadron decays

$\rightarrow E_T^{iso}(R = 0.4) < 4 \text{ GeV}$  (corrected for underlying event)

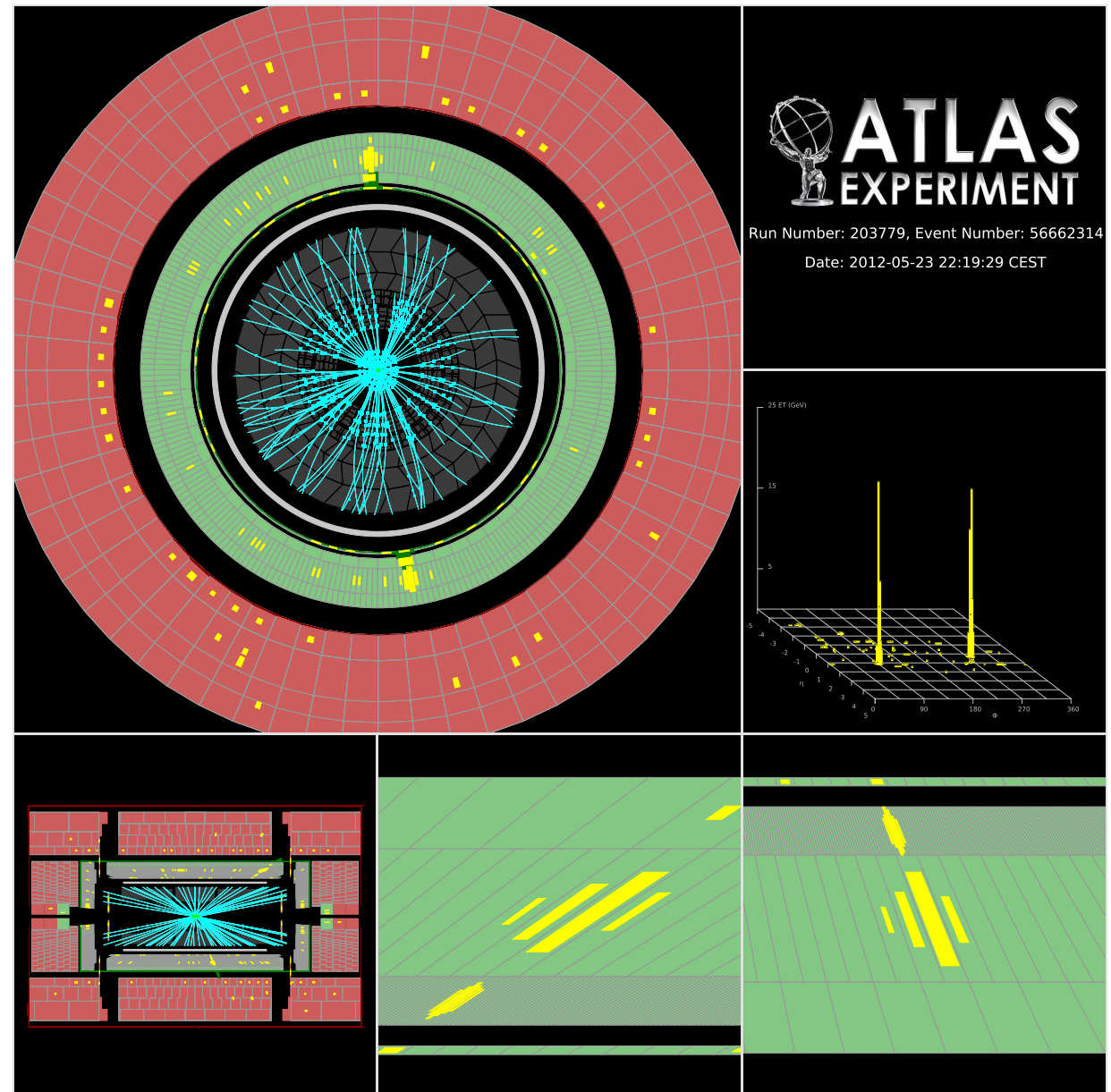
- Comparison to NLO QCD calculations with Jetphox



ATLAS PLB706-150

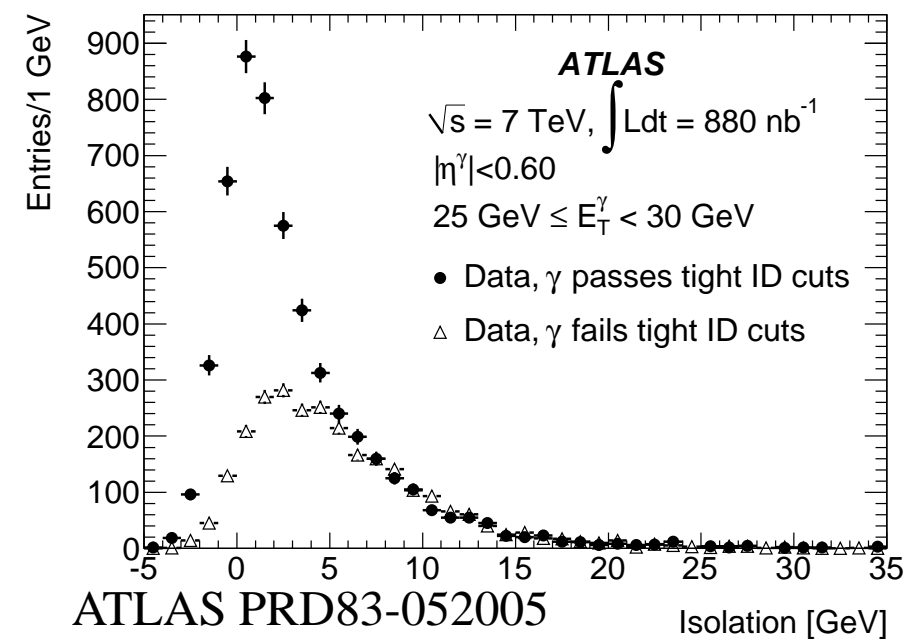
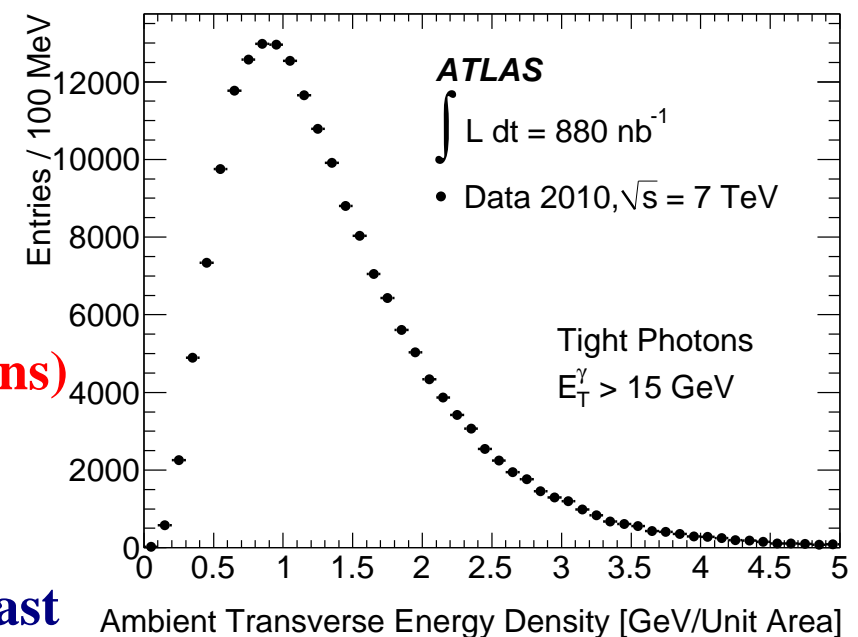
## Photon isolation in ATLAS

- $E_T^{iso}(R = 0.4)$  computed using the calorimeter cells (EM and HAD) in a cone  $R = 0.4$ , but excluding the contributions from  $3 \times 5$  EM cells around photon
- The leakage of the photon energy outside that region is subtracted (few %)
- The underlying event and pileup contribute to  $E_T^{iso}$ !



## Photon isolation in ATLAS

- $E_T^{iso}$  is corrected by subtracting the estimated contributions from the underlying event and pileup; the correction is computed on an event-by-event basis (to avoid the large fluctuations) using the jet-area method (M. Cacciari et al.)  
⇒ ambient transverse-energy density 540 MeV (in  $R = 0.4$  cone) for events with at least one photon candidate with  $E_T > 15$  GeV and exactly one PV (+170 MeV for each extra PV)
- After the correction the  $E_T^{iso}$  distribution is centered at zero with a width of 1.5 GeV in simulated signal events
- A photon candidate is considered isolated if  $E_T^{iso} < 3$  GeV
- Residual background still expected

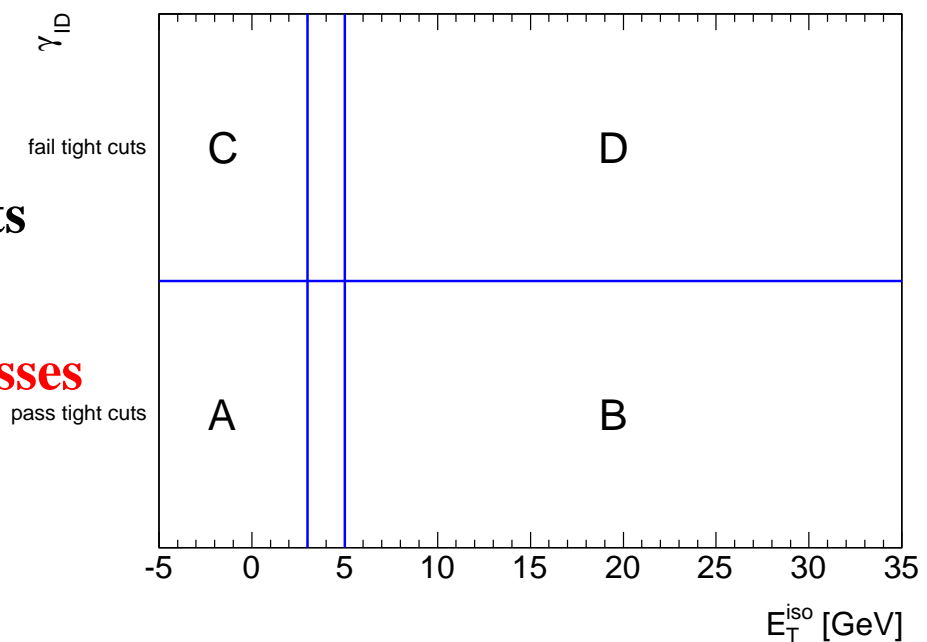


## Background subtraction

- Residual background still expected even after the tight identification and isolation requirements
- A data-driven method necessary to avoid relying on detailed simulations of the background processes
- The two-dimensional sideband method:
  - photon identification  $\gamma_{ID}$  vs  $E_T^{iso}$  plane
  - four regions are defined
    - region A (signal): tight and isolated photons ( $E_T^{iso} < 3$  GeV)
    - region B (bkg): tight and non-isolated photons ( $E_T^{iso} > 5$  GeV)
    - region C (bkg): non-tight and isolated photons ( $E_T^{iso} < 3$  GeV)
    - region D (bkg): non-tight and non-isolated photons ( $E_T^{iso} > 5$  GeV)
- It is assumed that for background events there is no correlation between  $\gamma_{ID}$  and  $E_T^{iso}$

$$\frac{N_A^{bkg}}{N_B^{bkg}} = \frac{N_C^{bkg}}{N_D^{bkg}} \quad \Rightarrow N_A^{sig} = N_A - N_B^{bkg} \frac{N_C^{bkg}}{N_D^{bkg}}$$

further assuming that signal contamination is small in B, C and D



## Background subtraction

- The effects of the small signal contaminations can be accounted for

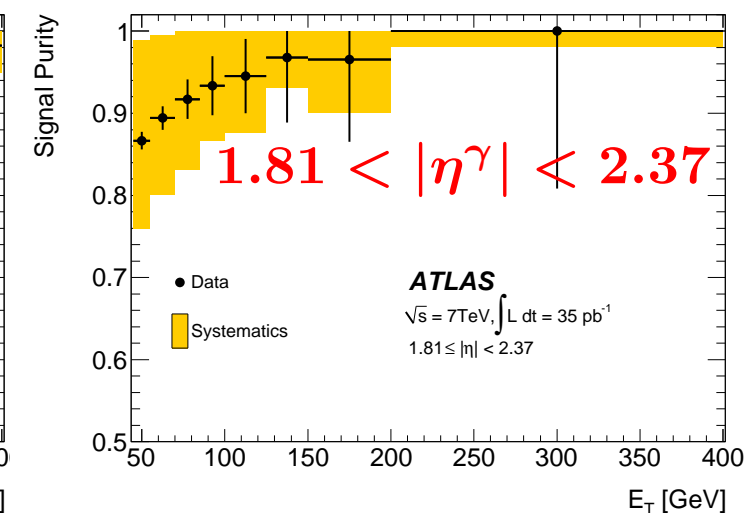
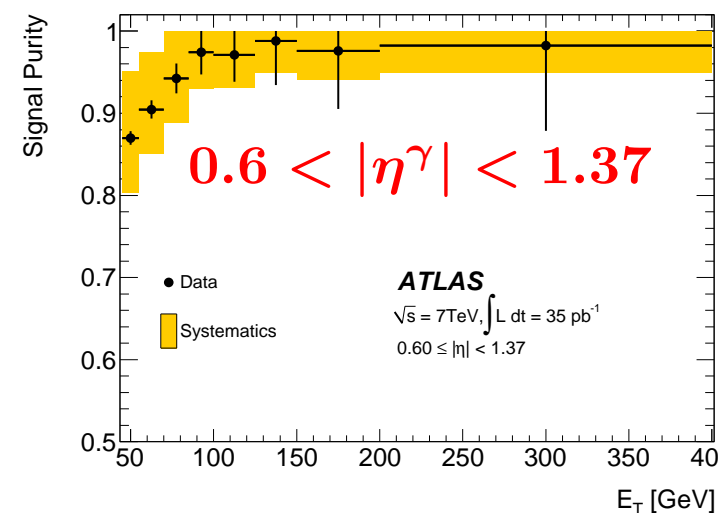
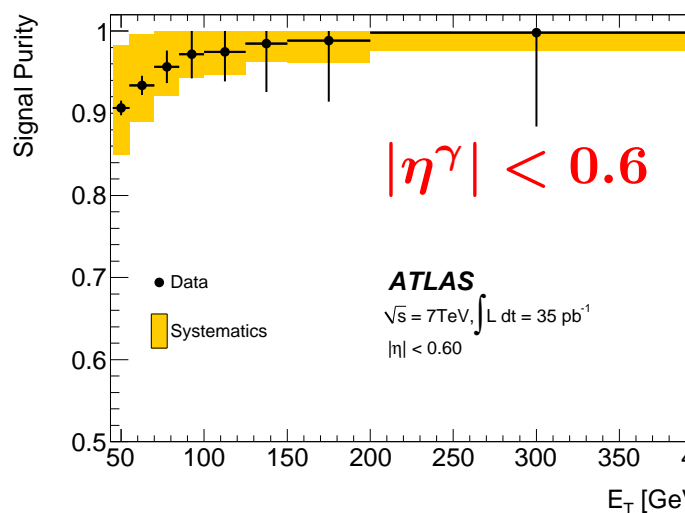
$$\frac{N_A^{bkg}}{N_B^{bkg}} = \frac{N_C^{bkg}}{N_D^{bkg}} \Rightarrow \frac{N_A - N_A^{sig}}{N_B - \epsilon_B N_A^{sig}} = \frac{N_C - \epsilon_C N_A^{sig}}{N_D - \epsilon_D N_A^{sig}}$$

where the leakage fractions ( $\epsilon_K$ ,  $K = B, C, D$ ) are estimated using MC samples of signal processes,  $\epsilon_K \equiv N_K^{sig} / N_A^{sig}$

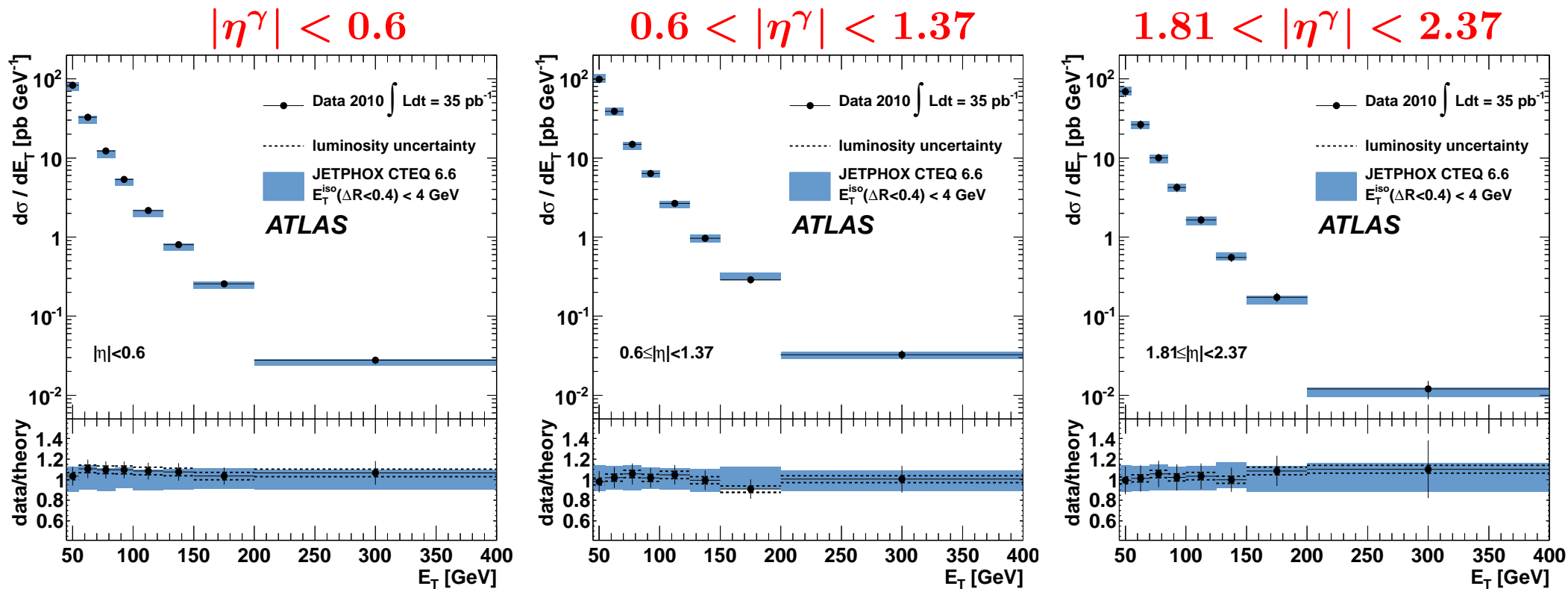
- Purity of the sample as a function of  $E_T^\gamma$  for different ranges in  $|\eta^\gamma|$

$\rightarrow$  purity  $\gtrsim 90\%$  for  $E_T^\gamma > 45$  GeV

ATLAS PLB706-150 (aux. mat. STDM-2011-04)



# Inclusive isolated-photon production in $pp$ collisions at $\sqrt{s} = 7$ TeV



- Uncertainties on the photon signal yields  $< 10\%$  and decrease with  $E_T^\gamma$ ; luminosity uncertainty 3.4%
- Comparison to NLO QCD (Jetphox) calculations using CTEQ6.6 PDFs and BFG set II  
→ theoretical uncertainties  $\sim 10\%$ , dominated by terms beyond NLO
- ⇒ Good description of the data by NLO QCD within uncertainties (exp  $\ll$  theo)

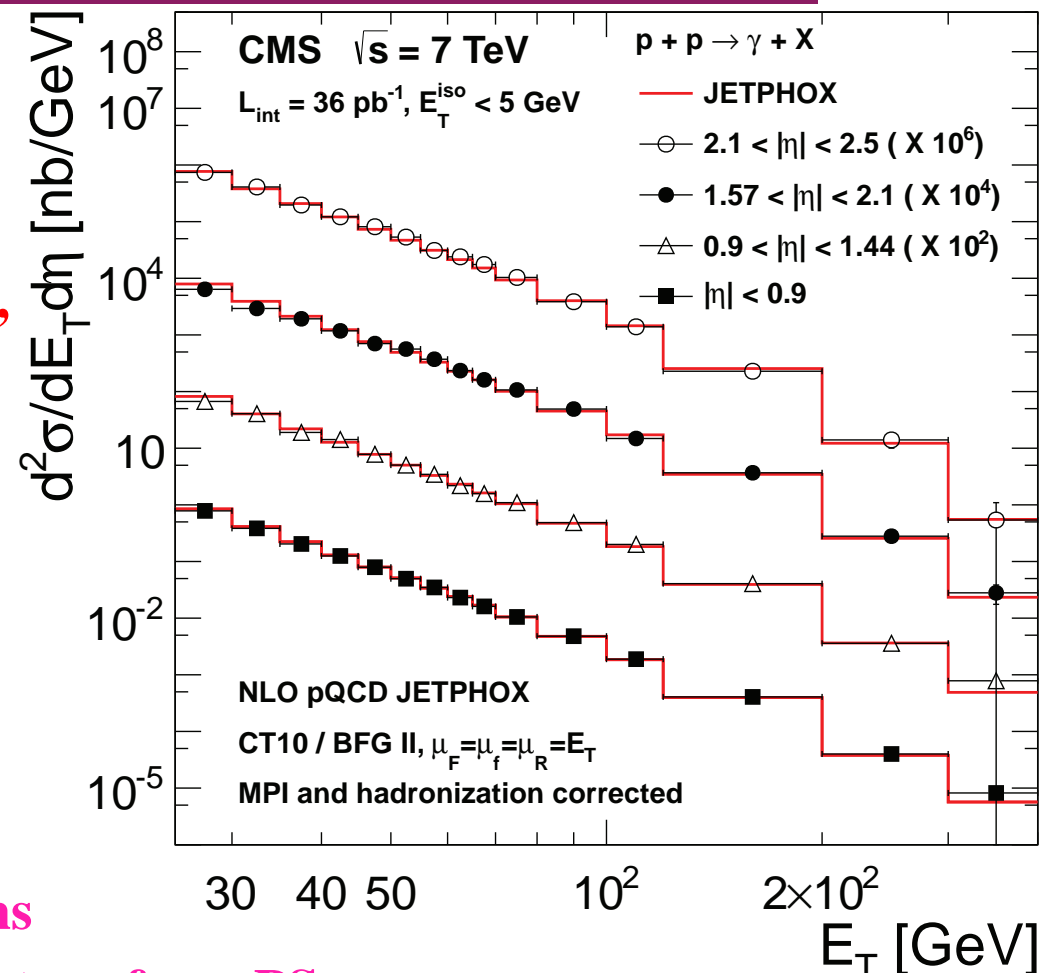
ATLAS PLB706-150

## Inclusive photon production in $pp$ collisions at $\sqrt{s} = 7 \text{ TeV}$

- Measurement of  $d^2\sigma/dE_T^\gamma d\eta^\gamma$  in the phase-space region defined by:  
 $\rightarrow 25 < E_T^\gamma < 400 \text{ GeV}$   
 $\rightarrow$  four regions in  $|\eta^\gamma|$ : [0,0.9], [0.9,1.44], [1.57,2.1] and [2.1,2.5],  
using  $\mathcal{L} = 36 \text{ pb}^{-1}$

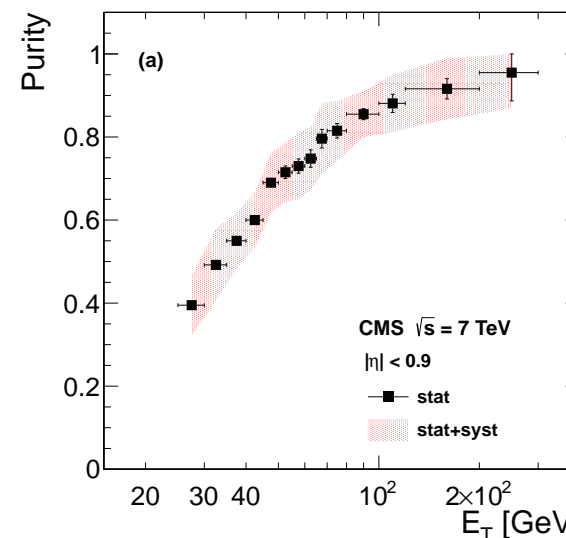
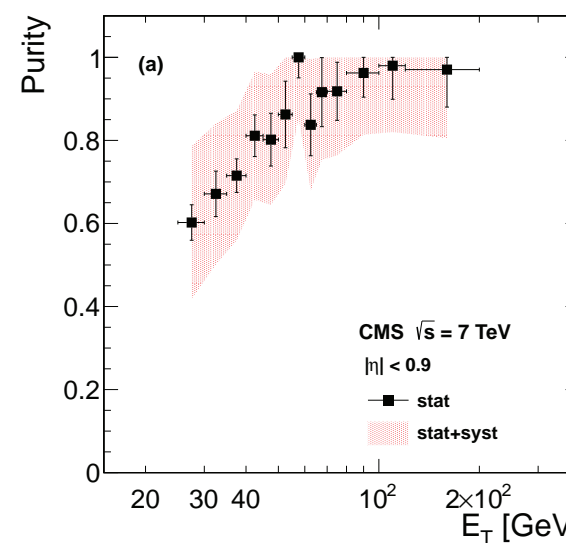
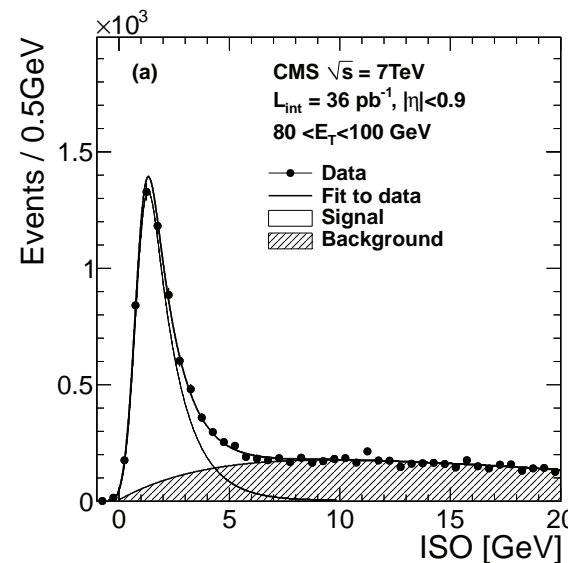
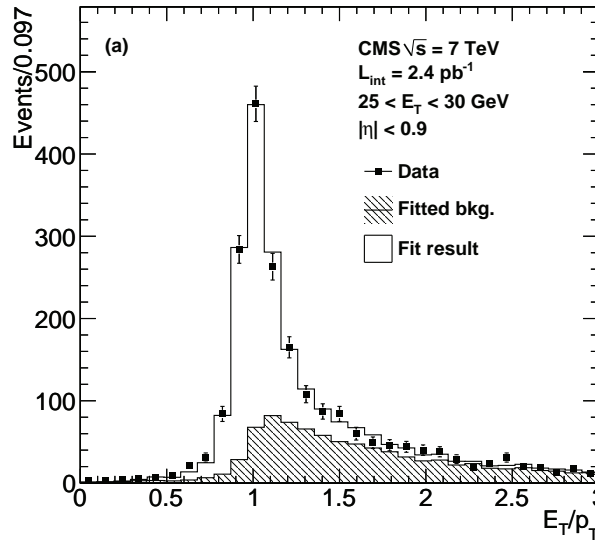
- Two methods used to extract signal:  
 $\rightarrow$  photon conversion method ( $E_T/p_T$ )  
 $\rightarrow$  isolation method  
 $\Rightarrow$  and results are combined

- Cross sections for isolated prompt photons  
 $\rightarrow$  “direct” photons, ISR/FSR photons, photons from PS  
 $\rightarrow E_T^{iso}(R = 0.4) < 5 \text{ GeV}$



CMS PRD84-052011

# Inclusive photon production in $pp$ collisions at $\sqrt{s} = 7$ TeV

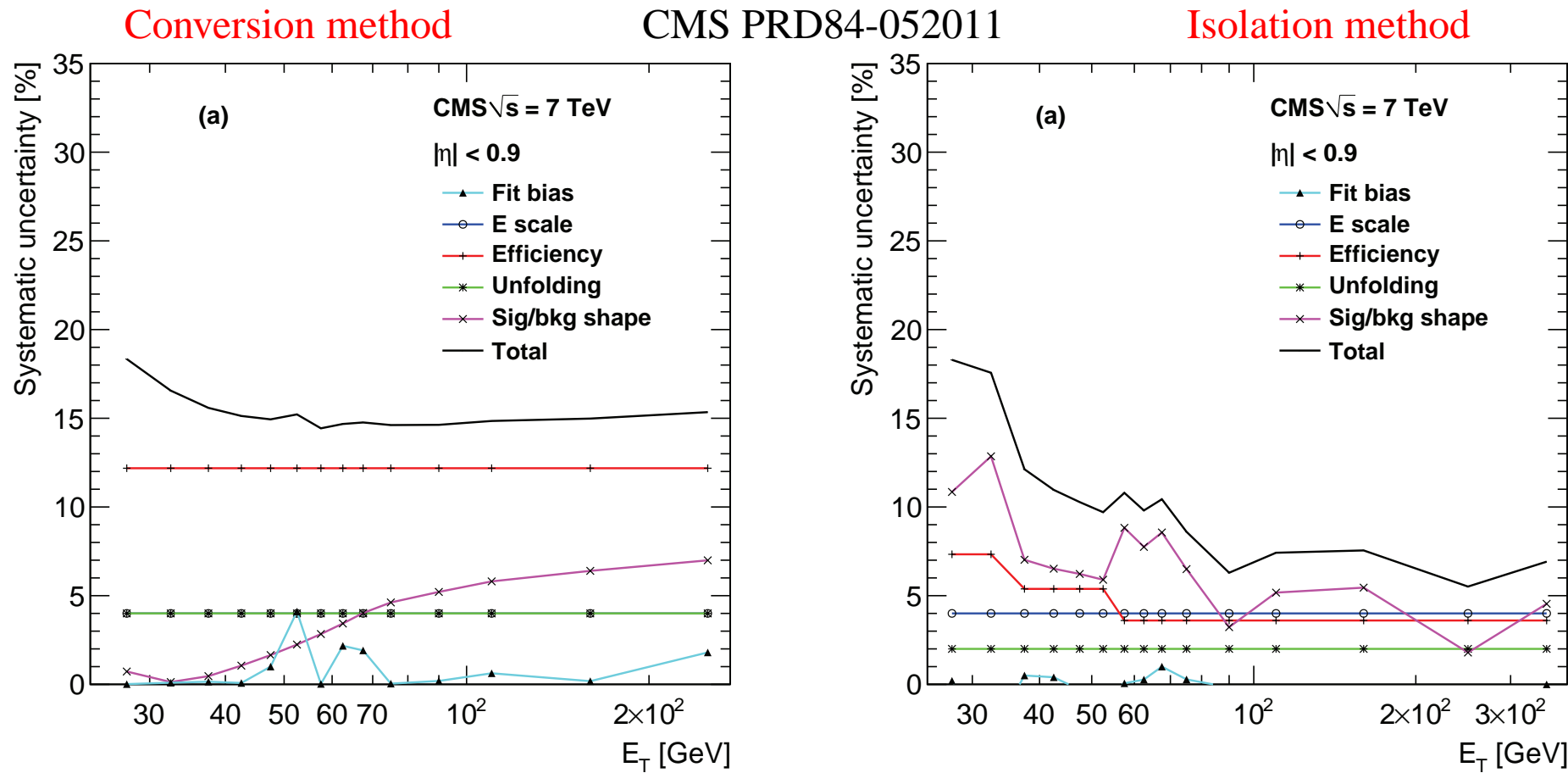


- Photon conversion method:  
ratio of  $E_T$  measured in ECAL  
over  $p_T$  measured in tracker  
for converted photons
  - statistically limited
  - restricted to  $E_T < 200$  GeV
  - high purity at low  $E_T$

- Isolation method:  
isolation sum measured in  
tracker, ECAL and HCAL
  - not statistically limited
  - no restriction in  $E_T$
  - low purity at low  $E_T$

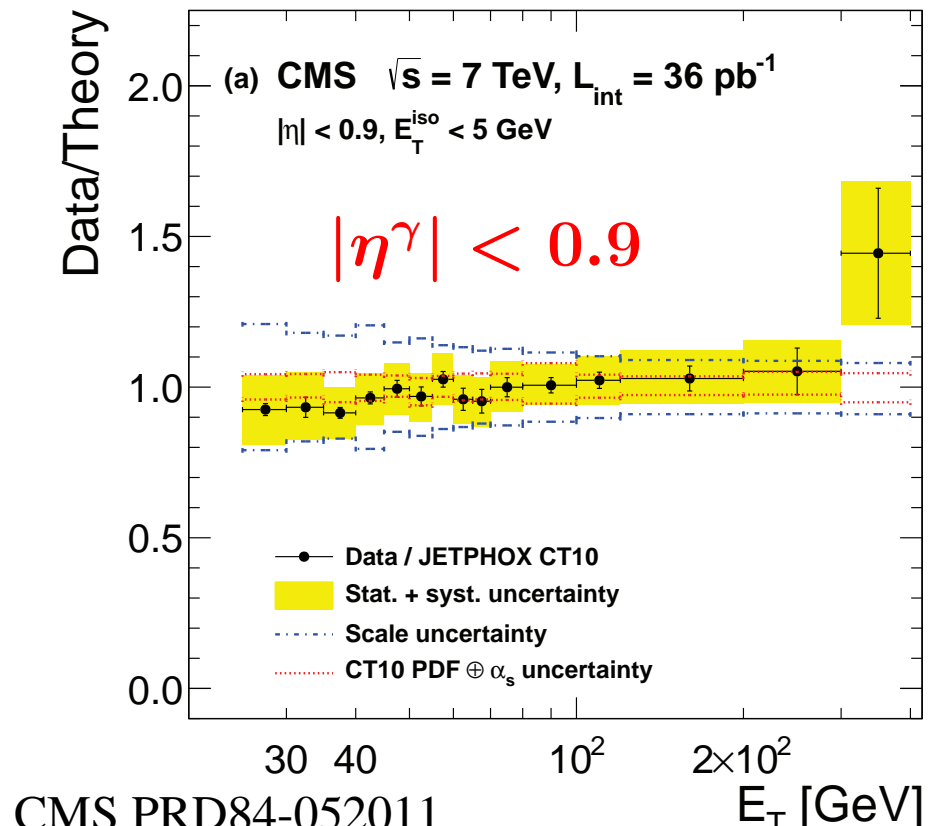
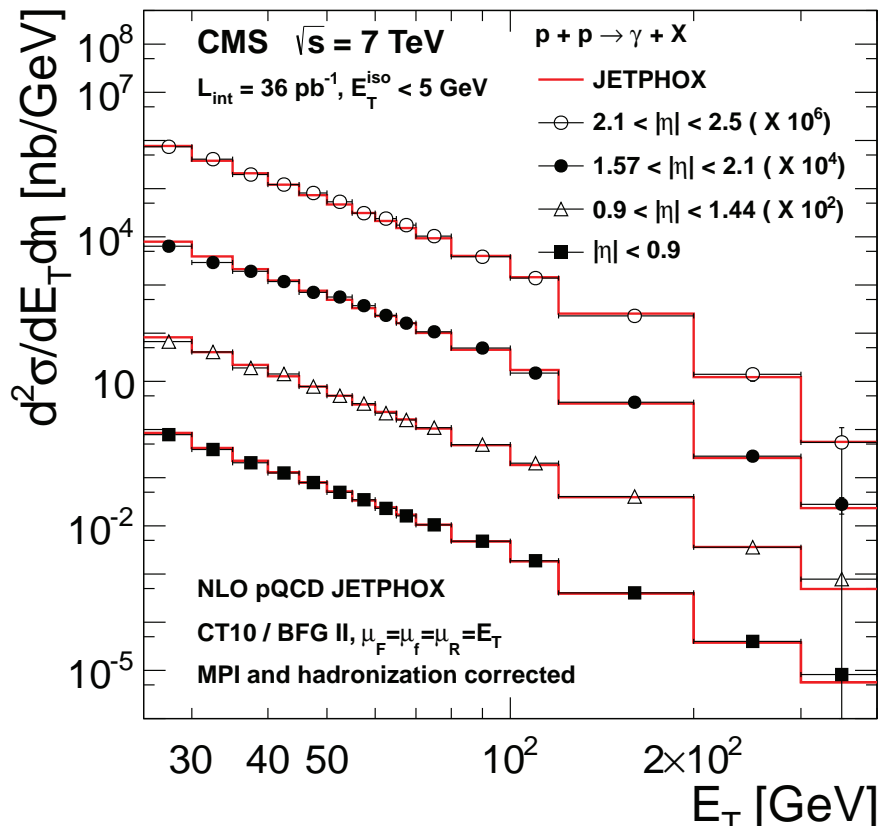
CMS PRD84-052011

# Inclusive photon production in $pp$ collisions at $\sqrt{s} = 7$ TeV



- Major systematic uncertainties: shape of signal and background and photon ID efficiency
  - Total ( $|\eta^\gamma| < 0.9$ ): 14-18% in conversion method; 3.8-18% in isolation method

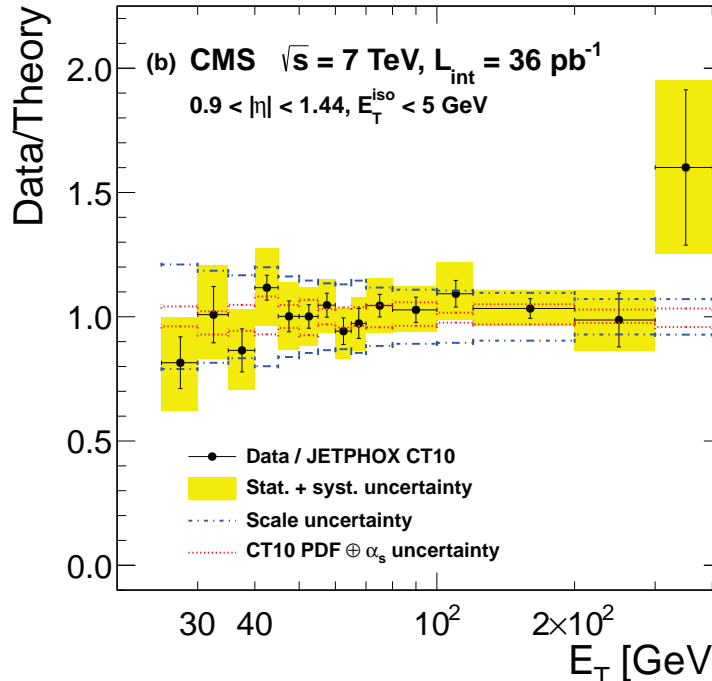
## Inclusive photon production in $pp$ collisions at $\sqrt{s} = 7 \text{ TeV}$



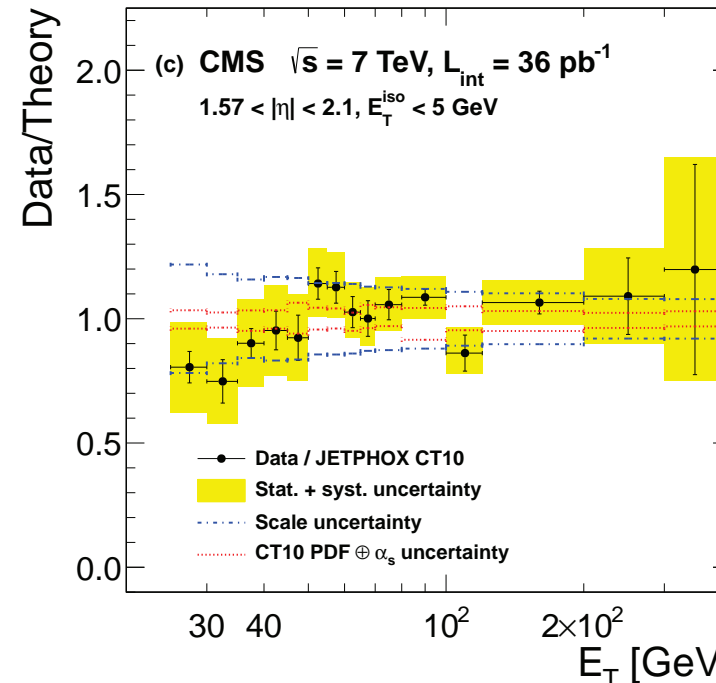
- Comparison to NLO QCD (Jetphox) calculations using  $\mu = E_T^\gamma$  and CT10 PDFs  
→ small non-perturbative effects:  $\bar{C} = 0.975 \pm 0.006$  multiplicative correction applied
- NLO QCD calculations agree with the measurement within uncertainties  
→ a “tendency” for NLO QCD to be above the data at low  $E_T$

## Inclusive photon production in $pp$ collisions at $\sqrt{s} = 7 \text{ TeV}$

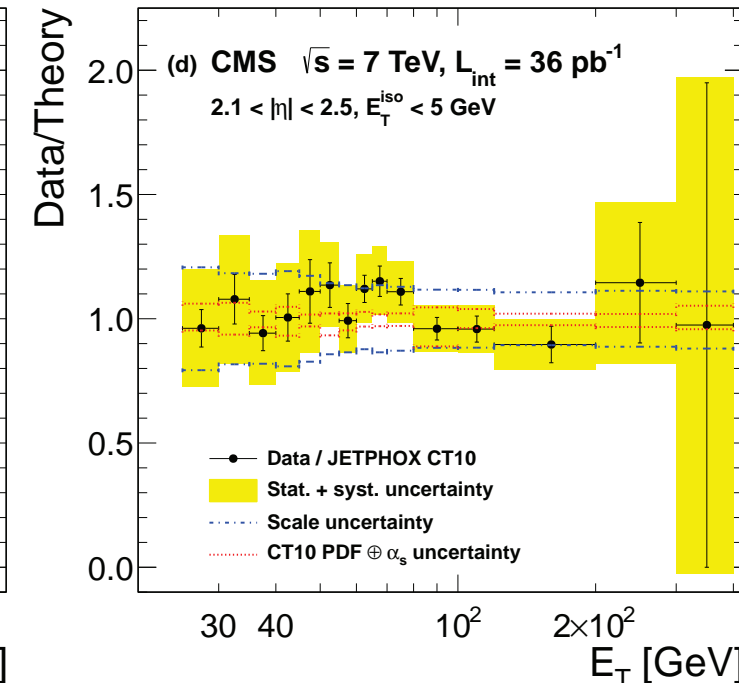
$0.9 < |\eta^\gamma| < 1.44$



CMS PRD84-052011  
 $1.57 < |\eta^\gamma| < 2.1$



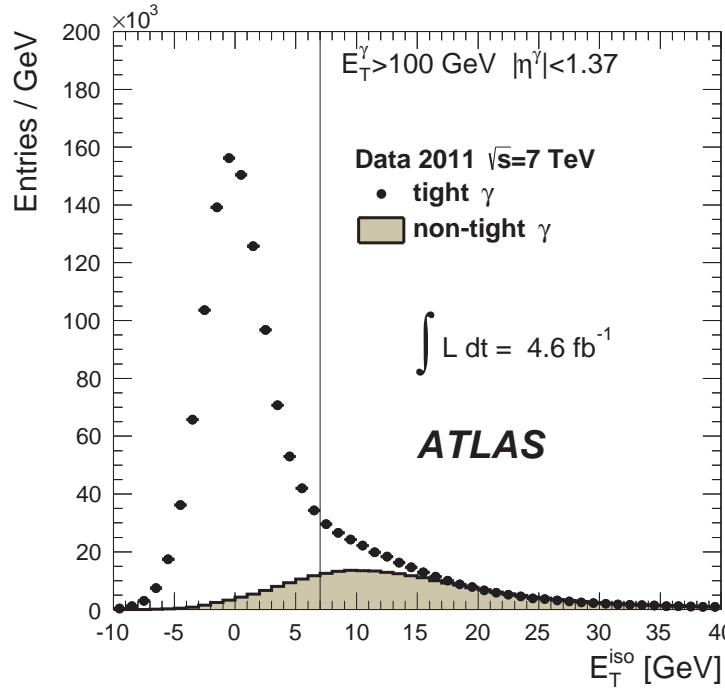
$2.1 < |\eta^\gamma| < 2.5$



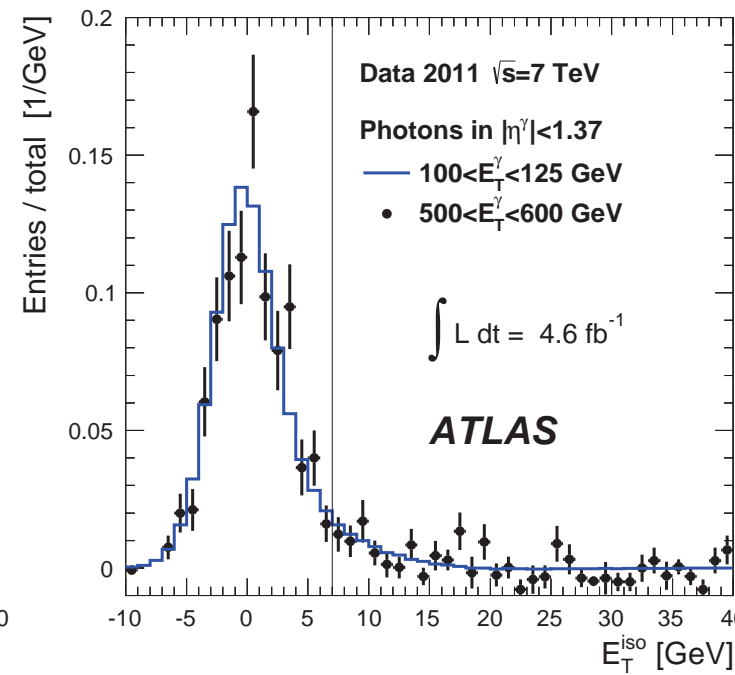
- Comparison to NLO QCD (Jetphox) calculations using  $\mu = E_T^\gamma$  and CT10 PDFs  
→ small non-perturbative effects:  $\bar{C} = 0.975 \pm 0.006$  multiplicative correction applied
- NLO QCD calculations agree with the measurement within uncertainties  
→ a “tendency” for NLO QCD to be above the data at low  $E_T$

# Inclusive photon production in $pp$ collisions at $\sqrt{s} = 7$ TeV using $4.6 \text{ fb}^{-1}$

$E_T^\gamma > 100 \text{ GeV}$

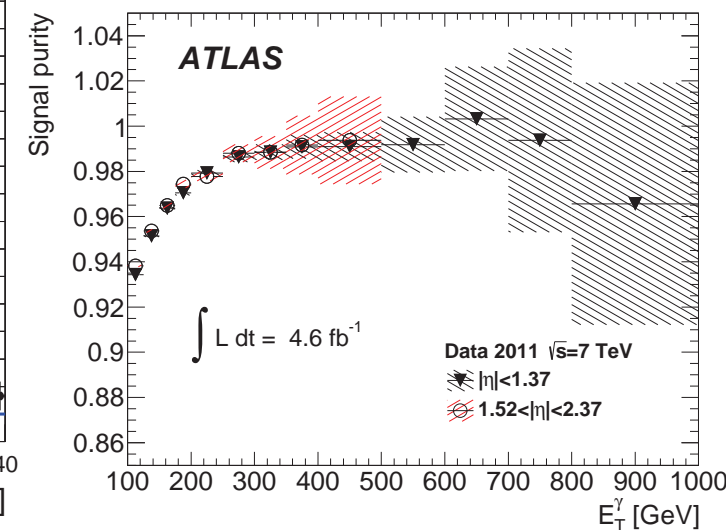


$500 < E_T^\gamma < 600 \text{ GeV}$



ATLAS PRD89-052004

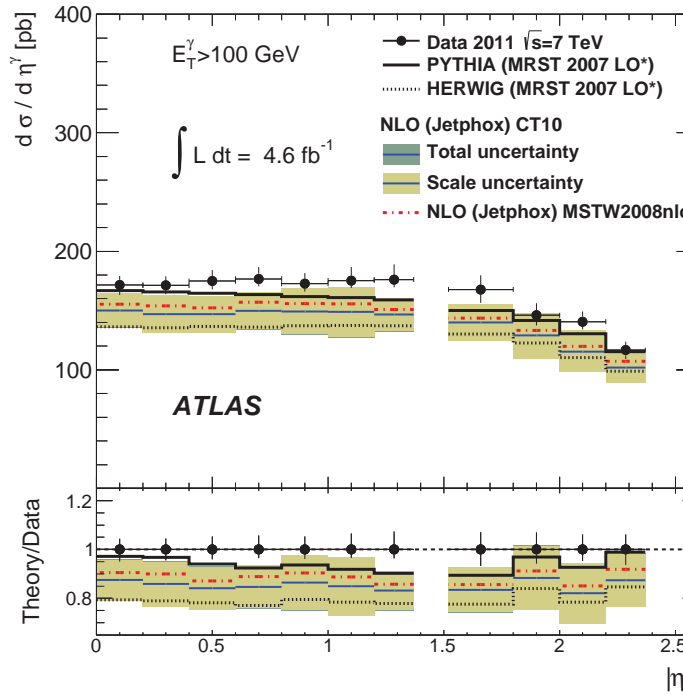
Signal purity



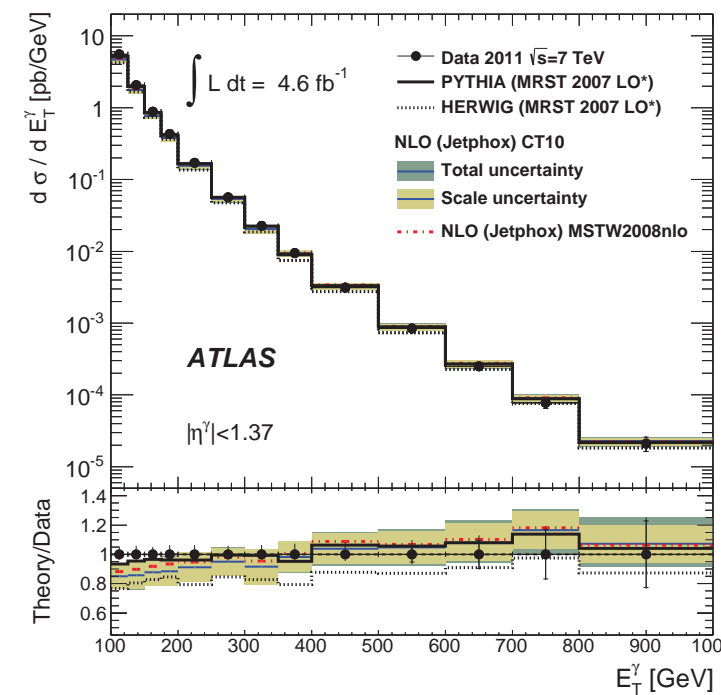
- Measurement of inclusive isolated-photon production for  $E_T^\gamma > 100 \text{ GeV}$  using  $\mathcal{L} = 4.6 \text{ fb}^{-1}$  of  $pp$  collision data at  $\sqrt{s} = 7 \text{ TeV}$  (higher pileup during 2011)
- Photon isolation requirement  $E_T^{iso} < 7 \text{ GeV}$  in order to optimize the signal purity and the photon reconstruction efficiency at high  $E_T^\gamma$

# Inclusive photon production in $pp$ collisions at $\sqrt{s} = 7$ TeV using $4.6 \text{ fb}^{-1}$

$E_T^\gamma > 100 \text{ GeV}$

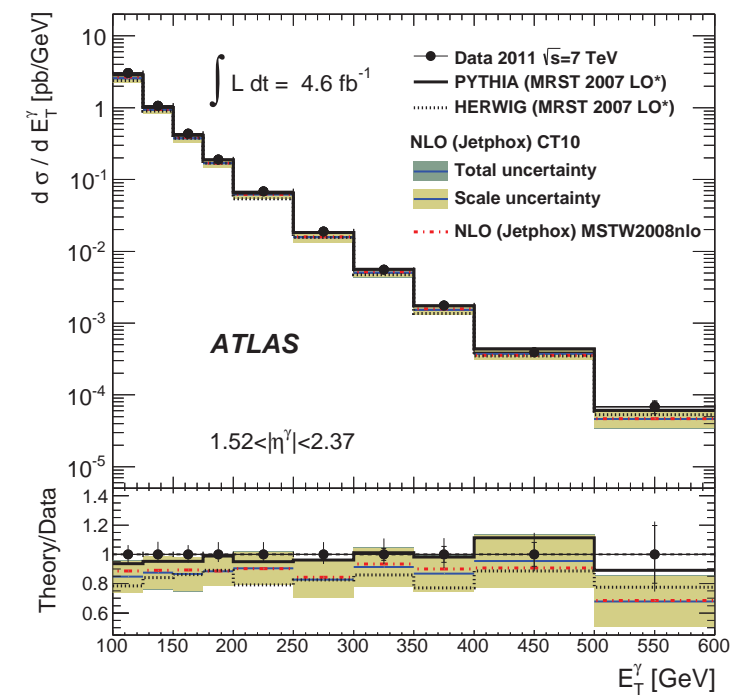


$| \eta^\gamma | < 1.37$



ATLAS PRD89-052004

$1.52 < | \eta^\gamma | < 2.37$



- Systematic uncertainties:  $\gamma$  energy scale (resolution) 2-6% (2%);  $\gamma$  ID up to 2%; MC model 2-4%; backg. subtraction 2-3%; luminosity 1.8% → total experimental uncertainty in barrel (end-cap) below 6% (7%)
- Good description of the data by NLO QCD (Jetphox) calculations up to  $\sim 1$  TeV
- Tendency in the data to be above NLO QCD at low  $E_T^\gamma$ , but in agreement within th.unc.

# Photon+jet production

# $\gamma + \text{jet}$ production in $pp$ collisions at $\sqrt{s} = 7 \text{ TeV}$

- Further experimental information can be extracted from photon production data by measuring the recoiling jet and
  - Measuring  $\gamma + \text{jet}$  for different angular configurations (same side vs opposite side) and different ranges in  $|y^{\text{jet}}|$

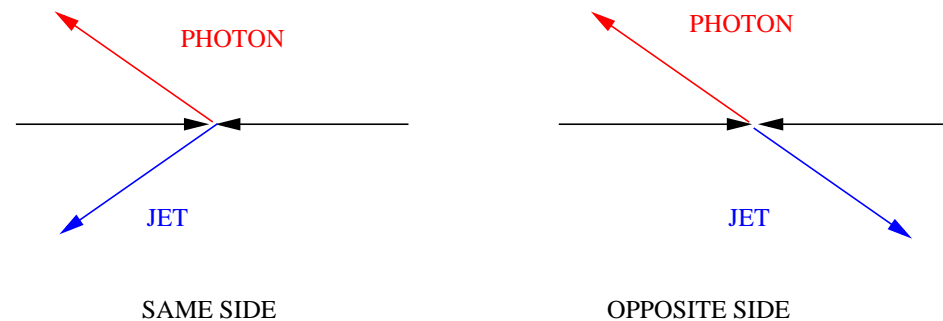
⇒ allows the separation of contributions from different  $x$  values

$$x_1 = E_T^\gamma (e^{+\eta^\gamma} + e^{+y^{\text{jet}}})/\sqrt{s} \quad x_2 = E_T^\gamma (e^{-\eta^\gamma} + e^{-y^{\text{jet}}})/\sqrt{s}$$

⇒ allows the comparison with theory in regions where fragmentation contributions are different: fragmentation contribution in OS is 20-50% higher than in SS

- Measurement of  $d\sigma/dE_T^\gamma$  in the phase-space region defined by  $E_T^\gamma > 25 \text{ GeV}$ ,  $|\eta^\gamma| < 1.37$ ,  $p_T^{\text{jet}} > 20 \text{ GeV}$  and three ranges in  $y^{\text{jet}}$ :  $|y^{\text{jet}}| < 1.2$ ,  $1.2 < |y^{\text{jet}}| < 2.8$  and  $2.8 < |y^{\text{jet}}| < 4.4$  (leading jet, reconstructed using the anti- $k_t$  algorithm with  $R = 0.4$ ), both for OS and SS;  $E_T^{\text{iso}*} < 4 \text{ GeV}$  and  $\Delta R_{\gamma j} > 1$
  - The measurements cover the region  $x \gtrsim 10^{-3}$  and  $625 < Q^2 < 1.6 \cdot 10^5 \text{ GeV}^2$

ATLAS PRD85-092014



# NLO QCD calculations and non-perturbative effects

ATLAS PRD85-092014

- NLO QCD calculations of  $\gamma + \text{jet}$  production

$$\rightarrow \mu_R = \mu_F = \mu_f = E_T^\gamma$$

 $\rightarrow \text{CT10 proton PDFs}$ 
 $\rightarrow \text{NLO photon fragmentation function (BFG set II)}$ 
 $\rightarrow \text{photon-isolation requirement at parton level}$ 

$$E_T^{\text{iso}}(\text{partons}) < 4 \text{ GeV}$$

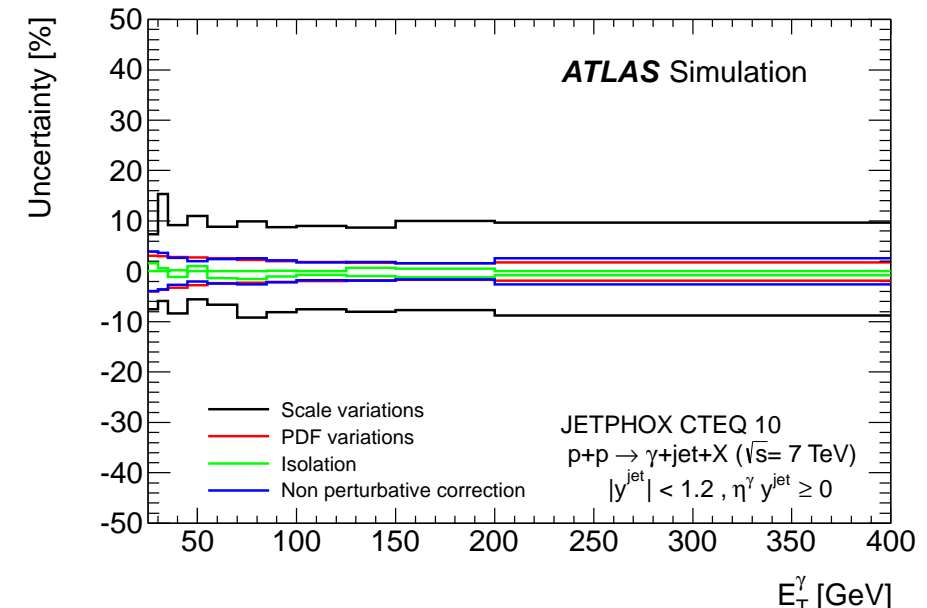
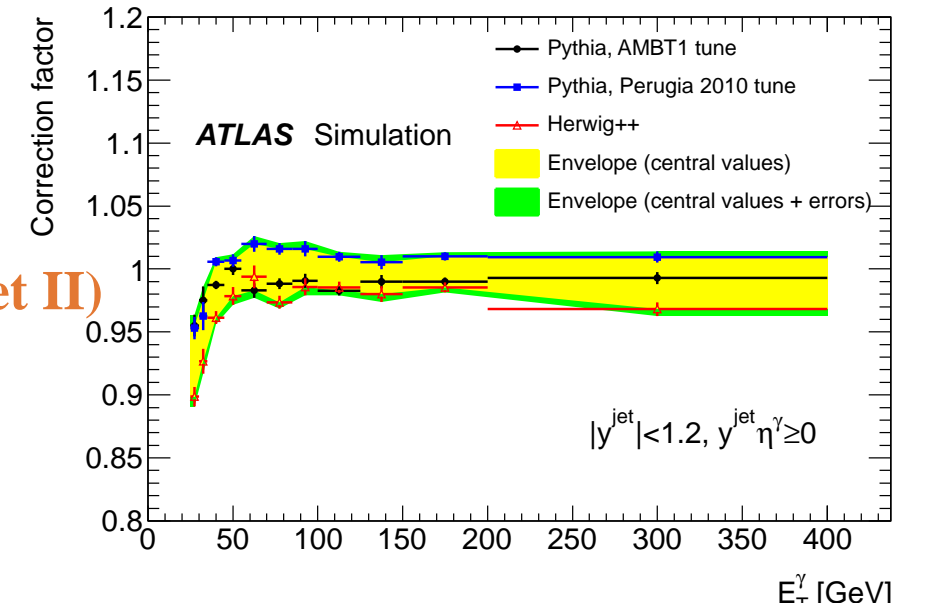
- Corrections for non-perturbative effects

(hadronisation and underlying event) using

**PYTHIA (AMBT1 and Perugia2010 tunes)** and

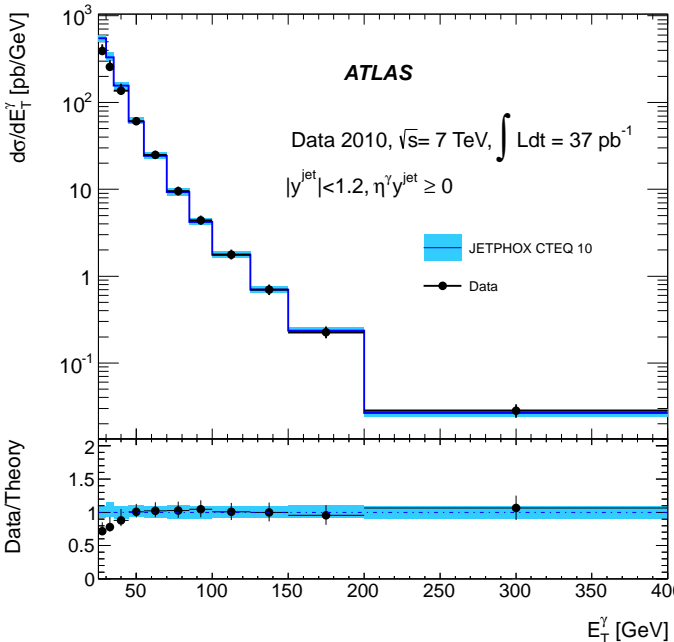
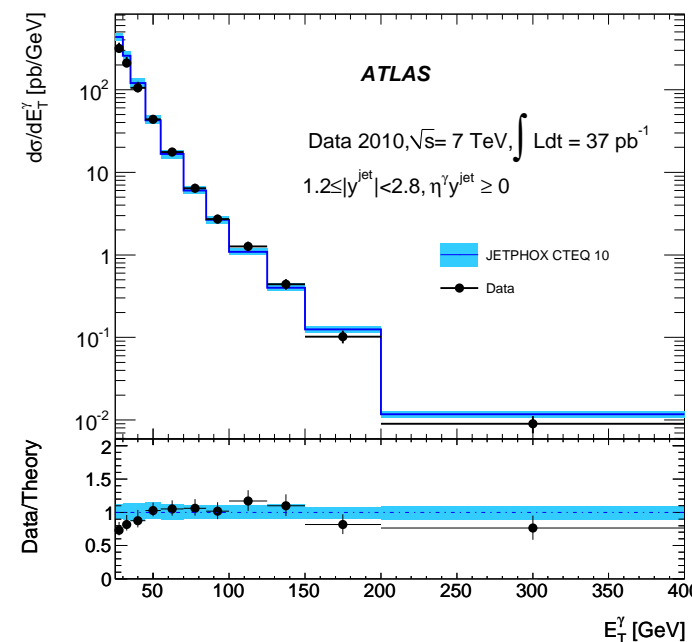
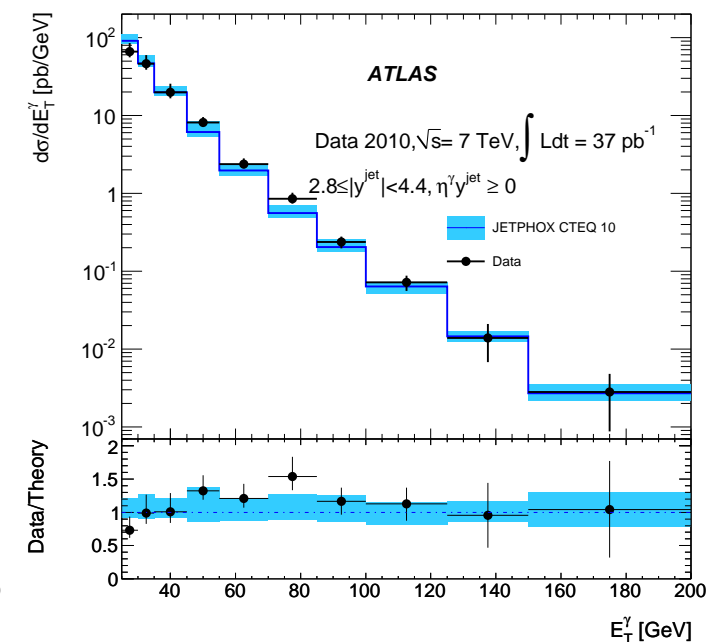
**HERWIG (UE7000-2 tune)**

- Theoretical uncertainties

 $\rightarrow \text{terms beyond NLO (variations of } \mu_R, \mu_F, \mu_f)$ 
 $\rightarrow \text{PDF-induced uncertainties}$ 
 $\rightarrow \text{correspondence parton/particle-level isolation}$ 
 $\rightarrow \text{non-perturbative correction}$ 


## $\gamma + \text{jet production: same side}, \eta^\gamma \cdot y^{\text{jet}} \geq 0$

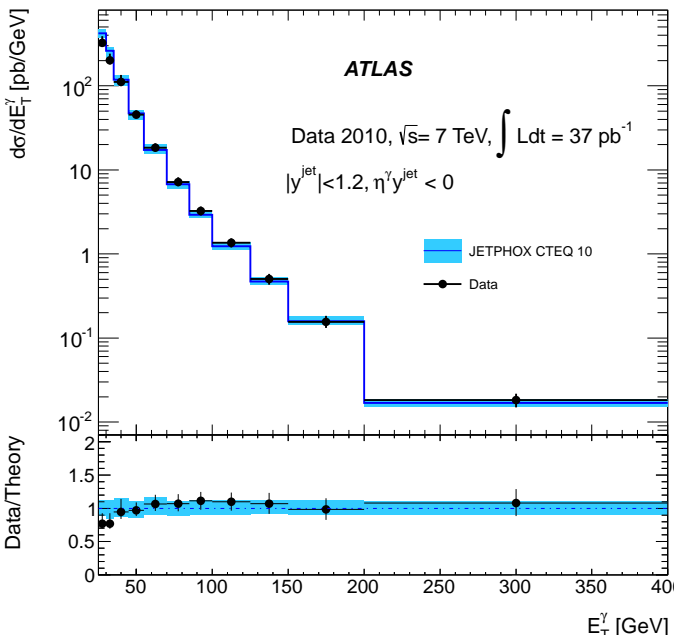
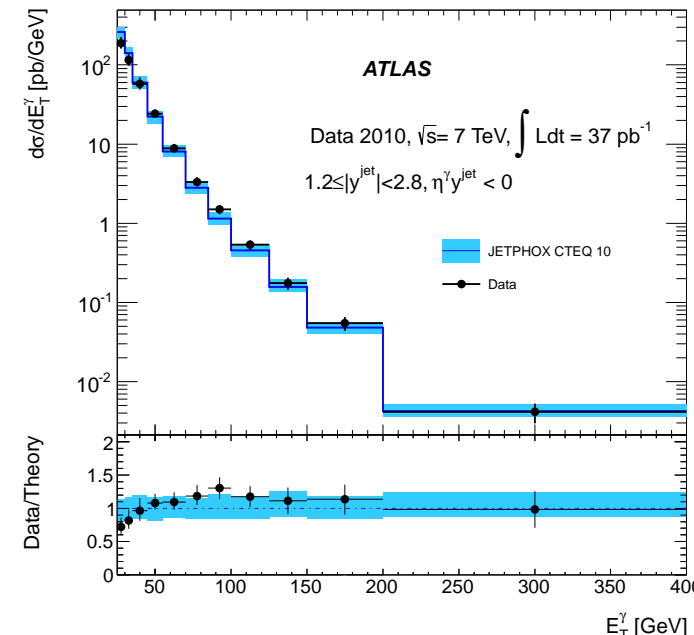
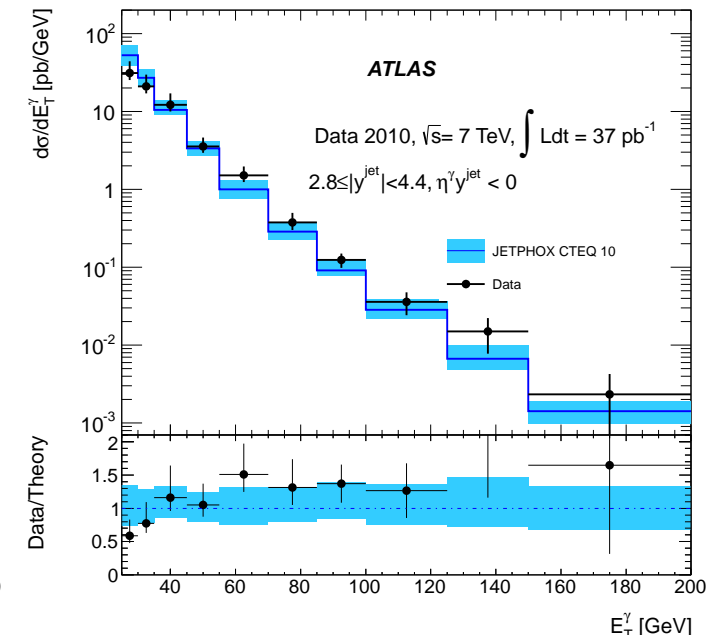
ATLAS PRD85-092014

 $|y^{\text{jet}}| < 1.2$  $1.2 < |y^{\text{jet}}| < 2.8$  $2.8 < |y^{\text{jet}}| < 4.4$ 

- NLO QCD calculations corrected for non-perturbative effects are in fair agreement with the measurements within the uncertainties except for  $E_T^\gamma < 45$  GeV
- Data consistently lower than the calculations for  $E_T^\gamma < 45$  GeV  
→ Inadequacy of the NLO QCD calculations at low  $E_T^\gamma$ ? higher-order effects?

# $\gamma + \text{jet production: opposite side, } \eta^\gamma \cdot y^{\text{jet}} < 0$

ATLAS PRD85-092014

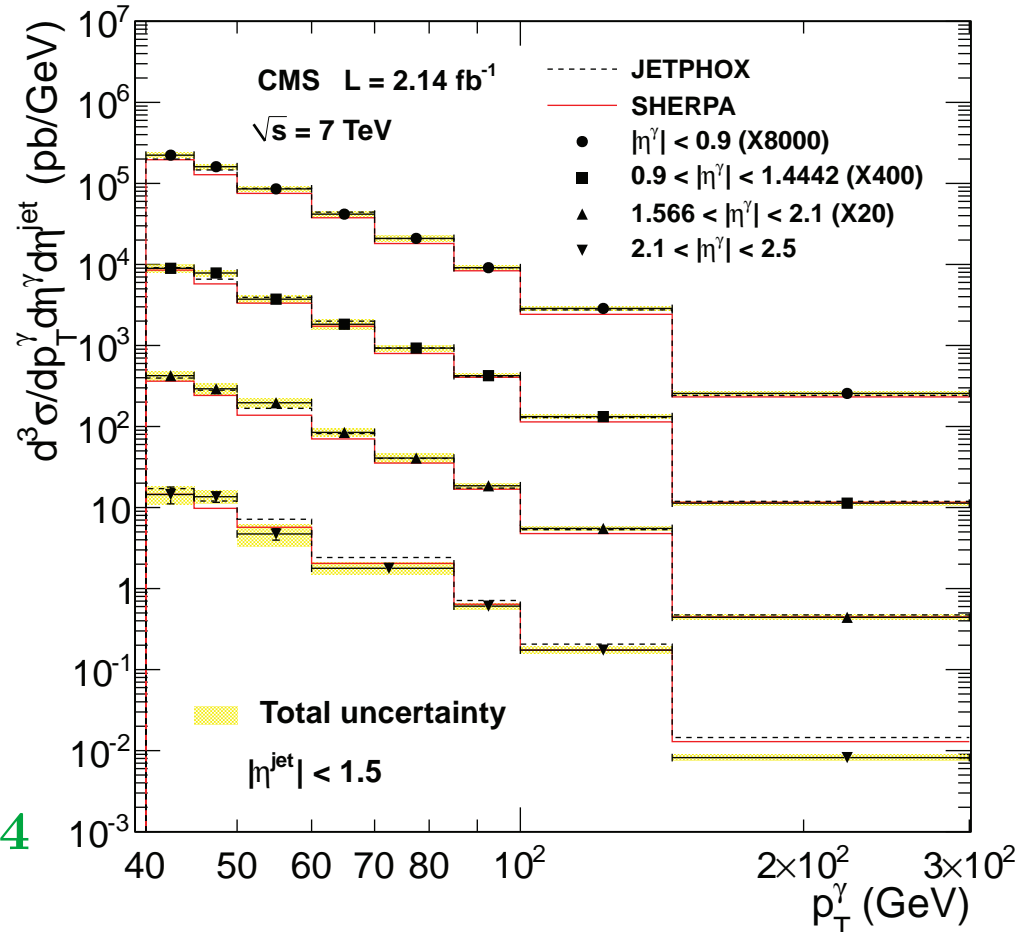
 $|y^{\text{jet}}| < 1.2$  $1.2 < |y^{\text{jet}}| < 2.8$  $2.8 < |y^{\text{jet}}| < 4.4$ 

- NLO QCD calculations corrected for non-perturbative effects are in fair agreement with the measurements within the uncertainties except for  $E_T^\gamma < 45$  GeV
- Data consistently lower than the calculations for  $E_T^\gamma < 45$  GeV  
→ Inadequacy of the NLO QCD calculations at low  $E_T^\gamma$ ? higher-order effects?
- The data have the potential to contribute to the determination of the proton PDFs

# $\gamma + \text{jet}$ production in $pp$ collisions at $\sqrt{s} = 7 \text{ TeV}$

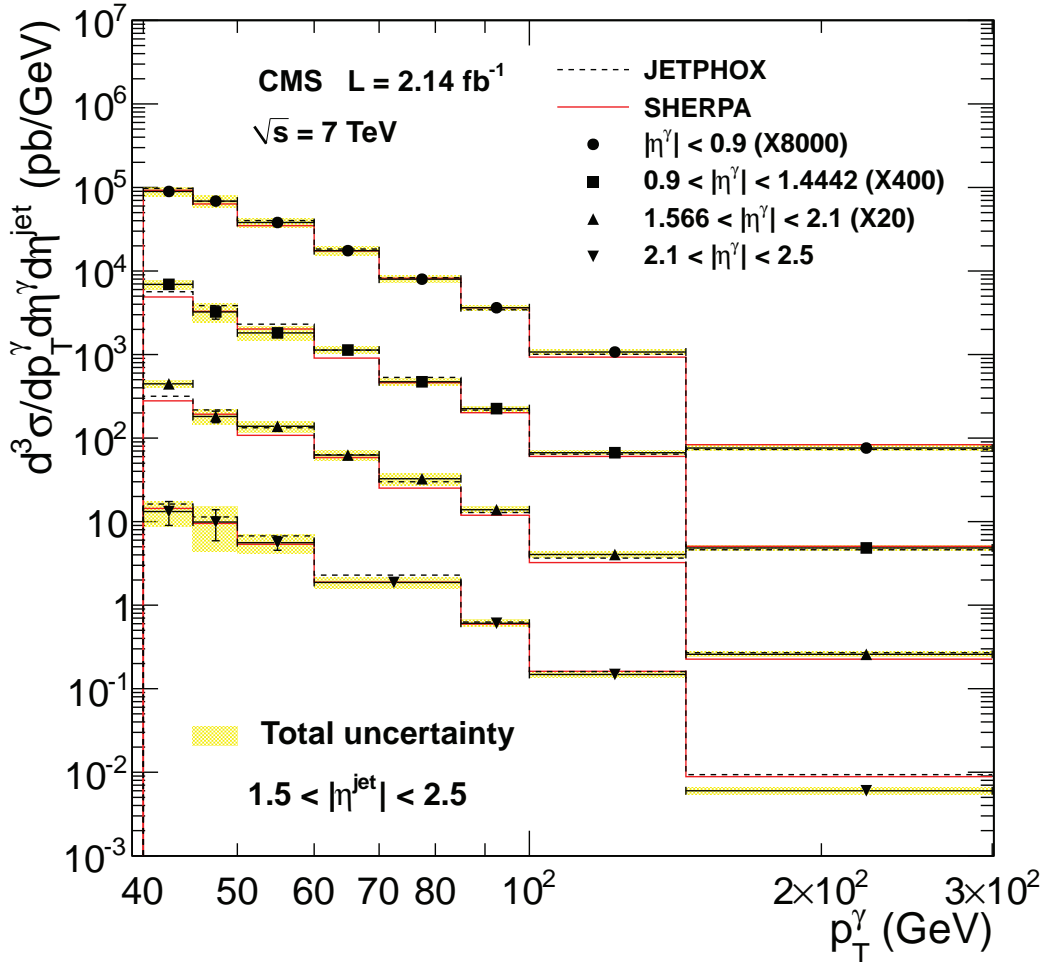
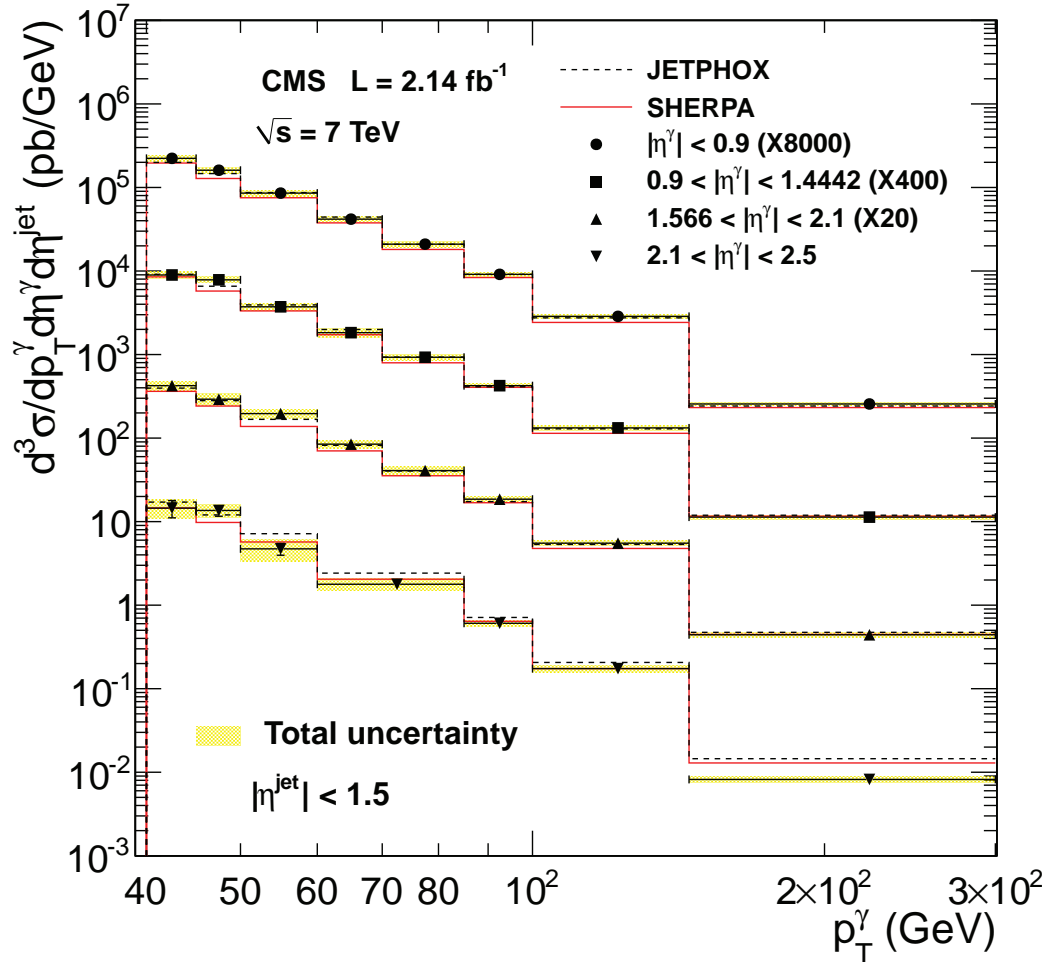
CMS JHEP06-2014-009

- Measurement of  $d^3\sigma/dp_T^\gamma d\eta^\gamma d\eta^{\text{jet}}$  in the phase-space region defined by:
  - $\rightarrow 40 < p_T^\gamma < 300 \text{ GeV}$
  - $\rightarrow p_T^{\text{jet}} > 30 \text{ GeV}$
  - $\rightarrow$  four regions in  $|\eta^\gamma|$ : [0,0.9], [0.9,1.44], [1.57,2.1] and [2.1,2.5],
  - $\rightarrow$  two regions in (leading jet)  $|\eta^{\text{jet}}|$ : [0,1.5], [1.5,2.5]
 using the anti- $k_t$  algorithm with  $R = 0.5$  and  $\mathcal{L} = 2.14 \text{ fb}^{-1}$
- The measurements cover  $0.002 \lesssim x \lesssim 0.4$  and  $1600 < Q^2 < 9 \cdot 10^4 \text{ GeV}^2$
- Experimental uncertainties 5-17% (7-48%) for central (forward) photons  
 $\rightarrow$  uncertainty on signal photon purity dominates
- Comparison to NLO QCD (Jetphox) and multi-leg MC (Sherpa,  $\gamma +$  up to 3 partons)  
 $\rightarrow$  To model exp. selection: energy in a cone ( $R = 0.4$ ) around the photon  $< 5 \text{ GeV}$



# $\gamma + \text{jet}$ production in $pp$ collisions at $\sqrt{s} = 7 \text{ TeV}$

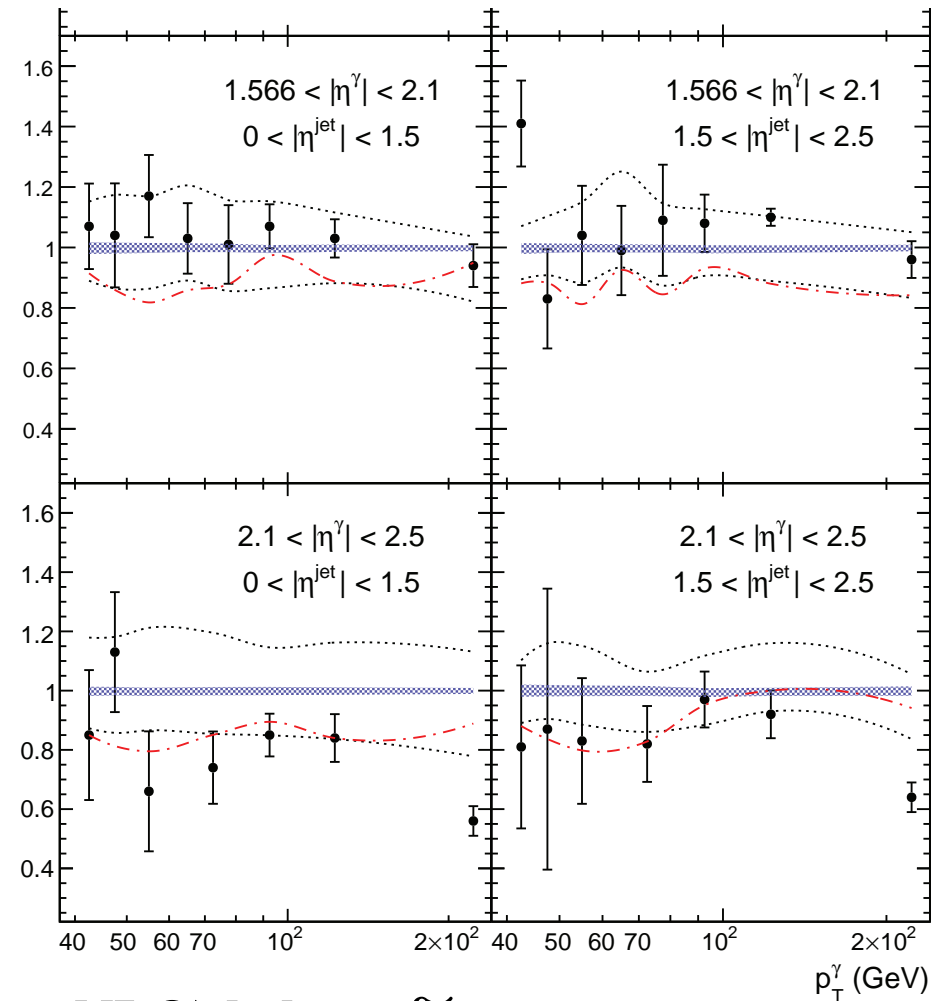
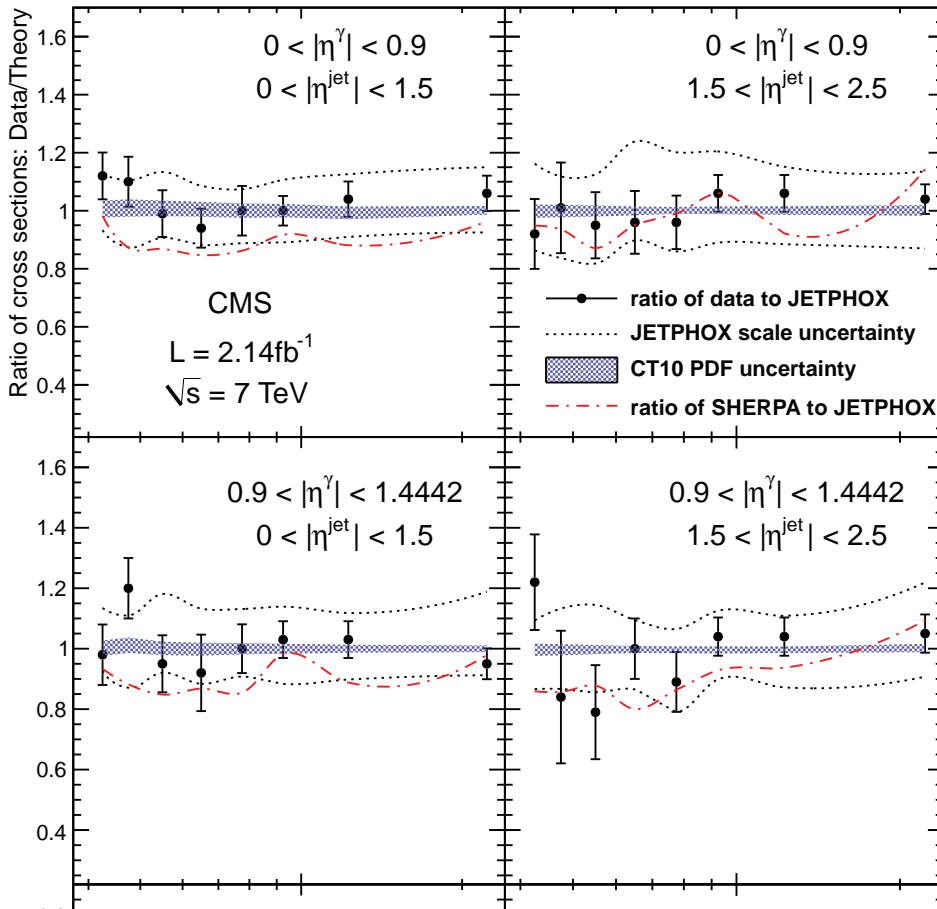
CMS JHEP06-2014-009



- Comparison to Sherpa predictions based on ME( $\gamma +$  up to 3 partons)+PS and CTEQ6
- Comparison to NLO QCD (Jetphox) calculations using CT10 PDFs and  $\mu = p_T^\gamma / 2$
- To model exp. selection: energy in a cone ( $R = 0.4$ ) around the photon  $< 5 \text{ GeV}$

# $\gamma + \text{jet}$ production in $pp$ collisions at $\sqrt{s} = 7 \text{ TeV}$

CMS JHEP06-2014-009



- Non-perturbative corrections (applied only to NLO) below 1%
- The predictions of Sherpa and NLO QCD (Jetphox) consistent with data  
→ except for photons measured in the largest  $\eta$  and  $p_T$  regions

## Dynamics of $\gamma + \text{jet}$ production in $pp$ collisions at $\sqrt{s} = 7 \text{ TeV}$

- Study of the  $\gamma + \text{jet}$  dynamics by measuring the differential cross sections as functions of

→ Photon:  $E_T^\gamma$

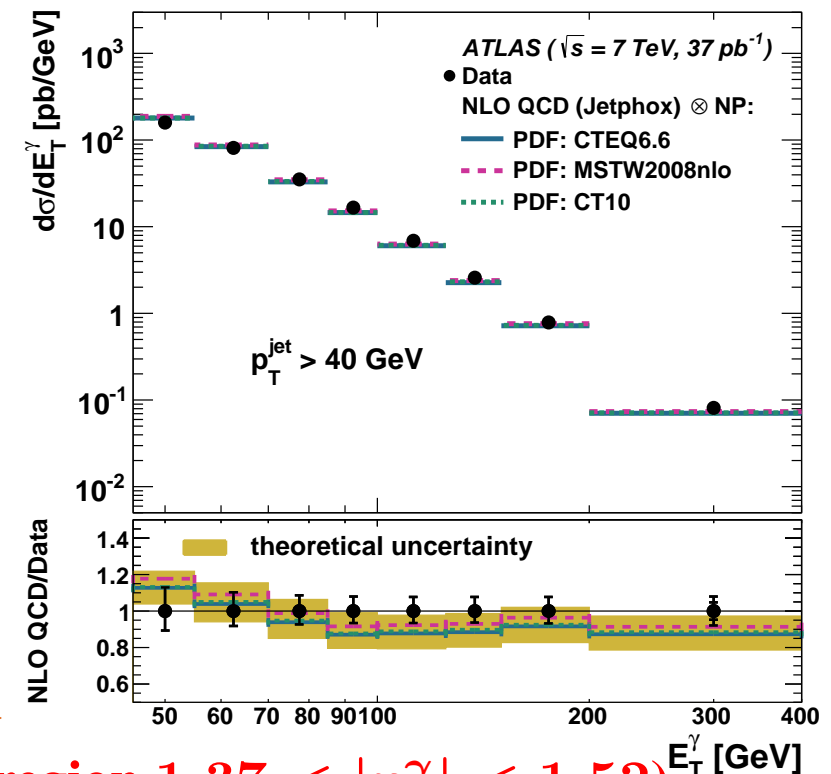
→ Jet:  $p_T^{\text{jet}}$ ,  $y^{\text{jet}}$

→ Photon+Jet:  $\Delta\phi^{\gamma j}$ ,  $m^{\gamma j}$ ,  $\cos\theta^{\gamma j}$

where  $\cos\theta^{\gamma j} = \tanh\frac{1}{2}(y^{\text{jet}} - \eta^\gamma)$

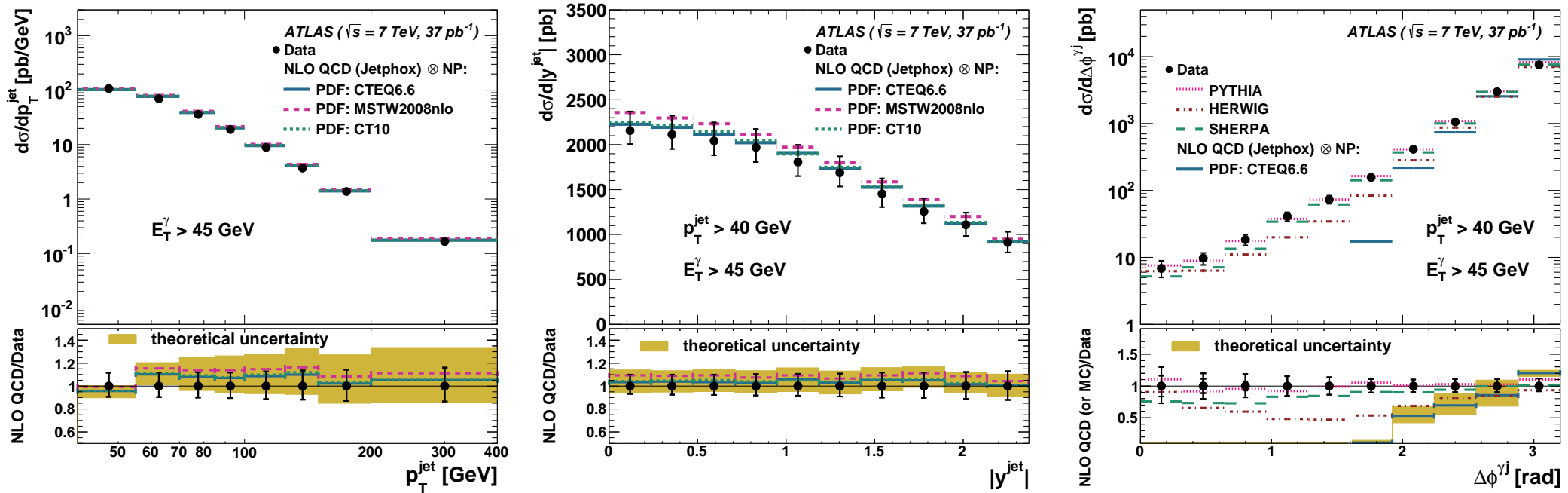
$\theta^{\gamma j}$  = scattering angle in centre-of-mass frame  
for  $2 \rightarrow 2$  hard collinear scattering

- Measurements in the phase-space region defined by:  $E_T^\gamma > 45 \text{ GeV}$ ,  $|\eta^\gamma| < 2.37$  (excluding the region  $1.37 < |\eta^\gamma| < 1.52$ )  
 $p_T^{\text{jet}} > 40 \text{ GeV}$ ,  $|y^{\text{jet}}| < 2.37$  for the leading jet (anti- $k_t$  algorithm with  $R = 0.6$ )  
 $E_T^{\text{iso}*} < 4 \text{ GeV}$  and  $\Delta R_{\gamma j} > 1$
- Comparison to NLO QCD calculation (JETPHOX) corrected for non-perturbative effects
- Small experimental and theoretical uncertainties:  $\sim 10\%$
- Good description of the measured  $d\sigma/dE_T^\gamma$  by the NLO QCD calculations



# Dynamics of $\gamma + \text{jet}$ production in $pp$ collisions

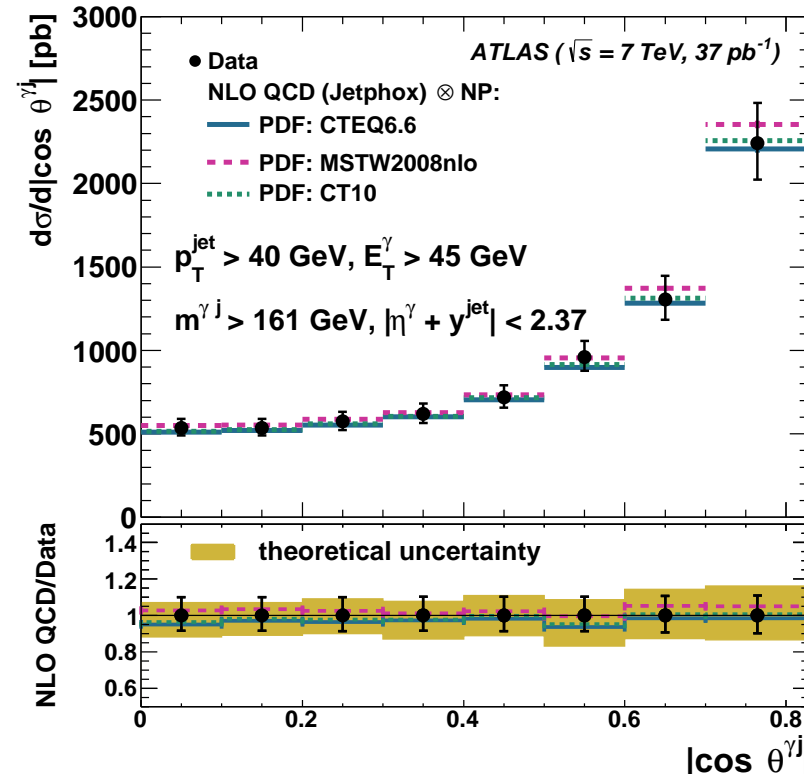
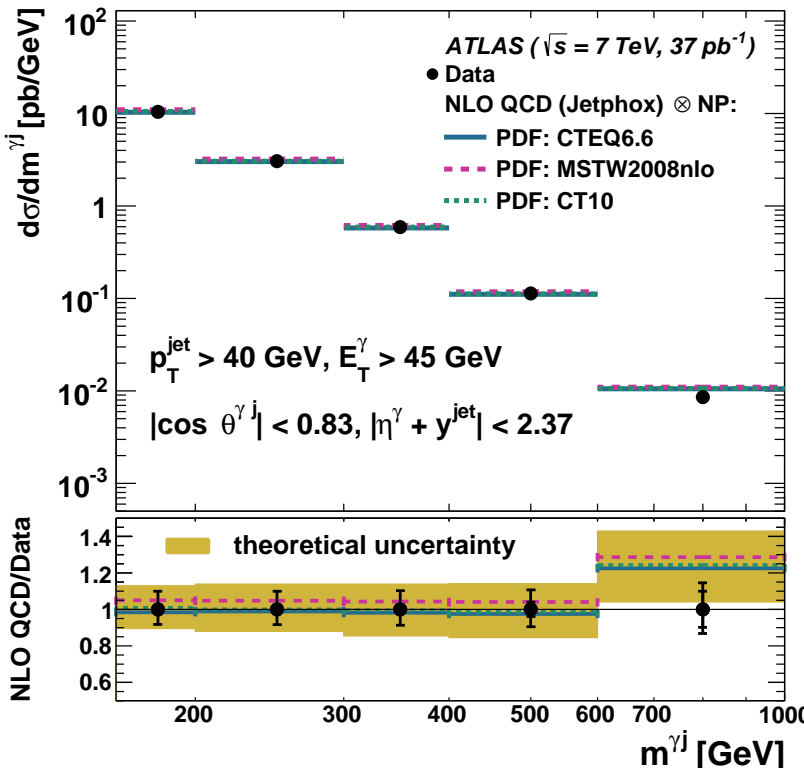
ATLAS NPB875-483



- Good description of the measured  $d\sigma/dp_T^{\text{jet}}$  and  $d\sigma/d|y^{\text{jet}}|$  by the NLO QCD calculations both in normalisation and shape
- Not unexpectedly, NLO QCD calculations fail to describe  $d\sigma/d\Delta\phi^{\gamma j}$ : with up to three final-state particles, the photon and the leading jet cannot be in the same hemisphere in the transverse plane  $\Rightarrow \Delta\phi^{\gamma j} \geq \pi/2$
- PYTHIA and SHERPA MC models give a good description of  $d\sigma/d\Delta\phi^{\gamma j}$

# Dynamics of $\gamma + \text{jet}$ production in $pp$ collisions

ATLAS NPB875-483



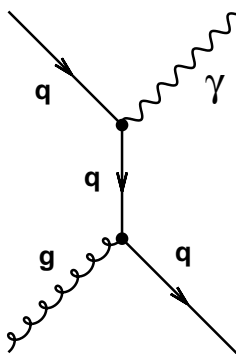
$$|\eta^\gamma + y^{\text{jet}}| < 2.37, \quad |\cos \theta^{\gamma j}| < 0.83, \quad m^{\gamma j} > 161 \text{ GeV}$$

- In the selected (unbiased) region the angular distribution increases as  $|\cos \theta^{\gamma j}|$  increases
- Good description of the data by the NLO QCD calculations within the (small) experimental and theoretical uncertainties  $\Rightarrow$  validation of the description of the dynamics of  $\gamma + \text{jet}$  production in  $pp$  collisions at  $\mathcal{O}(\alpha_{em}\alpha_s^2)$

## Dynamics of $\gamma + \text{jet}$ production in $pp$ collisions

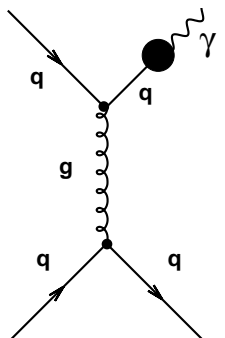
ATLAS NPB875-483

- Angular distribution  $d\sigma/d|\cos \theta^{\gamma j}|$  sensitive to the spin of the exchanged (virtual) particle: quark(1/2) vs gluon(1)



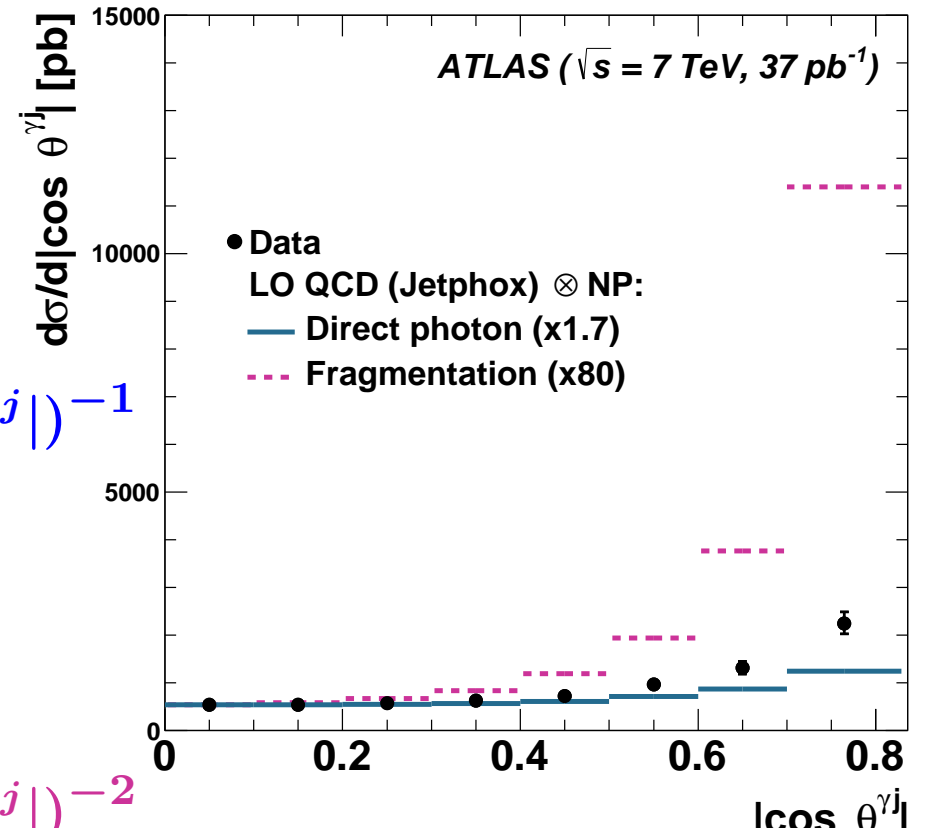
**direct-photon process**

$$d\sigma/d|\cos \theta^{\gamma j}| \sim (1 - |\cos \theta^{\gamma j}|)^{-1}$$



**fragmentation process**

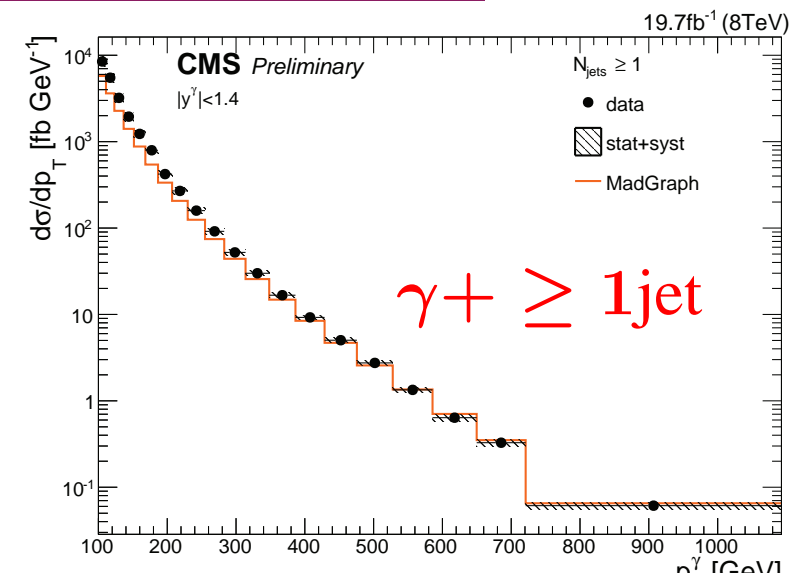
$$d\sigma/d|\cos \theta^{\gamma j}| \sim (1 - |\cos \theta^{\gamma j}|)^{-2}$$



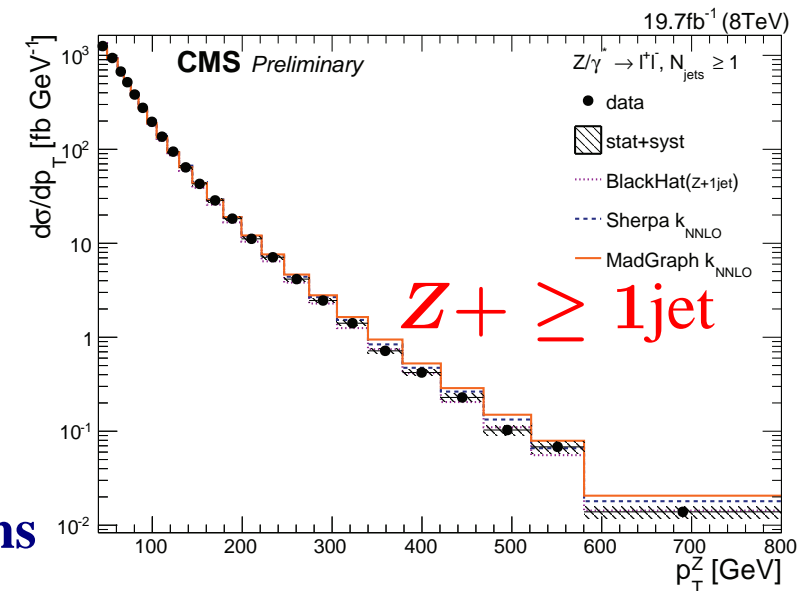
- Measured angular distribution closer to that of direct-photon processes than fragm.  
⇒ consistent with the dominance of processes in which a virtual quark is exchanged

## $\sigma(Z + \text{jets})/\sigma(\gamma + \text{jets})$ in $pp$ collisions at $\sqrt{s} = 8 \text{ TeV}$

- Measurement of cross sections and ratios for  $Z + \text{jets}$  and  $\gamma + \text{jets}$  with the aim of
  - testing QCD calculations
  - (improved) modelling of  $Z(\rightarrow \nu\bar{\nu}) + \text{jets}$  in  $n_{\text{jets}} \geq 1, 2, 3$  and large  $H_T$  final states
- Phase-space region defined by
  - $p_T^{V=\gamma, Z} > 100 \text{ GeV}$  and  $|y^\gamma| < 1.4$   
( $|y^Z| < 1.4$  for ratios  $Z/\gamma$ )
  - $p_T^{\text{jet}} > 30 \text{ GeV}$  and  $|\eta^{\text{jet}}| < 2.4$
 using the anti- $k_t$  algorithm with  $R = 0.5$  and  $\mathcal{L} = 19.7 \text{ fb}^{-1}$
- Reduced experimental and theoretical uncertainties in the ratios
- Comparison to NLO QCD (BlackHat, only for  $Z$ ) and multi-leg MC (Sherpa, MadGraph) calculations

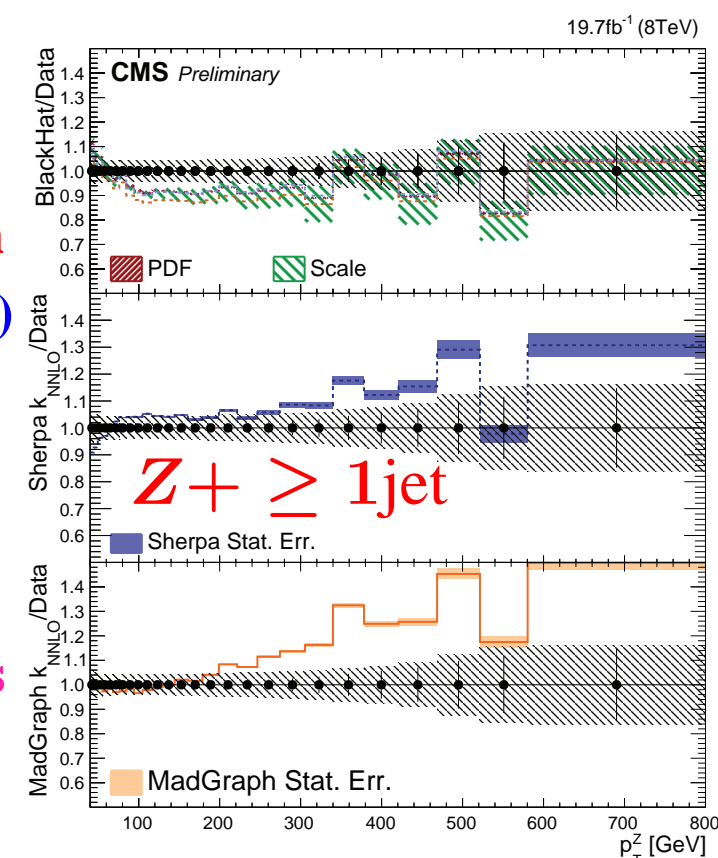
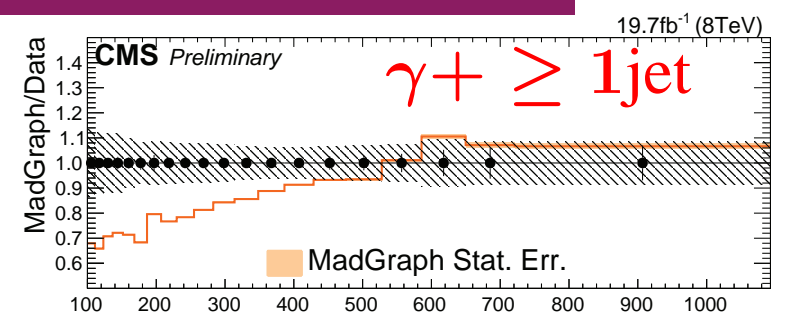


CMS PAS SMP-14-005

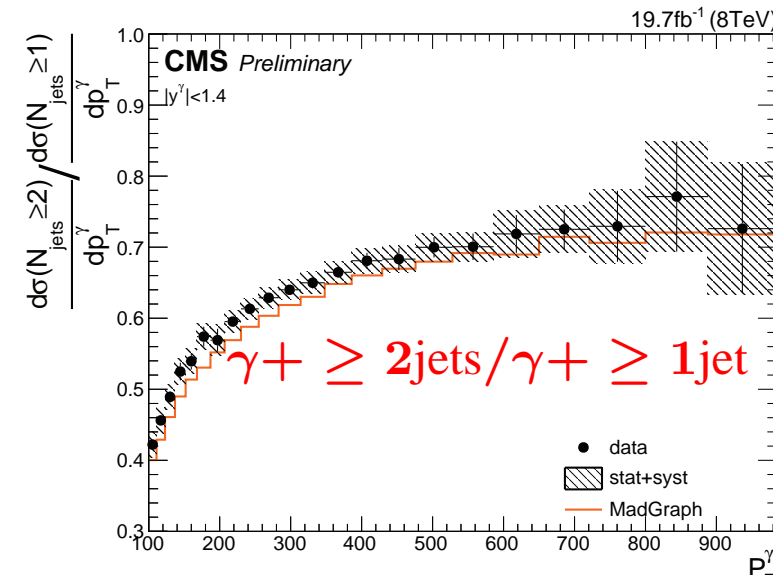
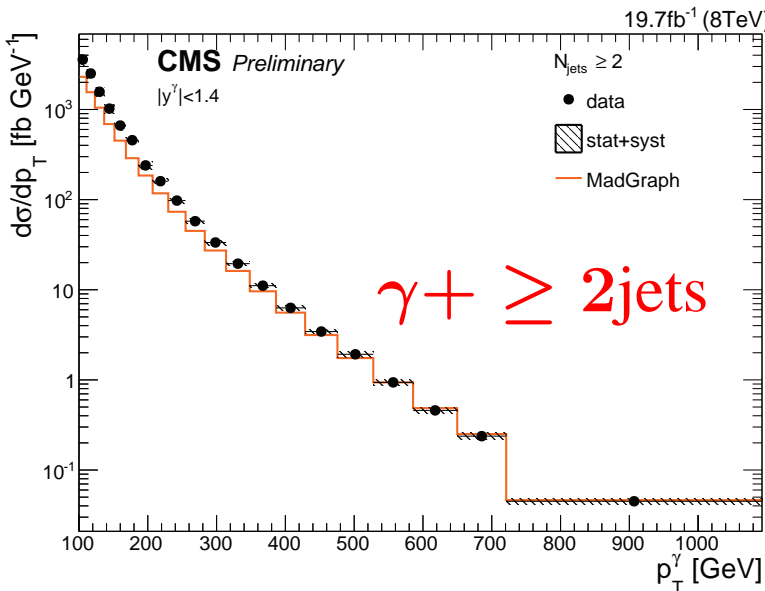


## $\sigma(Z + \text{jets})$ and $\sigma(\gamma + \text{jets})$ in $pp$ collisions at $\sqrt{s} = 8 \text{ TeV}$

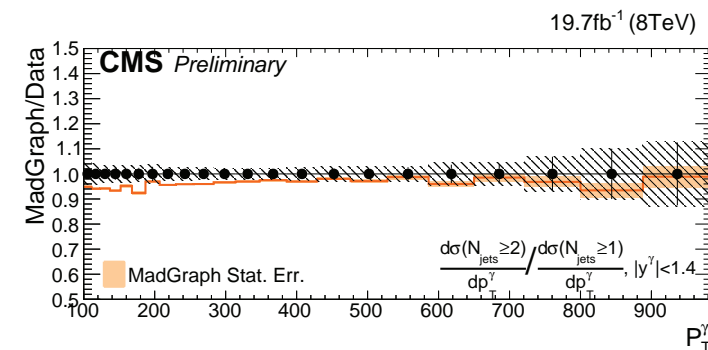
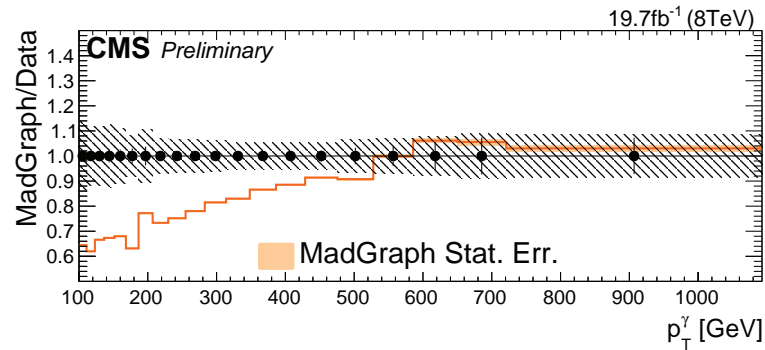
- Isolation requirements on the photon are imposed separately on pileup-corrected scalar  $p_T$  sum of PF-neutral and charged hadrons and PF photons inside a cone of  $R = 0.3$  around photon candidate
- Photon signal purity: data-driven method based on fitting signal+backg. templates to photon isolation (scalar  $p_T$  sum) distribution → corrected for pileup (using random cones) and energy deposit from photon → signal purity from 70% (low  $p_T$ ) to 90% (high  $p_T$ )
- Experimental systematic uncertainties ( $\gamma + \text{jets}$ ):  
 → uncertainty on the signal purity (4-10%)  
 → uncertainty on the integrated luminosity (2.6%)  
 → uncertainty on the jet energy scale: 5-10% for  $n_{\text{jets}} \geq 2, 3$  and 5-7% for  $H_T > 300 \text{ GeV}$  selections  
 → uncertainty on photon energy scale (< 3%)  
 → uncertainty on unfolding (2%)



# $\sigma(\gamma + \text{jets})$ in $pp$ collisions at $\sqrt{s} = 8 \text{ TeV}$

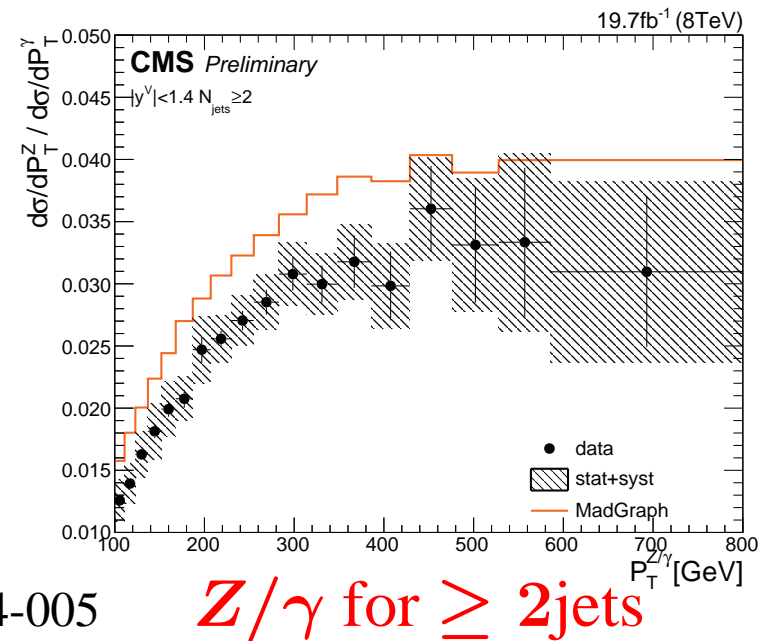
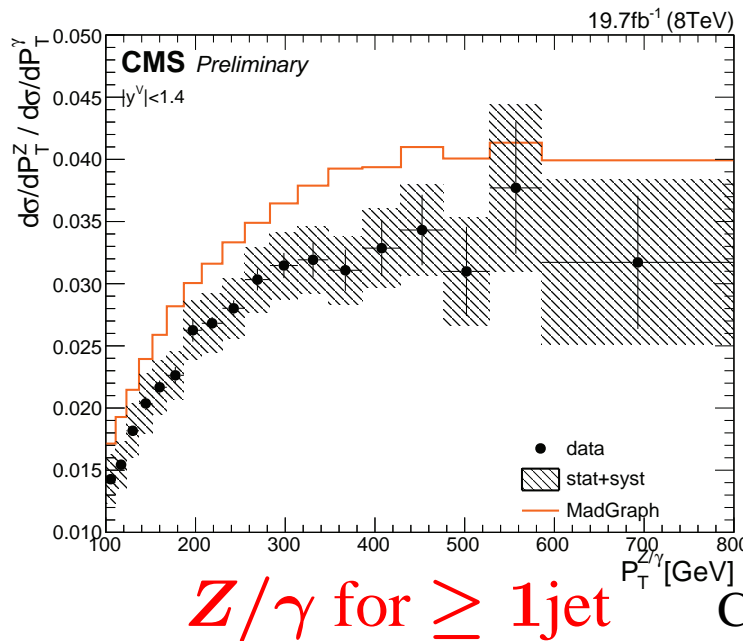


CMS PAS SMP-14-005

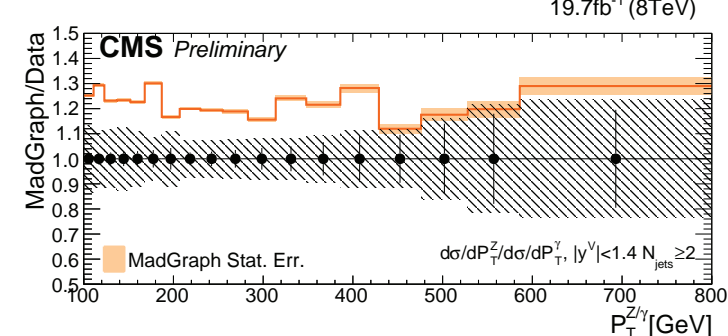
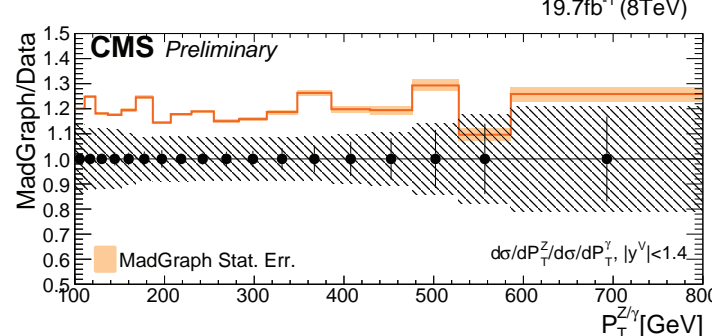


- Cross sections for isolated prompt photons with  $E_T^{iso}(R = 0.4) < 5 \text{ GeV}$
- Comparison to Madgraph including up to four-quark final states  
→ good description of the ratio  $\sigma(\gamma + \geq 2\text{jets})/\sigma(\gamma + \geq 1\text{jet})$

# $\sigma(Z + \text{jets})/\sigma(\gamma + \text{jets})$ in $pp$ collisions at $\sqrt{s} = 8 \text{ TeV}$



CMS PAS SMP-14-005



- **Cancelation of jet energy scale and resolution and luminosity uncertainties**
- **Observation of a turn-on of the ratio and plateau around  $p_T \simeq 300\text{-}350 \text{ GeV}$**   
→ good description of the shape by MadGraph (but  $\sim 20\%$  higher than data)
- ⇒ These ratios are suitable to predict invisible decays of  $Z$  for searches

# Photon pair production

## Isolated-photon pair production in $pp$ collisions

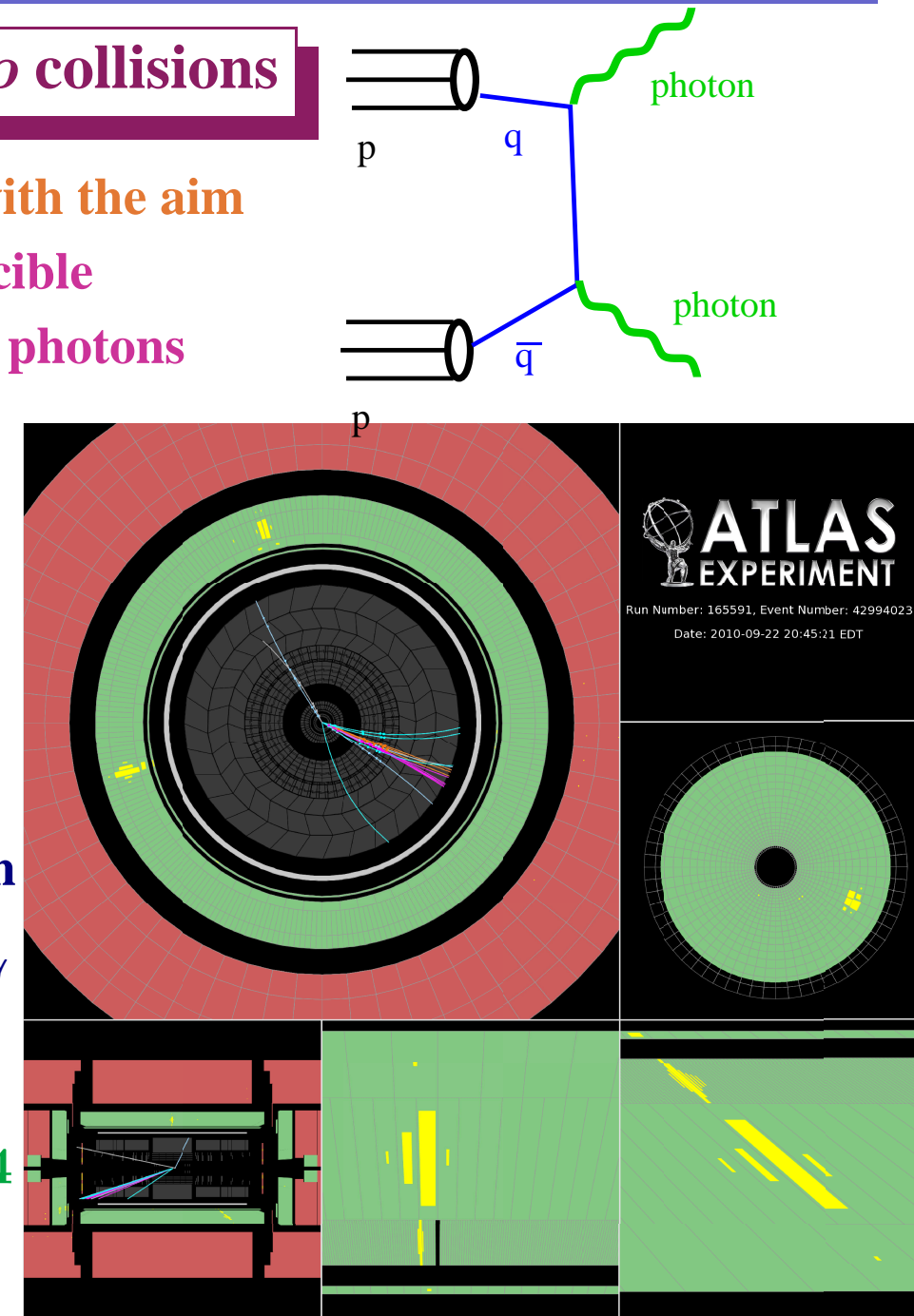
- Measurements of the process  $pp \rightarrow \gamma\gamma + X$  with the aim of testing pQCD and understanding the irreducible background to new physics processes involving photons or  $H \rightarrow \gamma\gamma$

- Measurement of differential cross sections as functions of

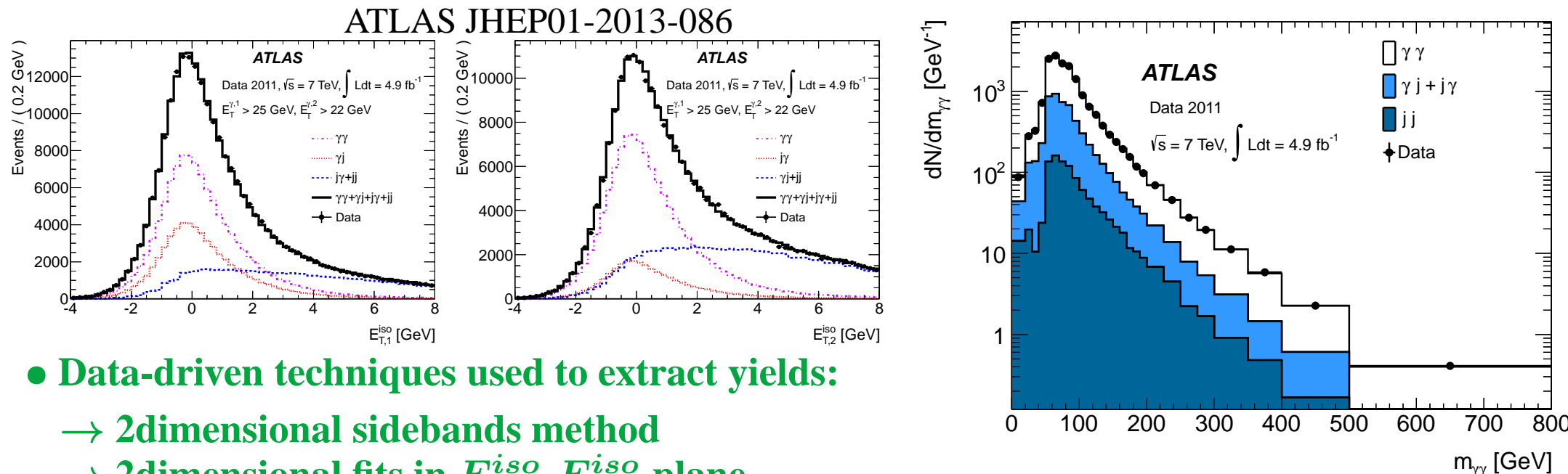
- diphoton invariant mass,  $m_{\gamma\gamma}$
- diphoton transverse momentum,  $p_{T,\gamma\gamma}$
- azimuthal separation in LAB frame,  $\Delta\phi_{\gamma\gamma}$
- cosine of the polar angle of highest- $E_T$  photon in the Collins-Soper diphoton rest frame,  $\cos\theta_{\gamma\gamma}^*$

in the phase-space region defined by:

$E_T^{\gamma 1,2} > 25(22)$  GeV,  $|\eta^\gamma| < 2.37$  (excluding the region  $1.37 < |\eta^\gamma| < 1.52$ ),  $\Delta R_{\gamma\gamma} > 0.4$  and  $E_T^{iso*} < 4$  GeV using  $\mathcal{L} = 4.9 \text{ fb}^{-1}$



# Isolated-photon pair production in $pp$ collisions at $\sqrt{s} = 7$ TeV



- Data-driven techniques used to extract yields:

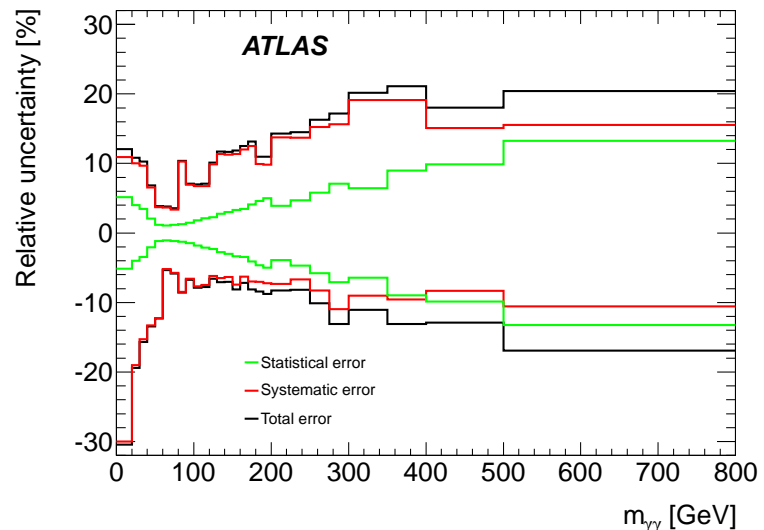
- 2dimensional sidebands method
- 2dimensional fits in  $E_{T,1}^{iso}$ - $E_{T,2}^{iso}$  plane

⇒  $\gamma\gamma, \gamma j + j\gamma, jj$  decomposition

- Data-driven subtraction of  $e^+e^-$  background

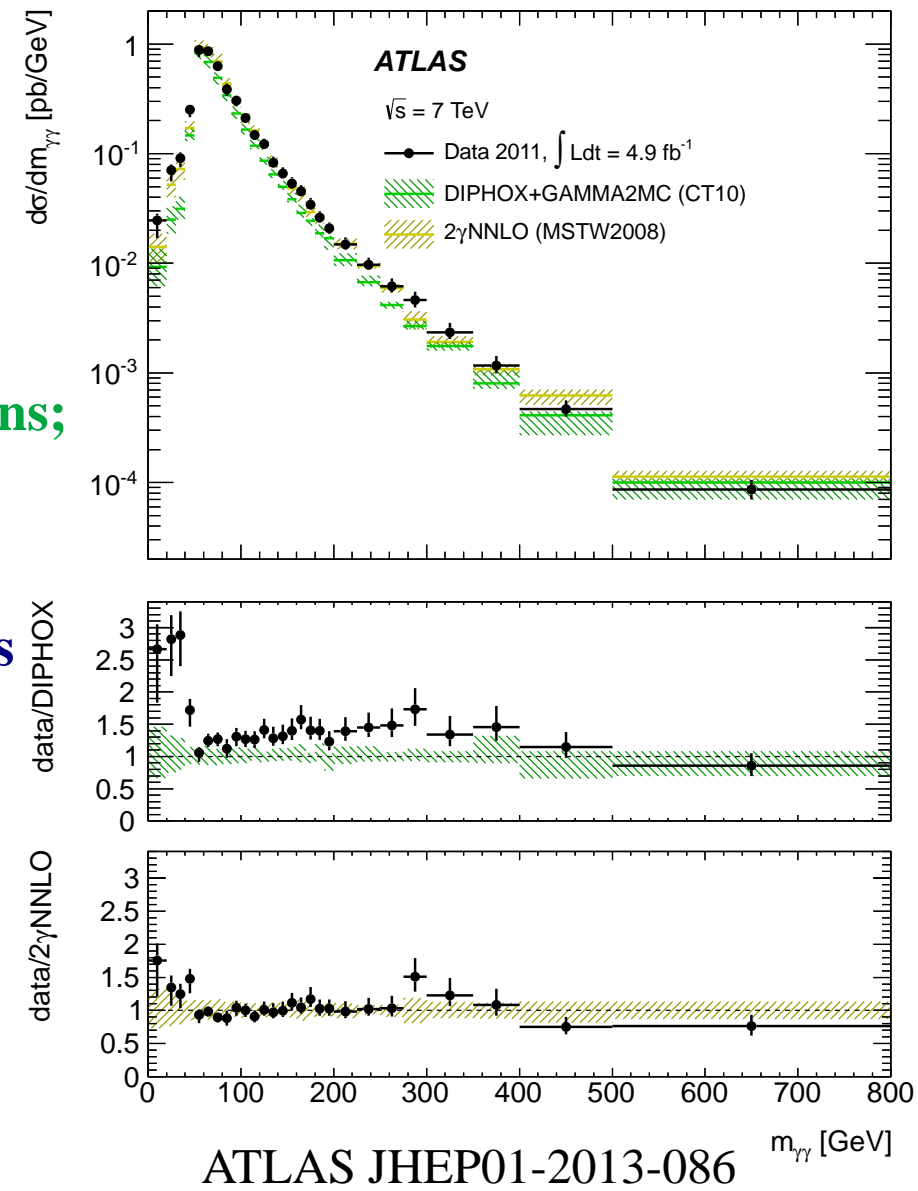
- Experimental uncertainties:

- background  $E_T^{iso}$  distribution ( $^{+3\%}_{-6\%}$ )
- signal  $E_T^{iso}$  distribution ( $^{+2\%}_{-3\%}$ )
- alternative MC model and budget material ( $^{+2\%}_{-5\%}$ )
- integrated luminosity ( $\pm 3.9\%$ )

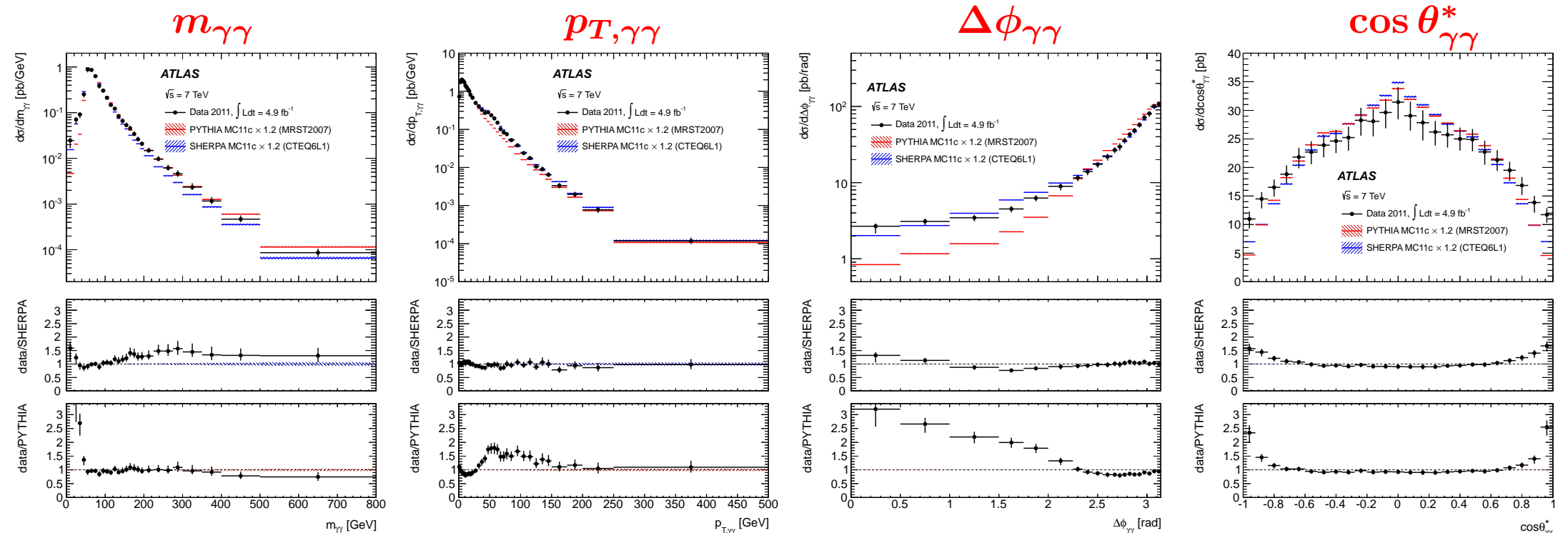


## Isolated-photon pair production in $pp$ collisions at $\sqrt{s} = 7$ TeV

- Comparison to theoretical calculations
- Fixed-order QCD calculations (NP corrected)
  - $2\gamma$ NNLO program; NNLO calculation of direct-photon contribution (no fragm.)
  - DIPHOX program; NLO calculation of direct-photon and fragmentation contributions; box diagram  $gg \rightarrow \gamma\gamma$  (at NLO) included using GAMMA2MC
- Matrix-elements plus parton shower calculations
  - PYTHIA ( $2 \rightarrow 2 + PS$ )
  - SHERPA ( $2 \rightarrow 2(3,4) + PS$ )
- The contribution from  $H \rightarrow \gamma\gamma$  is neglected (1%)
- PYTHIA and SHERPA MC diphoton samples used to estimate hadronization and underlying event effects → typical correction of 0.95



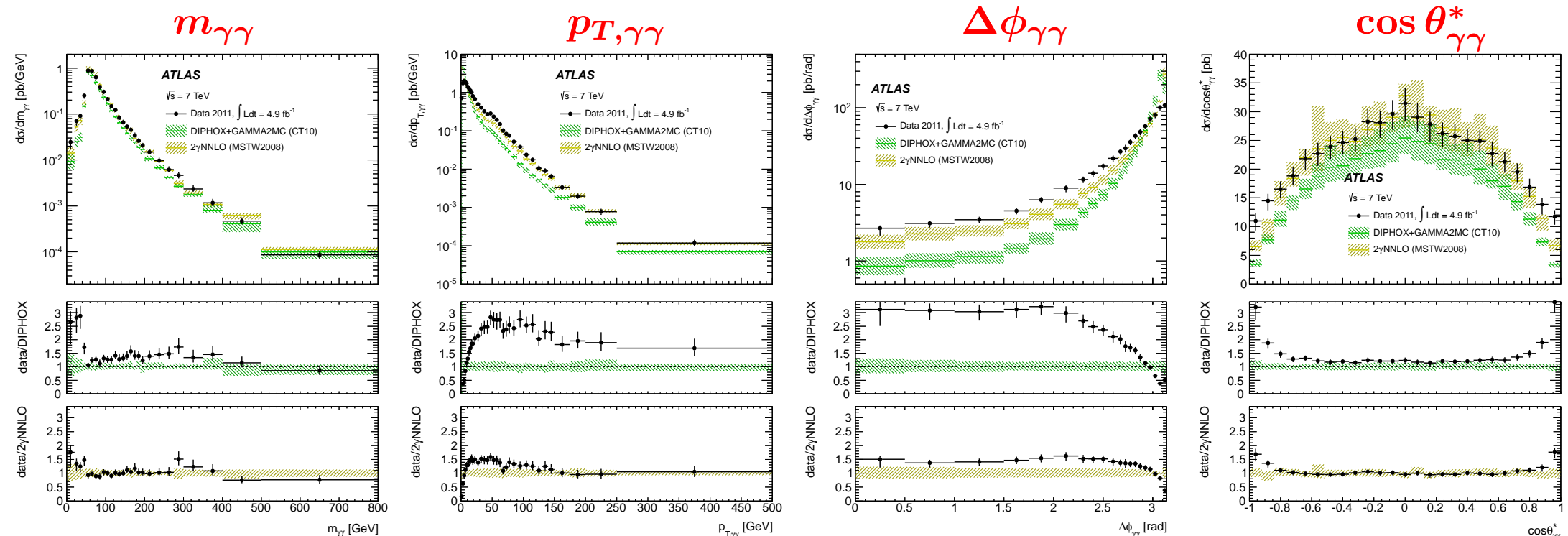
# Isolated-photon pair production in $pp$ collisions at $\sqrt{s} = 7$ TeV



- Comparison to matrix-elements plus parton shower calculations of PYTHIA and SHERPA
  - MC normalisations rescaled by 1.2 to compare shapes
  - $\Delta\phi_{\gamma\gamma} \sim \pi$  and low  $p_{T,\gamma\gamma}$  (soft gluon resummation important): both MCs do well
  - low  $\Delta\phi_{\gamma\gamma}$  and low  $m_{\gamma\gamma}$ : PYTHIA fails
  - SHERPA performs well except for high  $m_{\gamma\gamma}$

ATLAS JHEP01-2013-086

# Isolated-photon pair production in $pp$ collisions at $\sqrt{s} = 7$ TeV



- Comparison to fixed-order calculations of  $2\gamma$ NNLO and DIPHOX+GAMMA2MC
  - no re-scaling of the normalisations! (absolute predictions)
  - $\Delta\phi_{\gamma\gamma} \sim \pi$  and low  $p_{T,\gamma\gamma}$  (soft gluon resummation important): both fail
  - DIPHOX+GAMMA2MC predictions underestimate the data
  - inclusion of h.o. ( $2\gamma$ NNLO) improves dramatically the description of the data

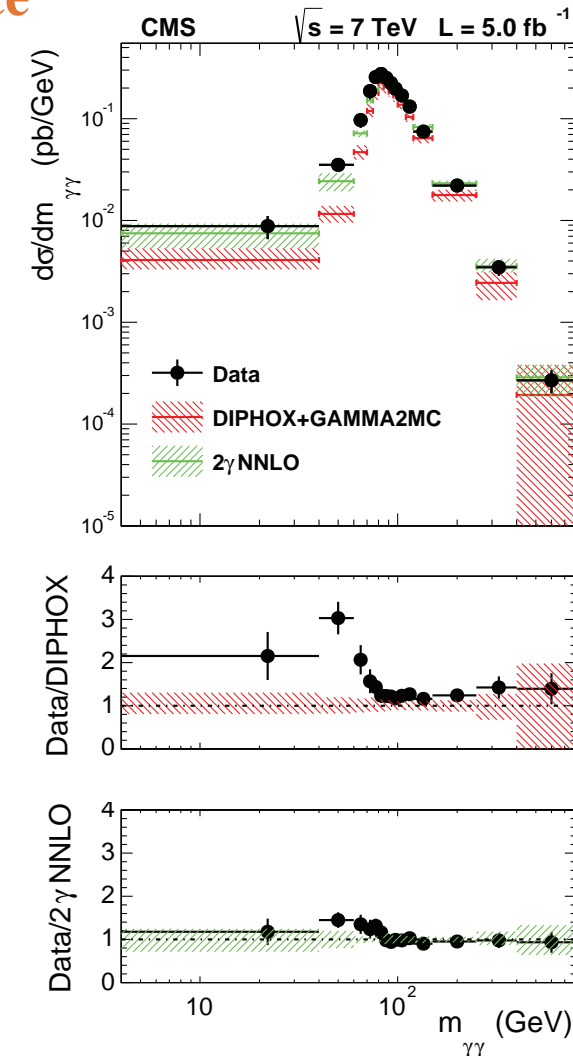
ATLAS JHEP01-2013-086

# Diphoton production in $pp$ collisions at $\sqrt{s} = 7 \text{ TeV}$ using $5 \text{ fb}^{-1}$

- Measurement of diphoton production in the phase-space region defined by:

$\rightarrow E_T^{\gamma 1} > 40 \text{ GeV}, E_T^{\gamma 2} > 25 \text{ GeV}$   
 $\rightarrow |\eta^\gamma| < 2.5$  (except [1.44,1.57])  
 $\rightarrow \Delta R(\gamma_1, \gamma_2) > 0.45$

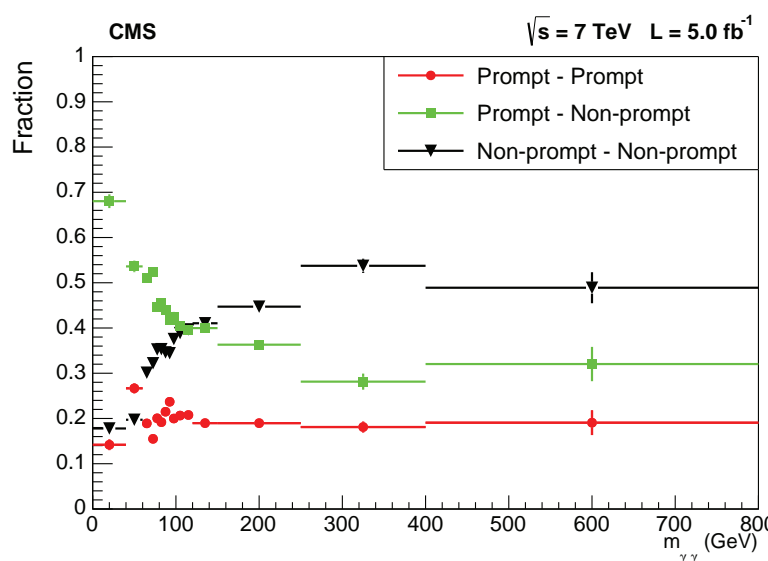
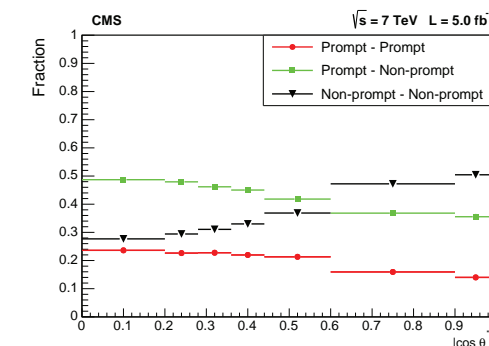
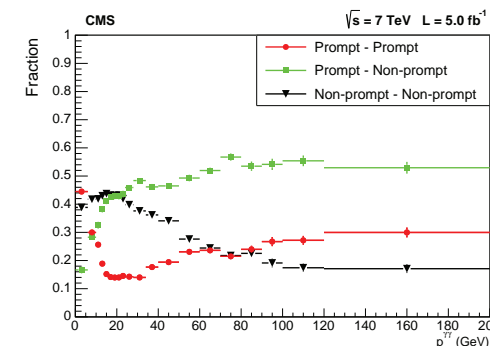
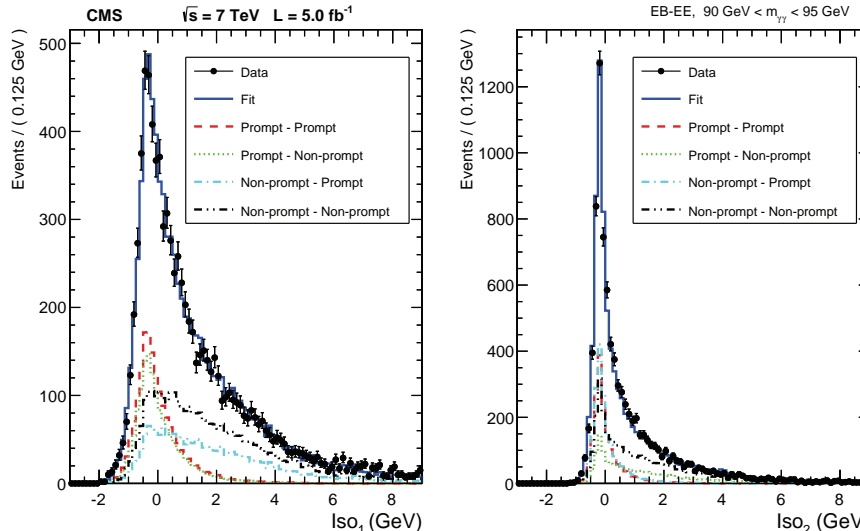
- Data-driven method to extract prompt diphoton yield
  - using photon component of particle flow isolation
  - pileup subtraction using Jet-area/median method
  - corrected for energy deposit from photon candidate
- Cross sections for isolated prompt photons
  - $\rightarrow E_T^{iso}(R = 0.4) < 5 \text{ GeV}$
- Comparison to (N)NLO (resummed) QCD calculations and multi-leg MC calculations



CMS EPJC74-3129

# Diphoton production in $pp$ collisions at $\sqrt{s} = 7 \text{ TeV}$ using $5 \text{ fb}^{-1}$

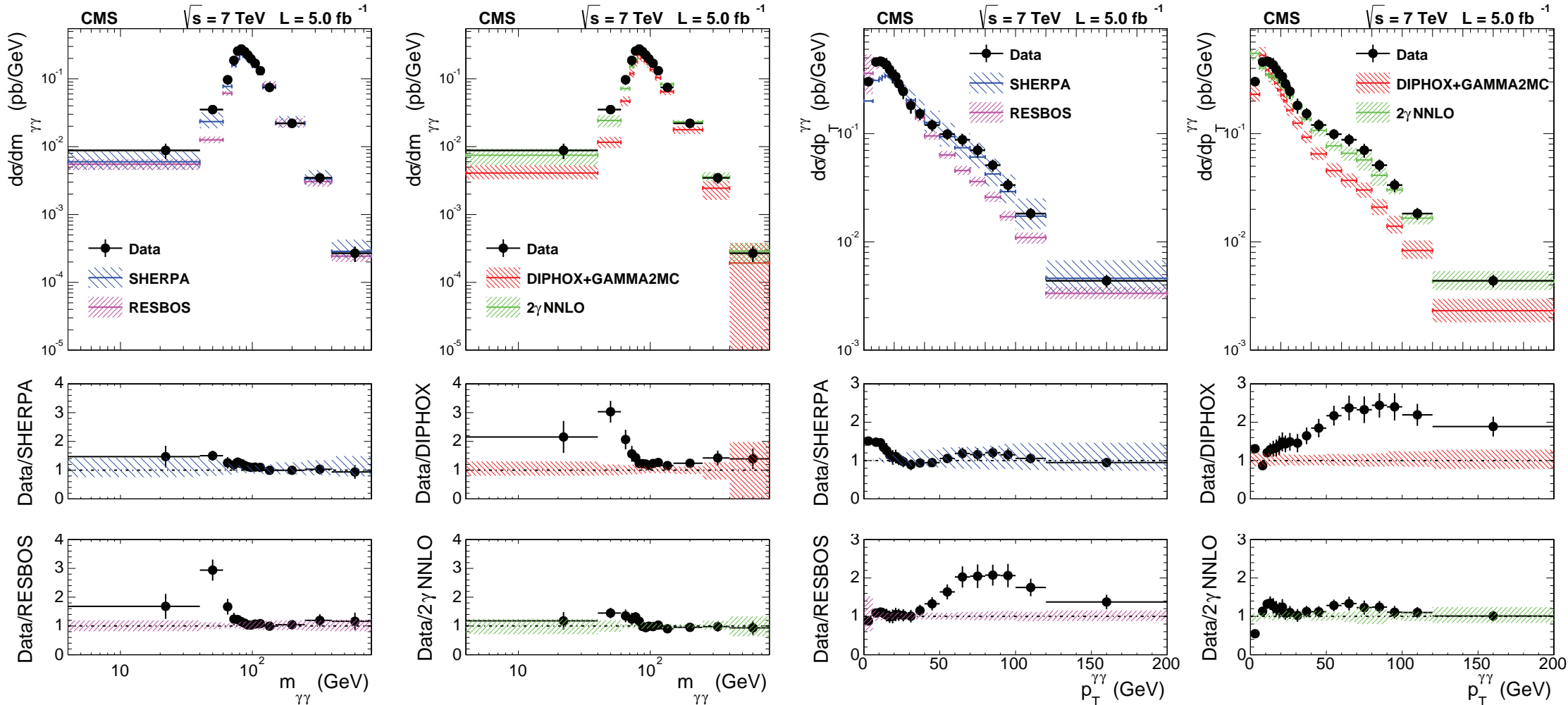
CMS EPJC74-3129



- 2dimensional binned maximum likelihood fit in isolation-1 and isolation-2 plane using templates  
→ extraction of the components: prompt-prompt, prompt-non-prompt, non-prompt-non-prompt

- Experimental uncertainties:
  - (non) prompt template shape 3-5% (5-10%)
  - template statistical 3%, fragmen. compon. 1.5%
  - selection efficiency 2-4%, unfolding 1%
  - luminosity 2.2%
- ⇒ total experimental uncertainty: 8% both  $\gamma$ 's in barrel and 11% for the full acceptance

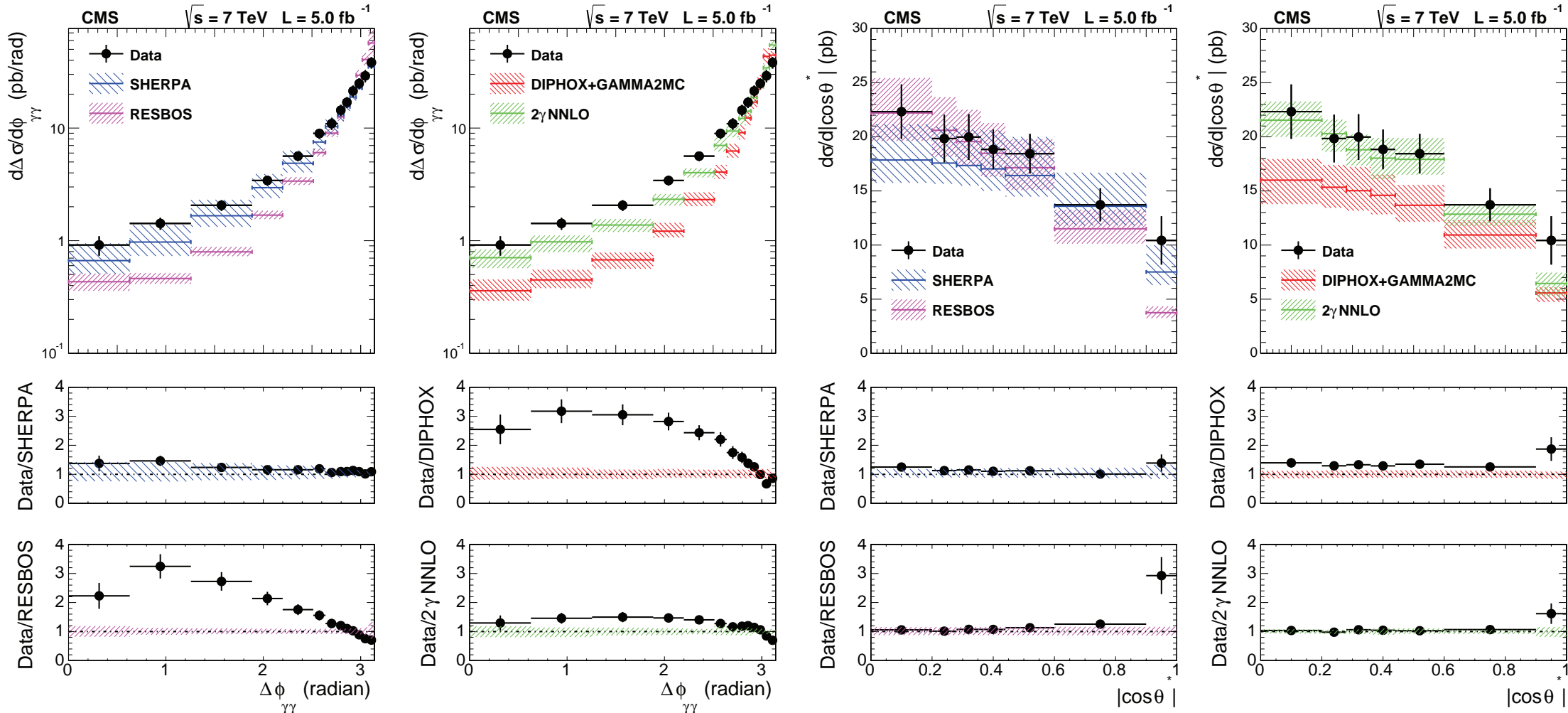
# Diphoton production in $pp$ collisions at $\sqrt{s} = 7 \text{ TeV}$ using $5 \text{ fb}^{-1}$



- Correction factor  $0.95 \pm 0.04$  for underlying event effects
- Comparison to NLO(Diphox+gamma2MC), NLO-resummed(Resbos), 2 $\gamma$ NNLO, Sherpa
- ⇒ Improved description of the data by 2 $\gamma$ NNLO and Sherpa

CMS EPJC74-3129

# Diphoton production in $pp$ collisions at $\sqrt{s} = 7 \text{ TeV}$ using $5 \text{ fb}^{-1}$



- Comparison to NLO(Diphox+gamma2MC), NLO-resummed(Resbos), 2 $\gamma$ NNLO, Sherpa
- ⇒ Improved description of the data by 2 $\gamma$ NNLO and Sherpa

CMS EPJC74-3129

# $V\gamma$ and $V\gamma\gamma$ production

# $W\gamma$ production in $pp$ collisions at $\sqrt{s} = 7$ TeV using $4.6 \text{ fb}^{-1}$

- Measurement of  $l\nu\gamma$  ( $l = e, \mu$ ) in the phase space

$\rightarrow p_T^l > 25 \text{ GeV}, |\eta_l| < 2.47, N_l = 1$

$\rightarrow p_T^\nu > 35 \text{ GeV}$

$\rightarrow E_T^\gamma > 15 \text{ GeV}, |\eta^\gamma| < 2.37, \Delta R(l, \gamma) > 0.7$

and  $\epsilon_h^p < 0.5$  (energy in cone  $R = 0.4$ /photon energy)

$\rightarrow$  jets: anti- $k_t$  algorithm with  $R = 0.4$

$E_T^{\text{jet}} > 30 \text{ GeV}, |\eta^{\text{jet}}| < 4.4, \Delta R(e/\mu/\gamma, \text{jet}) > 0.3$

- Inclusive ( $N_{\text{jet}} \geq 0$ ) and exclusive ( $N_{\text{jet}} = 0$ ) measurements

$\sigma_I(l\nu\gamma) = 2.77 \pm 0.03(\text{stat}) \pm 0.36(\text{syst}) \text{ pb}$

NNLO (arXiv 1407.1618)  $\sigma_I(l\nu\gamma) = 2.658 \pm 0.11 \text{ pb}$

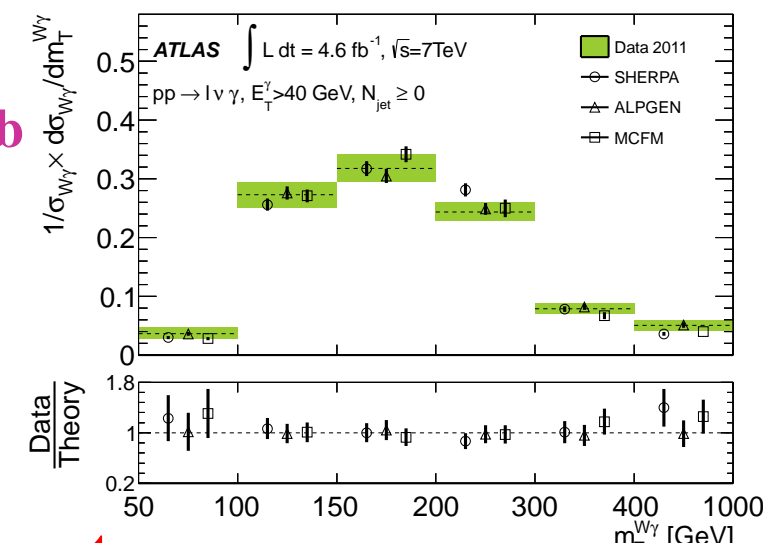
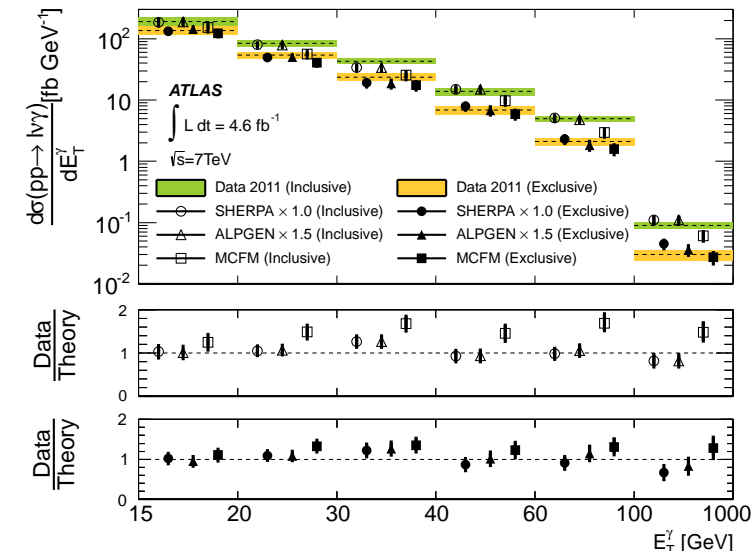
$\sigma_E(l\nu\gamma) = 1.76 \pm 0.03(\text{stat}) \pm 0.22(\text{syst}) \text{ pb}$

NNLO  $\sigma_E(l\nu\gamma) = 1.674^{+0.056}_{-0.064} \text{ pb}$

- NNLO corrections sizeable

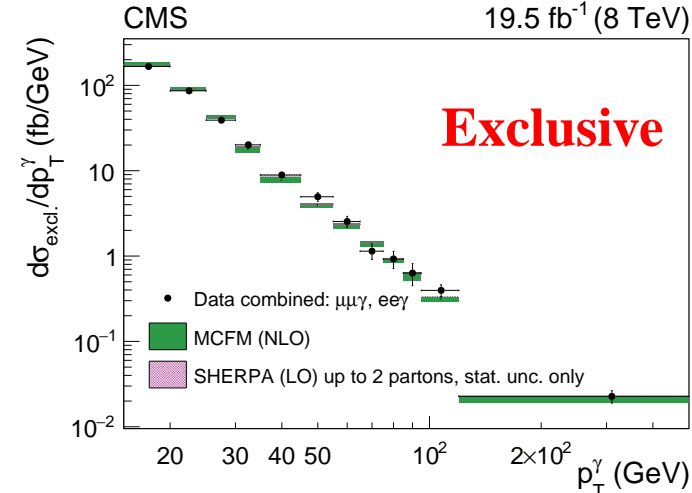
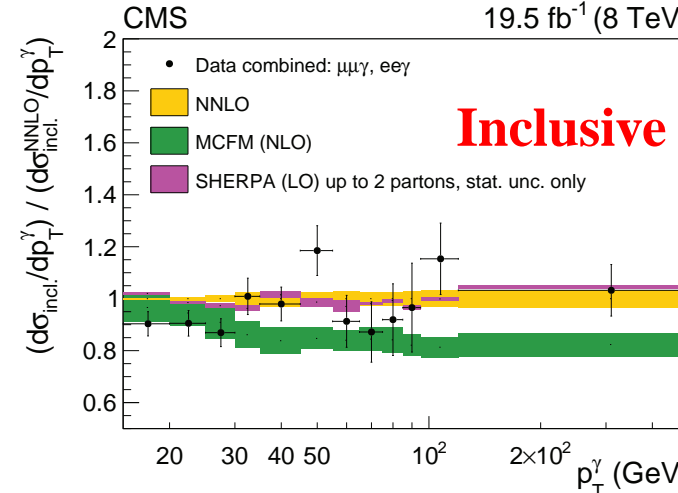
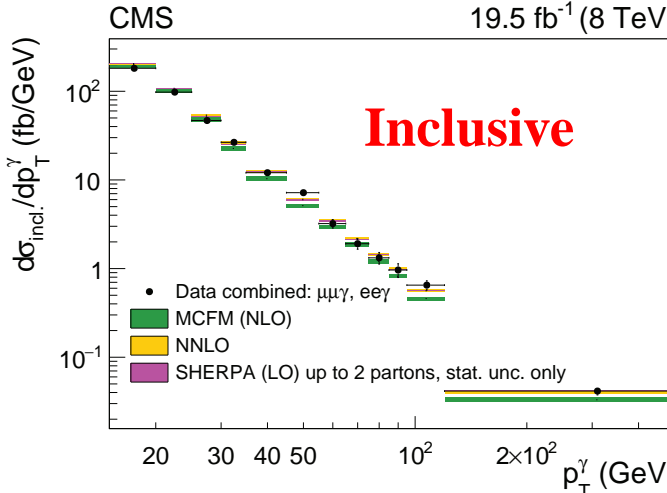
$\rightarrow$  deficit at high  $E_T^\gamma$  with NLO (MCFM)

- Sherpa and Alpgen (scaled to data) describe  $E_T^\gamma, m_T^{W\gamma}$  spectra

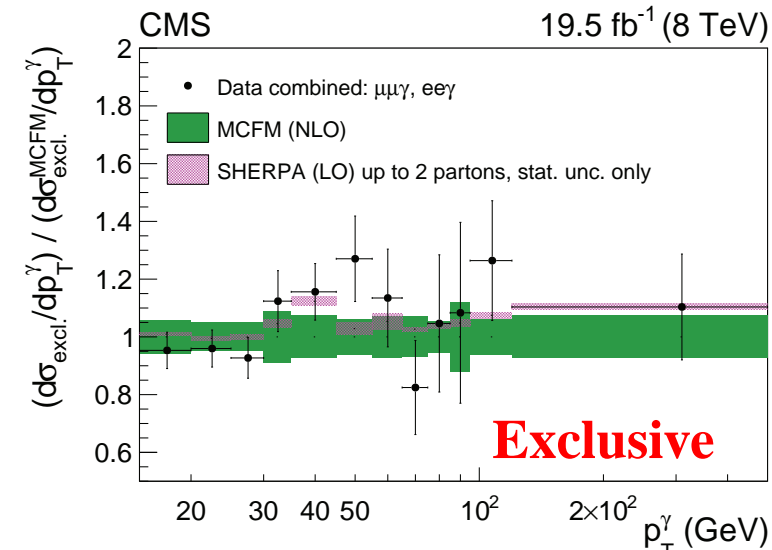


ATLAS PRD87-112003

# $Z(l^+l^-)\gamma$ production in $pp$ collisions at $\sqrt{s} = 8$ TeV using $19.5 \text{ fb}^{-1}$

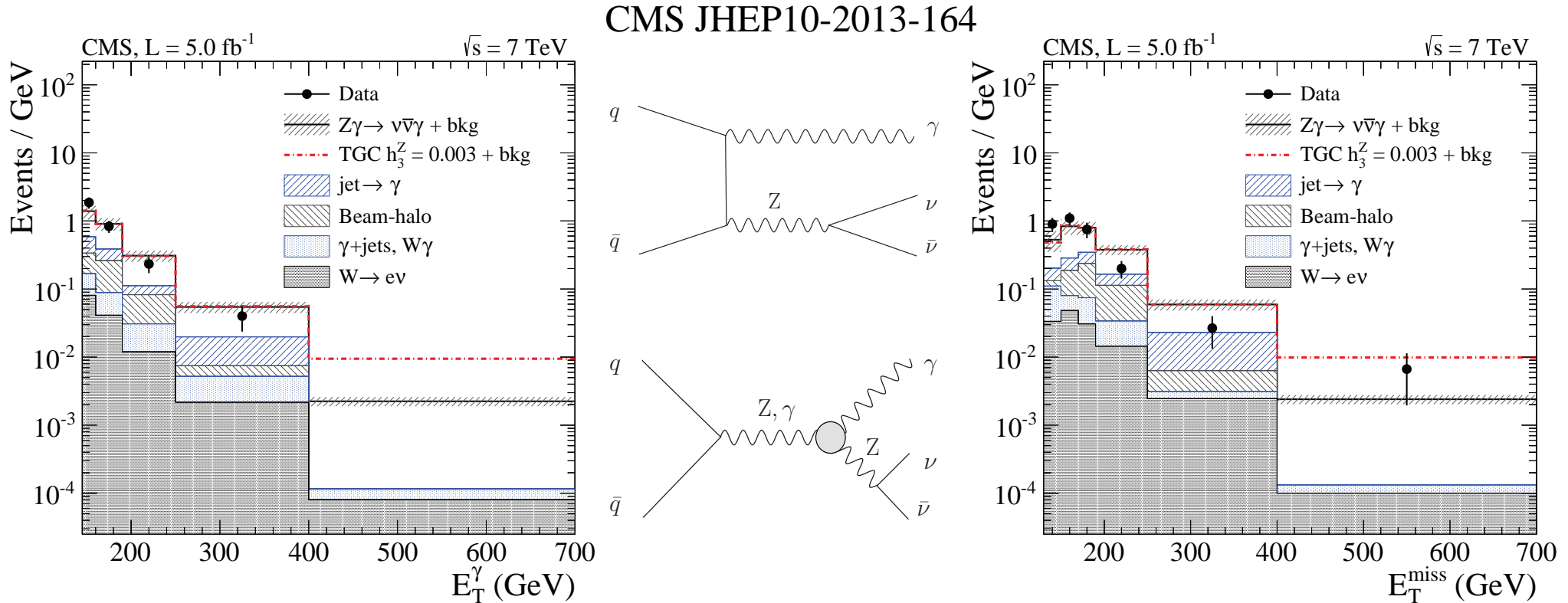


- Measurement of  $l^+l^-\gamma$  ( $l = e, \mu$ ) in the phase space
  - $\rightarrow p_T^l > 20 \text{ GeV}, |\eta_l| < 2.5, m_{l+l^-} > 50 \text{ GeV}$
  - $\rightarrow E_T^\gamma > 15 \text{ GeV}, |\eta^\gamma| < 2.5, \Delta R(l, \gamma) > 0.7$
  - and  $I_{\text{gen}}(R = 0.3) < 5 \text{ GeV}$
  - $\rightarrow$  anti- $k_t$   $R = 0.5$  jets:  $p_T^{\text{jet}} > 30 \text{ GeV}, |\eta^{\text{jet}}| < 2.4$
- Inclusive ( $N_{\text{jet}} \geq 0$ ) and exclusive ( $N_{\text{jet}} = 0$ ) measur.
- $\sigma_{\text{inc}} = 2063 \pm 19(\text{stat}) \pm 98(\text{syst}) \pm 54(\text{lumi}) \text{ fb}$   
NLO  $\sigma_{\text{inc}} = 2100 \pm 120 \text{ fb}$ ; NNLO  $2241 \pm 22(\text{scale}) \text{ fb}$
- $\sigma_{\text{exc}} = 1770 \pm 18(\text{stat}) \pm 115(\text{syst}) \pm 46(\text{lumi}) \text{ fb}$   
NLO  $\sigma_{\text{exc}} = 1800 \pm 120 \text{ fb}$
- $\Rightarrow$  NNLO important to describe inclusive high- $E_T^\gamma$  data



CMS JHEP04-2015-164

# $Z(\nu\bar{\nu})\gamma$ production in $pp$ collisions at $\sqrt{s} = 7$ TeV using $5 \text{ fb}^{-1}$



- Measurement of  $\nu\bar{\nu}\gamma$  for  $E_T^\gamma > 145$  GeV and  $|\eta^\gamma| < 1.4$

$$\sigma(pp \rightarrow Z\gamma + X \rightarrow \nu\bar{\nu}\gamma + X) = 21.1 \pm 4.2(\text{stat}) \pm 4.3(\text{syst}) \pm 0.5(\text{lum}) \text{ fb}$$

NLO (MCFM)  $\sigma = 24.6 \pm 2.5$  fb in agreement with the data

# Evidence of $W\gamma\gamma$ production in $pp$ at $\sqrt{s} = 8$ TeV using $20 \text{ fb}^{-1}$

- Measurement of  $l\nu\gamma\gamma$  ( $l = e, \mu$ ) in the phase space

$\rightarrow p_T^l > 20 \text{ GeV}, |\eta_l| < 2.5, N_l = 1$

$\rightarrow p_T^\nu > 25 \text{ GeV}, m_T > 40 \text{ GeV}$

$\rightarrow E_T^\gamma > 20 \text{ GeV}, |\eta^\gamma| < 2.37, \Delta R(l, \gamma) > 0.7,$

$\Delta R(\gamma, \gamma) > 0.4$  and  $\epsilon_h^p < 0.5$

$\rightarrow$  jets: anti- $k_t$  algorithm with  $R = 0.4$

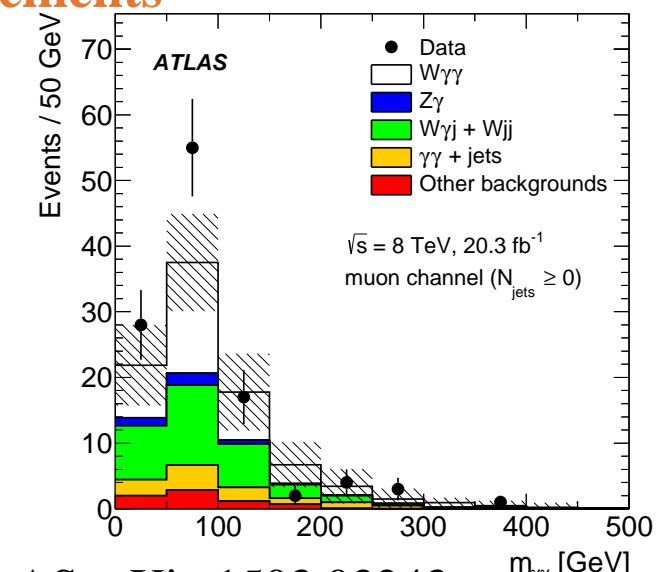
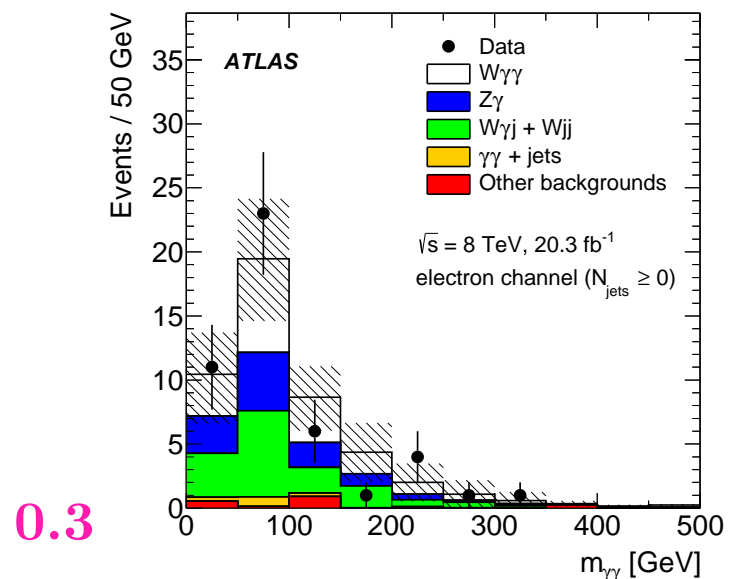
$E_T^{\text{jet}} > 30 \text{ GeV}, |\eta^{\text{jet}}| < 4.4, \Delta R(e/\mu/\gamma, \text{jet}) > 0.3$

- Inclusive ( $N_{\text{jet}} \geq 0$ ) and exclusive ( $N_{\text{jet}} = 0$ ) measurements

	$\sigma^{\text{fid}}$ [fb]	$\sigma^{\text{MCFM}}$ [fb]
Inclusive ( $N_{\text{jet}} \geq 0$ )		
$\mu\nu\gamma\gamma$	$7.1^{+1.3}_{-1.2}$ (stat.) $\pm 1.5$ (syst.) $\pm 0.2$ (lumi.)	
$e\nu\gamma\gamma$	$4.3^{+1.8}_{-1.6}$ (stat.) $\pm 1.9$ (syst.) $\pm 0.2$ (lumi.)	$2.90 \pm 0.16$
$\ell\nu\gamma\gamma$	$6.1^{+1.1}_{-1.0}$ (stat.) $\pm 1.2$ (syst.) $\pm 0.2$ (lumi.)	
Exclusive ( $N_{\text{jet}} = 0$ )		
$\mu\nu\gamma\gamma$	$3.5 \pm 0.9$ (stat.) $\pm 1.1$ (syst.) $\pm 0.1$ (lumi.)	
$e\nu\gamma\gamma$	$1.9^{+1.4}_{-1.1}$ (stat.) $\pm 1.1$ (syst.) $\pm 0.1$ (lumi.)	$1.88 \pm 0.20$
$\ell\nu\gamma\gamma$	$2.9^{+0.8}_{-0.7}$ (stat.) $\pm 1.0$ (syst.) $\pm 0.1$ (lumi.)	

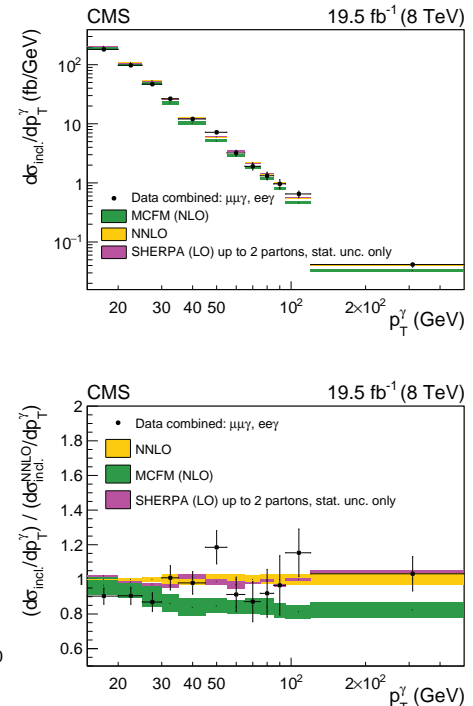
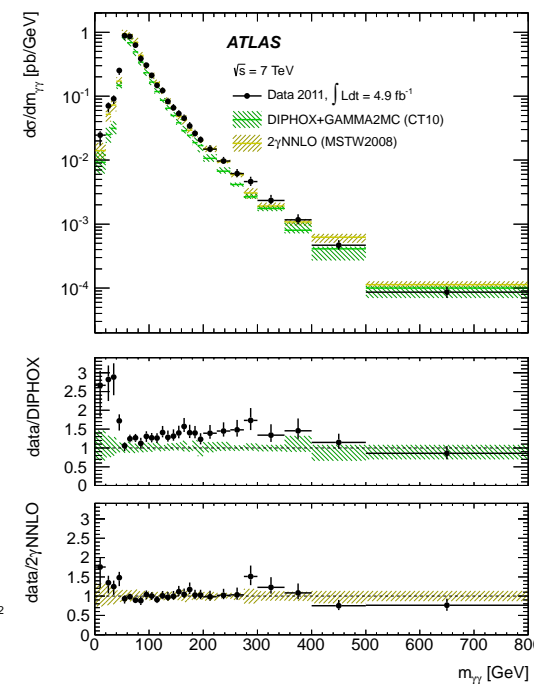
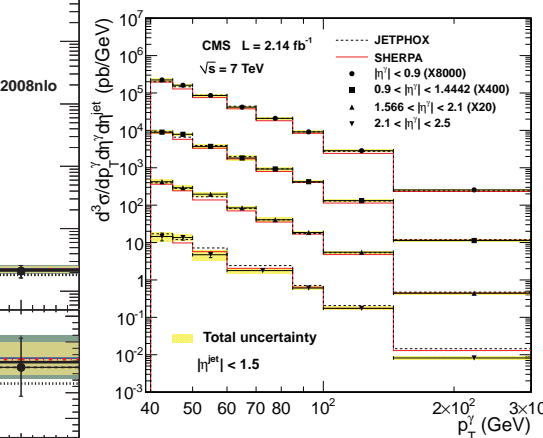
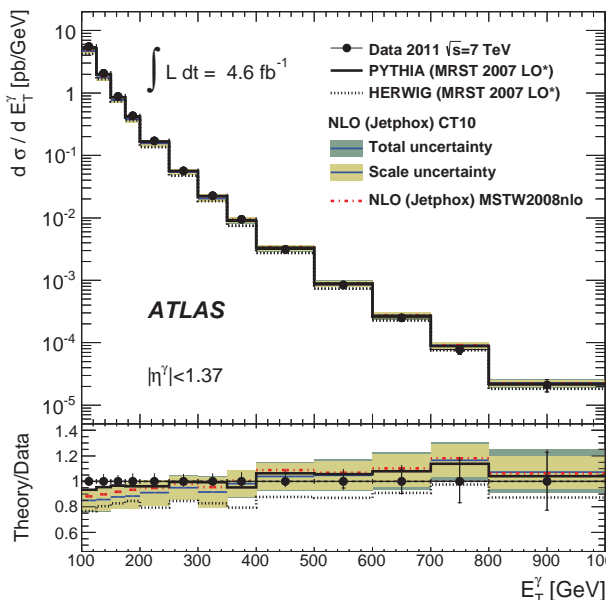
- Measurement of  $\sigma_{\text{inc}}$  higher than NLO by  $1.9\sigma$

$\rightarrow$  NNLO corrections to the rescue? (as for  $W\gamma$ )



ATLAS arXiv 1503.03243

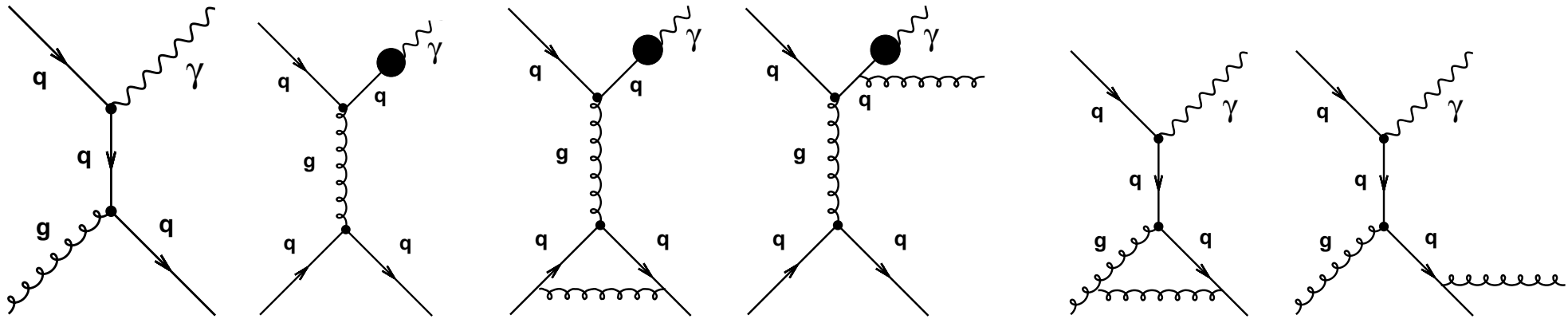
## Summary



- Exploration of isolated photon production in  $pp$  collisions up to  $E_T^\gamma \sim 1$  TeV  
⇒ additional experimental information on the gluon density in the proton
- Measurement of the dynamics of photon+jet and diphoton production  
⇒ understanding the background to Higgs into  $\gamma\gamma$  in terms of pQCD
- Measurement of  $W\gamma$ ,  $Z\gamma$  and  $W\gamma\gamma$  production  
⇒ testing the electroweak sector of the SM
- Overall, perturbative QCD succeeds in describing the data!
- But this is not yet the end: more 2012 data results +forthcoming LHC run at  $\sqrt{s} = 13$  TeV

**Backup**

## NLO QCD calculations for inclusive photon production



$$\sigma_{pp \rightarrow \gamma + X} = \sum_{i,j,a} \int_0^1 dx_1 f_{i/p}(x_1, \mu_F^2) \int_0^1 dx_2 f_{j/p}(x_2, \mu_F^2) \hat{\sigma}_{ij \rightarrow \gamma a^+}$$

$$\sum_{i,j,a,b} \int_{z_{min}}^1 dz D_a^\gamma(z, \mu_f^2) \int_0^1 dx_1 f_{i/p}(x_1, \mu_F^2) \int_0^1 dx_2 f_{j/p}(x_2, \mu_F^2) \hat{\sigma}_{ij \rightarrow ab}$$

- The calculations includes NLO corrections for both direct-photon and fragmentation contributions; beware the components are not distinguishable beyond LO
- The calculations implement the photon isolation requirement at “parton” level:  $E_T^{iso}$  calculated with the (few) final-state partons in the perturbative QCD calculation

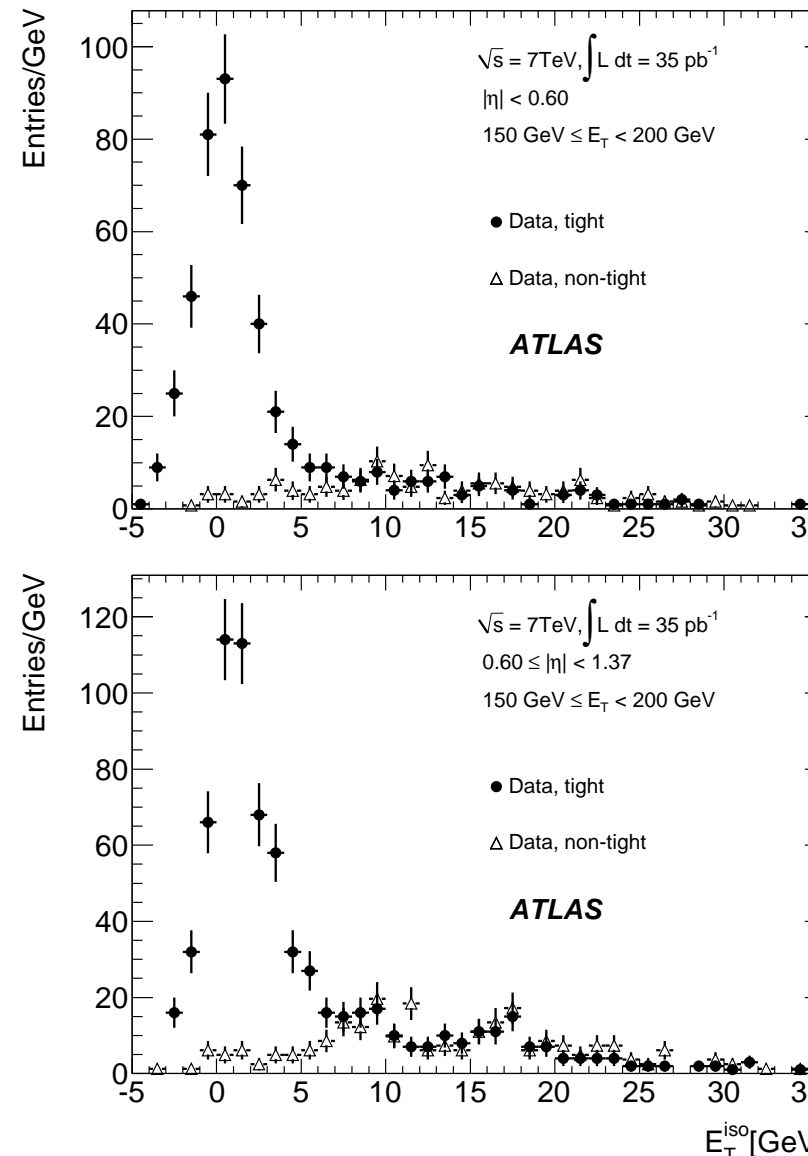
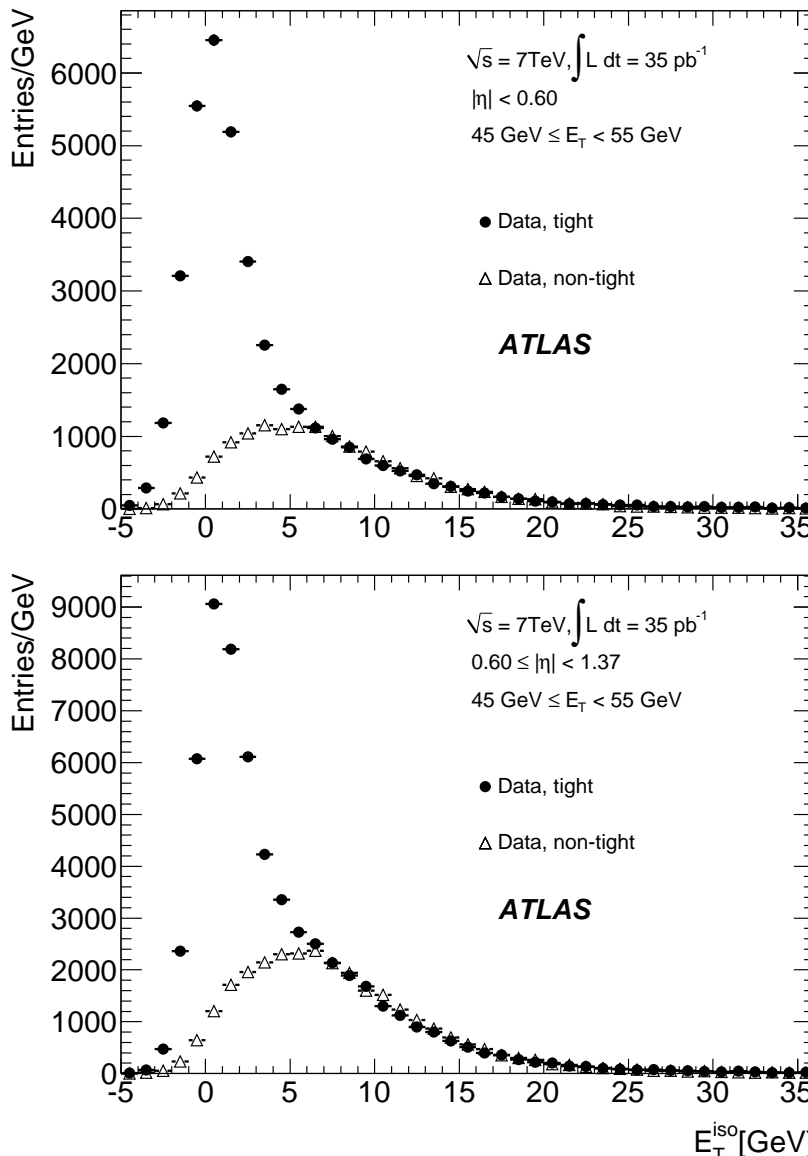
## NLO QCD calculations for inclusive photon production

$$\sigma_{pp \rightarrow \gamma + X} = \sum_{i,j,a} \int_0^1 dx_1 f_{i/p}(x_1, \mu_F^2) \int_0^1 dx_2 f_{j/p}(x_2, \mu_F^2) \hat{\sigma}_{ij \rightarrow \gamma a} +$$

$$\sum_{i,j,a,b} \int_{z_{min}}^1 dz D_a^\gamma(z, \mu_f^2) \int_0^1 dx_1 f_{i/p}(x_1, \mu_F^2) \int_0^1 dx_2 f_{j/p}(x_2, \mu_F^2) \hat{\sigma}_{ij \rightarrow ab}$$

- $\mu_R = \mu_F = \mu_f = E_T^\gamma$
- proton PDF set → CTEQ6.6, CT10, MSTW2008
- fragmentation function → BFG set II  
→ Corrections for hadronisation and underlying event needed
- Theoretical uncertainties:  
→ higher-order terms (beyond NLO); estimated by varying  $\mu_R, \mu_F, \mu_f$   
→ PDF-induced uncertainties; estimated using set of PDF eigenvectors  
→ uncertainty on  $\alpha_s$ ; estimated taking into account correlation with PDF  
→ uncertainty on non-perturbative correction; estimated with different MC and tunes

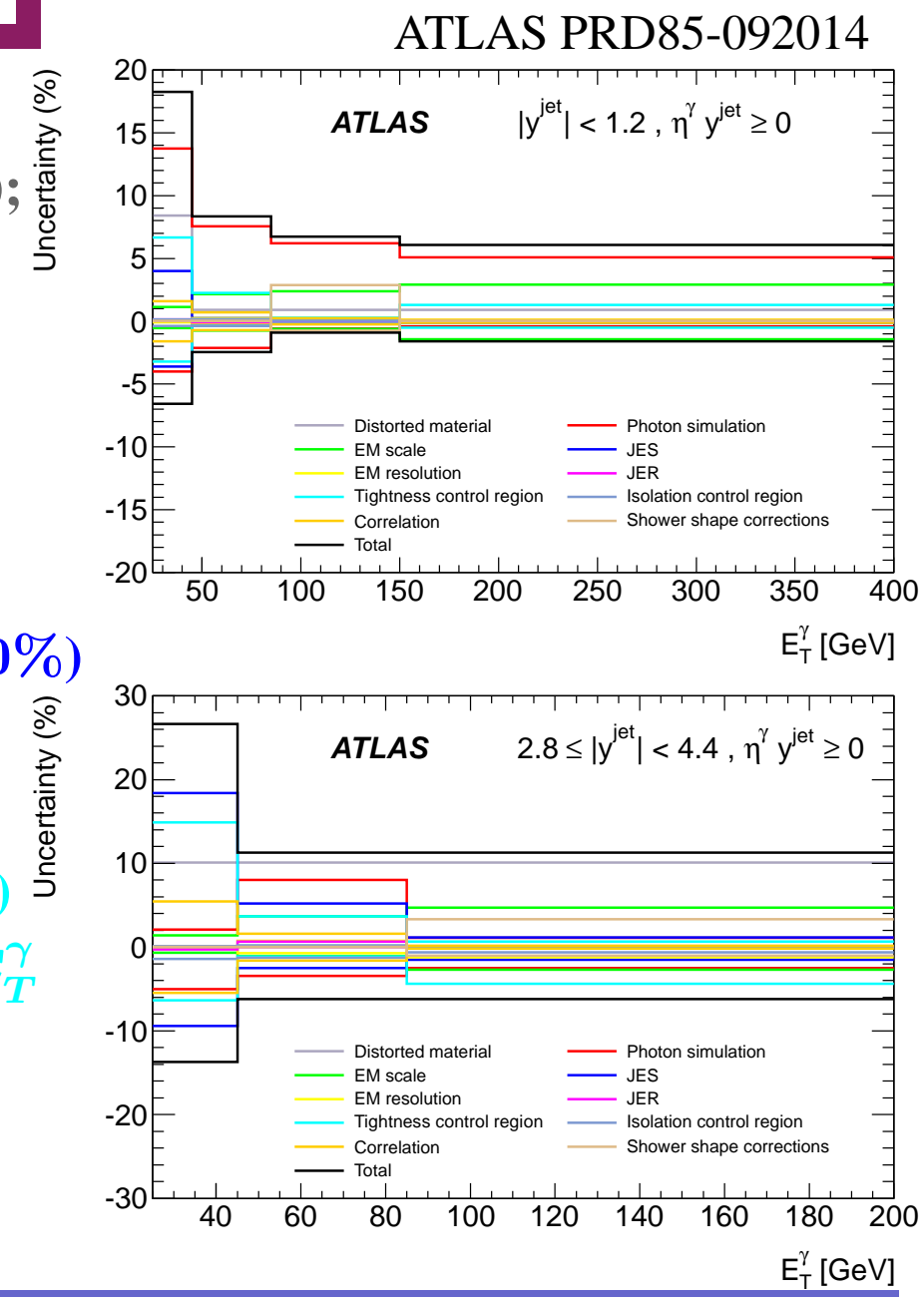
# Inclusive isolated photon production in $pp$ collisions at $\sqrt{s} = 7 \text{ TeV}$



ATLAS PLB706-150 (aux. mat. STDM-2011-04)

## Systematic experimental uncertainties

- Distorted material: simulation of the detector geometry (photon conversions and EM showers); 1-23% depending on  $E_T^\gamma$  and  $|y^{\text{jet}}|$
- Photon simulation: PYTHIA vs HERWIG; direct-photon vs photons radiated off quarks; 4-16% depending on  $E_T^\gamma$  and  $|y^{\text{jet}}|$
- Photon energy scale and resolution: negligible
- Jet energy scale: mostly 1st bin  $E_T^\gamma$ ; 3-7% (9-20%) for central/forward (very forward) jets
- Tightness control region: using a different set of background identification criteria; 5% (12%) for central (forward) jets and decreasing with  $E_T^\gamma$
- Trigger efficiency: 0.6% (0.4%) for  $E_T^\gamma < 45 \text{ GeV}$  ( $> 45 \text{ GeV}$ )
- Luminosity uncertainty: 3.4%



## $\gamma + \text{jet}$ production in $pp$ collisions

- Ratio of cross sections for different angular orientations between the photon and the leading jet

$\rightarrow |\eta^\gamma| < 0.9$

$\rightarrow$  two regions in (leading jet)  $|\eta^{\text{jet}}|$ :  
 $[0,1.5]$ ,  $[1.5,2.5]$

$\rightarrow$  SS ( $\eta^\gamma \cdot \eta^{\text{jet}} > 0$ ) and OS ( $\eta^\gamma \cdot \eta^{\text{jet}} < 0$ )

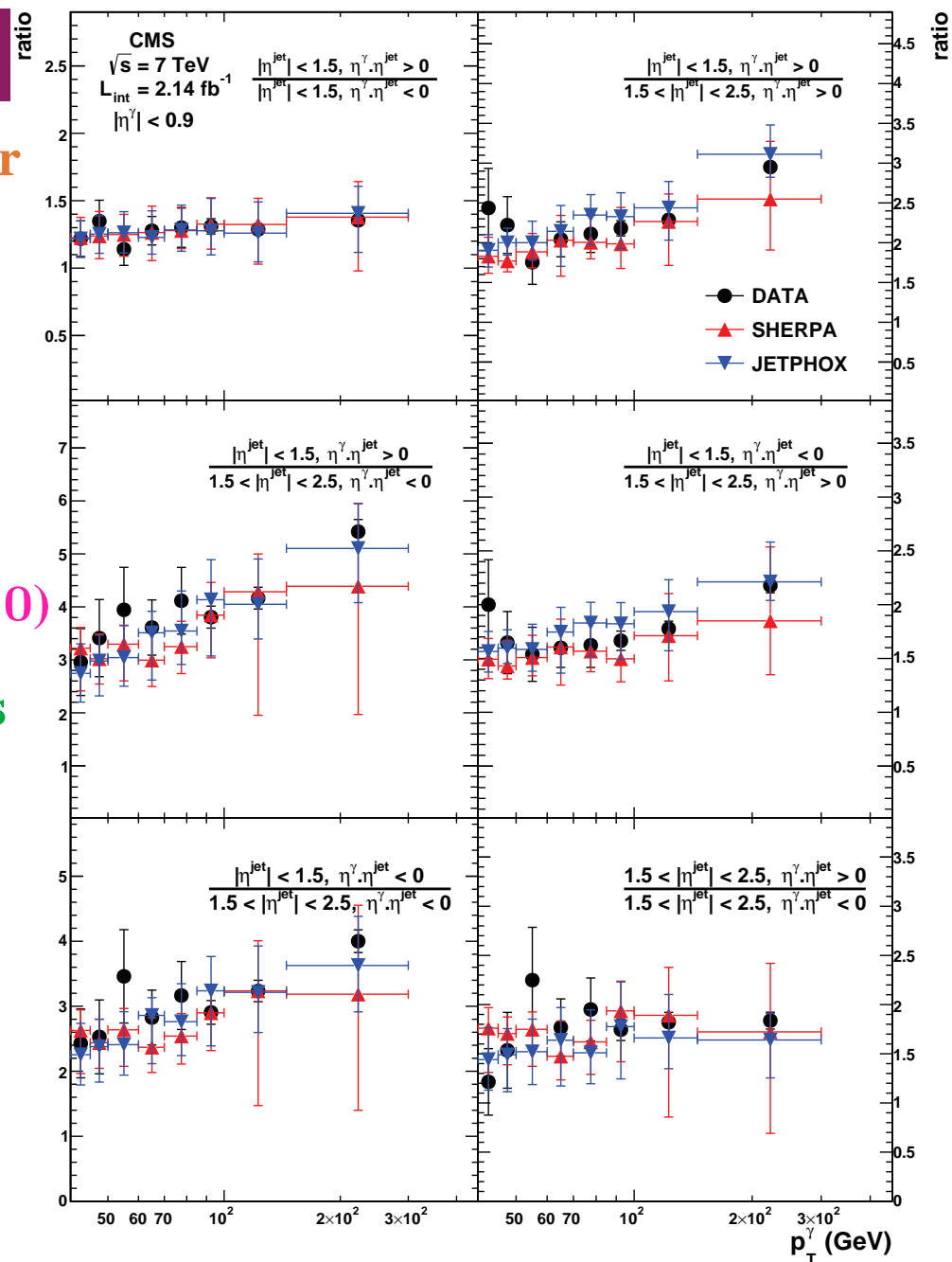
- Reduced uncertainties due to cancellations

- Comparison to Sherpa and NLO QCD

Jetphox calculations

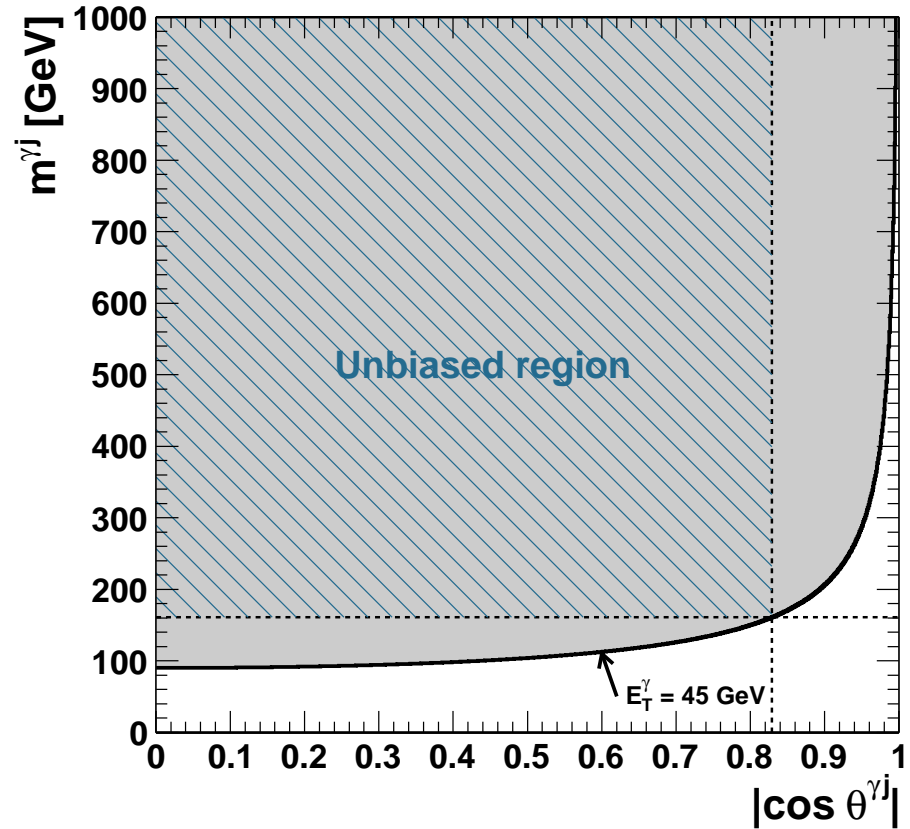
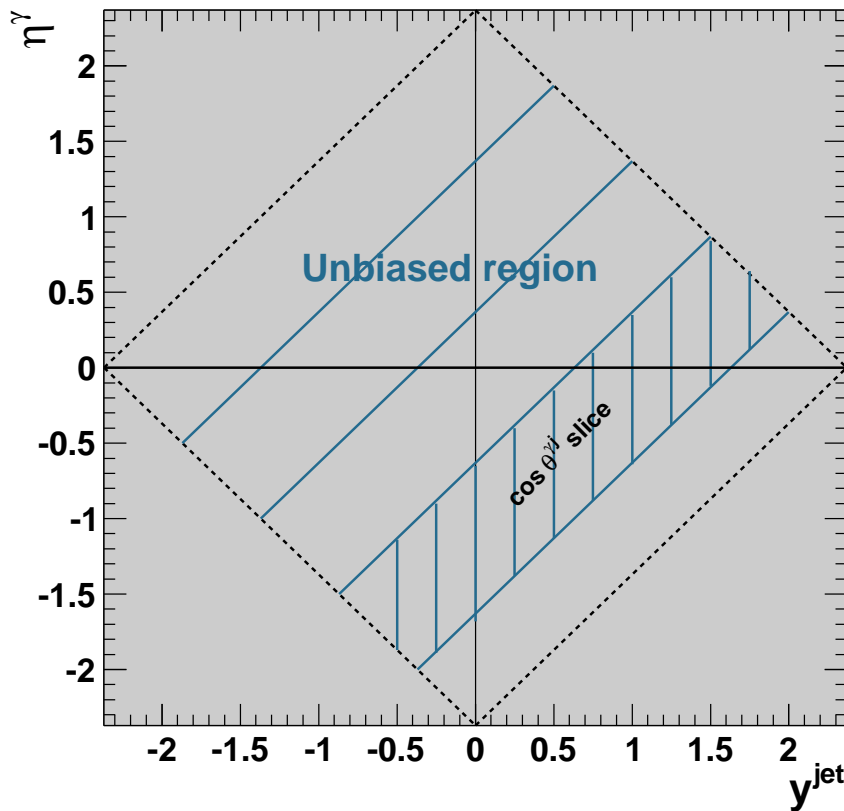
$\rightarrow$  consistent with the data

- All in all, multi-leg Sherpa is performing as well as NLO



CMS JHEP06-2014-009

## Selection of unbiased region to measure the $m^{\gamma j}$ and $\theta^{\gamma j}$ distributions

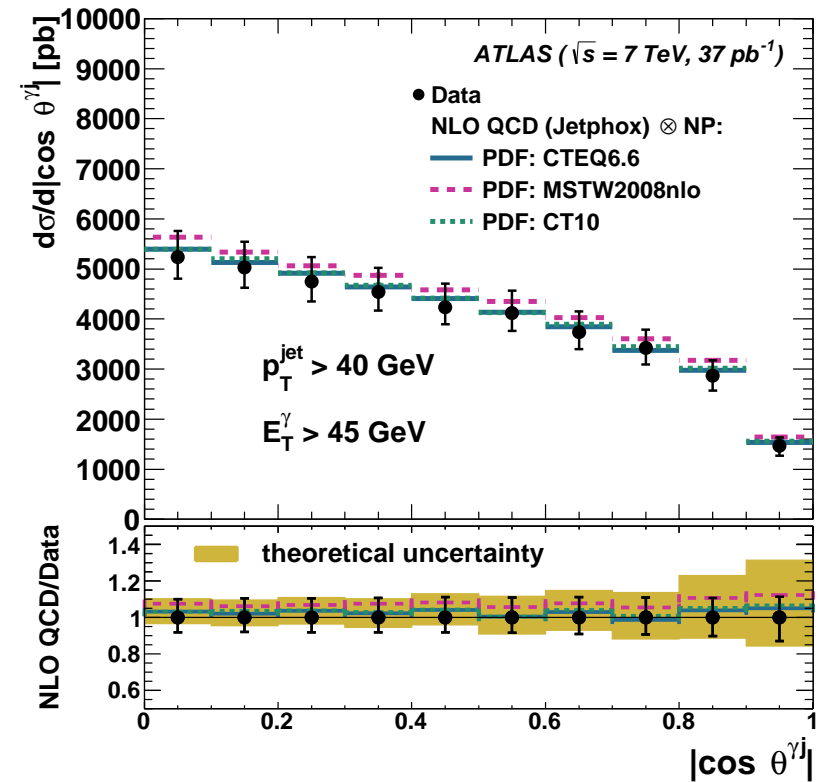
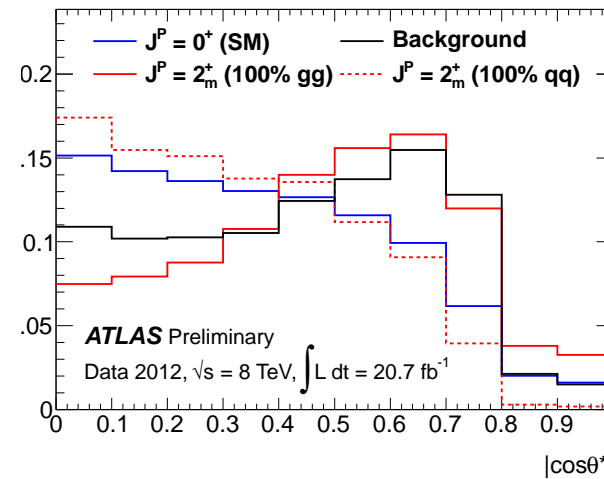
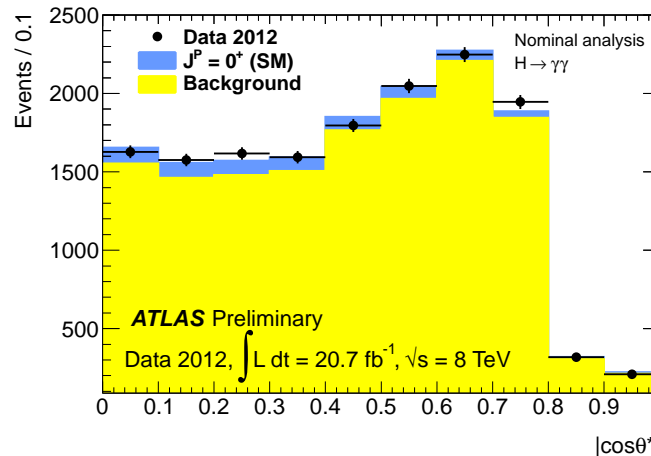


$$|\eta^\gamma + y_{\text{jet}}^{\text{jet}}| < 2.37 , \quad |\cos \theta^{\gamma j}| < 0.83 , \quad m^{\gamma j} > 161 \text{ GeV}$$

- First two requirements: avoiding the bias induced by cuts on  $\eta^\gamma$  and  $y_{\text{jet}}^{\text{jet}}$ ; slices of  $\cos \theta^{\gamma j}$  have the same length along the  $\eta^\gamma + y_{\text{jet}}^{\text{jet}}$  axis
- Third requirement: avoiding the bias due to  $E_T^\gamma > 45 \text{ GeV}$  in  $(|\cos \theta^{\gamma j}|, m^{\gamma j})$  plane

# Understanding the $\gamma + \text{jet}$ background to $H \rightarrow \gamma\gamma$

ATLAS NPB875-483



- $\gamma + \text{jet}$  production is the 2nd largest source of background to  $H \rightarrow \gamma\gamma$
- $\cos \theta^*$  distribution used to determine the spin of the Higgs-like particle discovered in 2012
- Measurement of  $d\sigma/d|\cos \theta^{\gamma j}|$  without additional requirements (no cut on  $m^{\gamma j}$ !)
- Good description of the measurement by NLO QCD calculations  
⇒ precise understanding of this background both in normalization and shape in terms of the Standard Model

## Rapidity distributions in $\gamma + \text{jet}$ events in $pp$ collisions at $\sqrt{s} = 7 \text{ TeV}$

- Measurement of  $1/\sigma \cdot d\sigma/dy$  for the production of a photon with a single jet as a function of → photon ( $y_\gamma$ ) and jet ( $y_{\text{jet}}$ ) rapidities

$$\rightarrow y_{\text{sum}} = |y_\gamma + y_{\text{jet}}|/2$$

$$\rightarrow y_{\text{dif}} = |y_\gamma - y_{\text{jet}}|/2$$

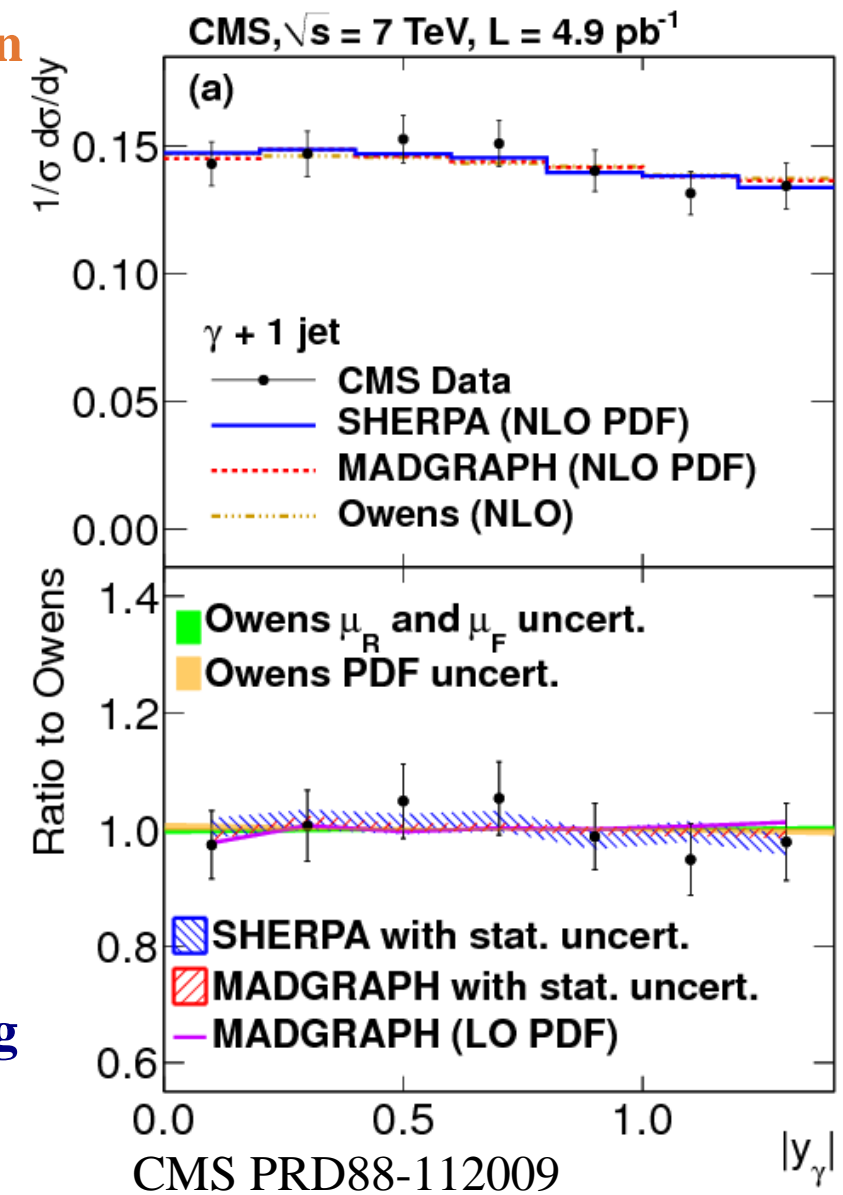
in the phase-space region defined by

$$\rightarrow p_T^\gamma > 40 \text{ GeV} \text{ and } |\eta^\gamma| < 1.44$$

$$\rightarrow p_T^{\text{jet}} > 30 \text{ GeV} \text{ and } |\eta^{\text{jet}}| < 2.4$$

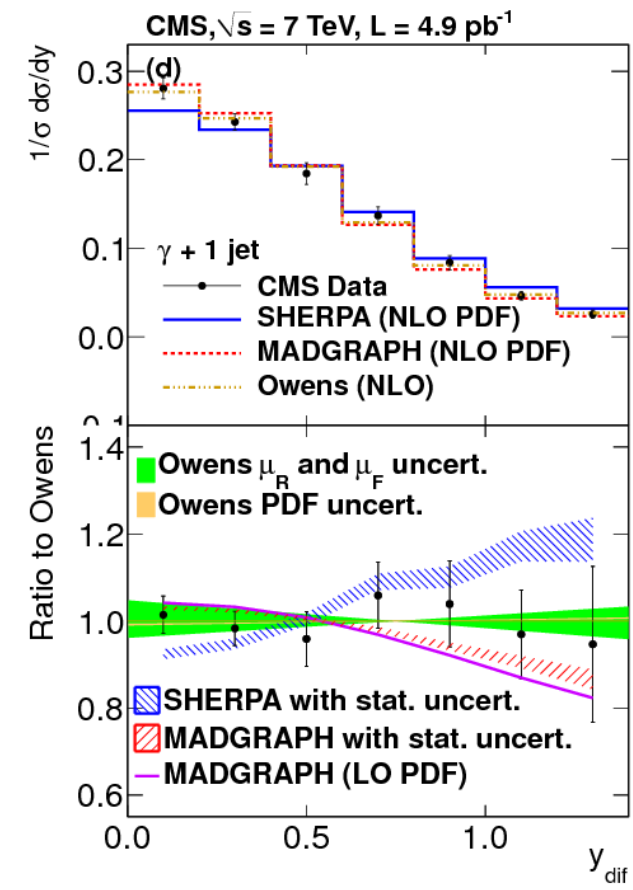
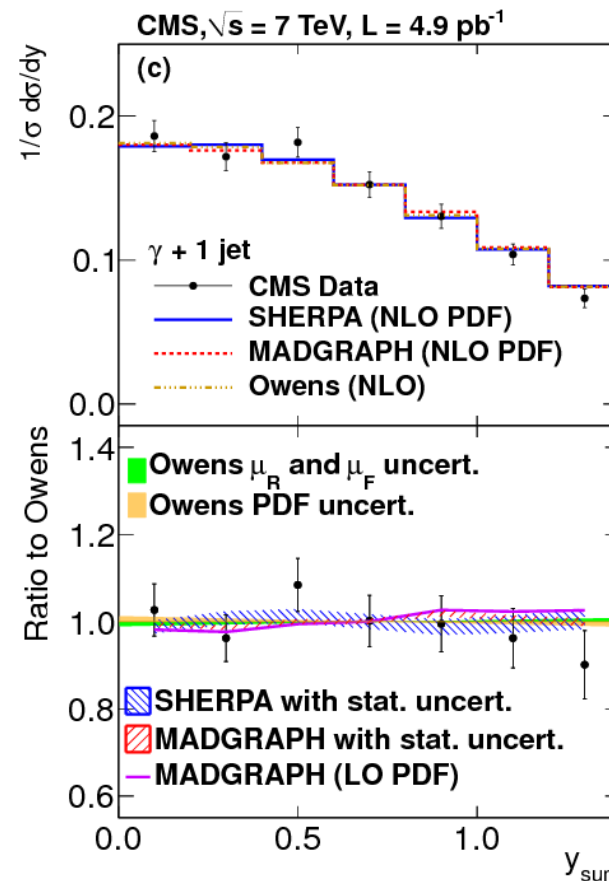
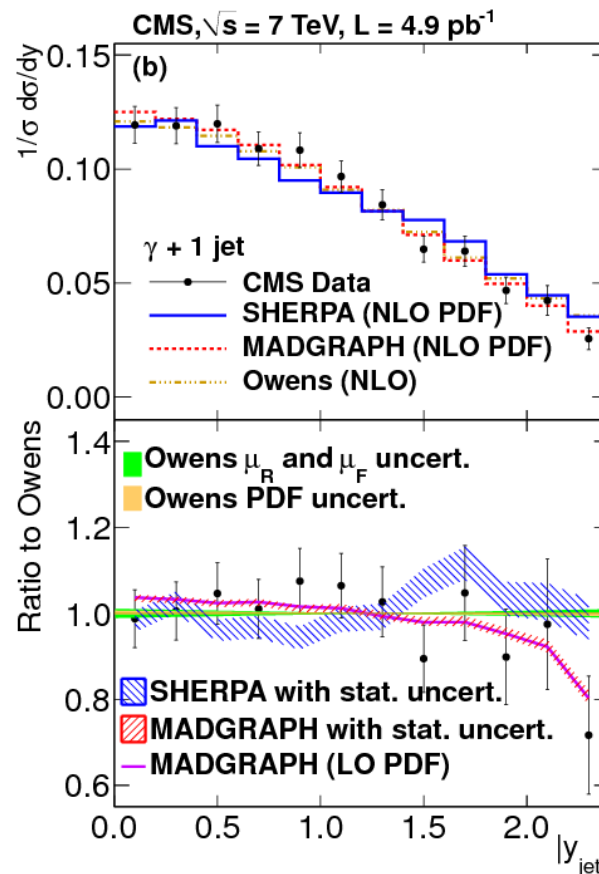
using the anti- $k_t$  algorithm with  $R = 0.5$  and  $\mathcal{L} = 4.9 \text{ pb}^{-1}$

- Reduced experimental and theoretical uncertainties (normalised cross sections)
- Comparison to NLO QCD (Owens) and multi-leg MC (Sherpa, MadGraph) calculations  
→ consistent with the data



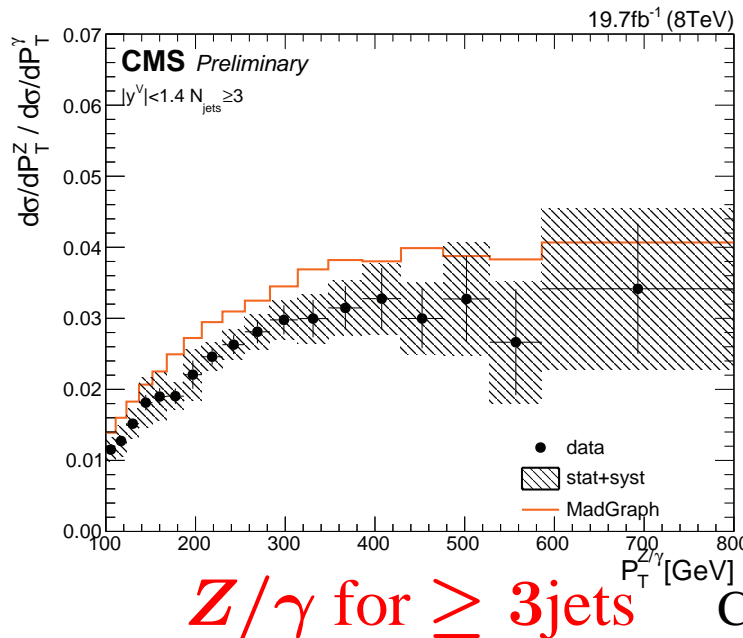
# Rapidity distributions in $\gamma +$ jet events in $pp$ collisions at $\sqrt{s} = 7$ TeV

CMS PRD88-112009



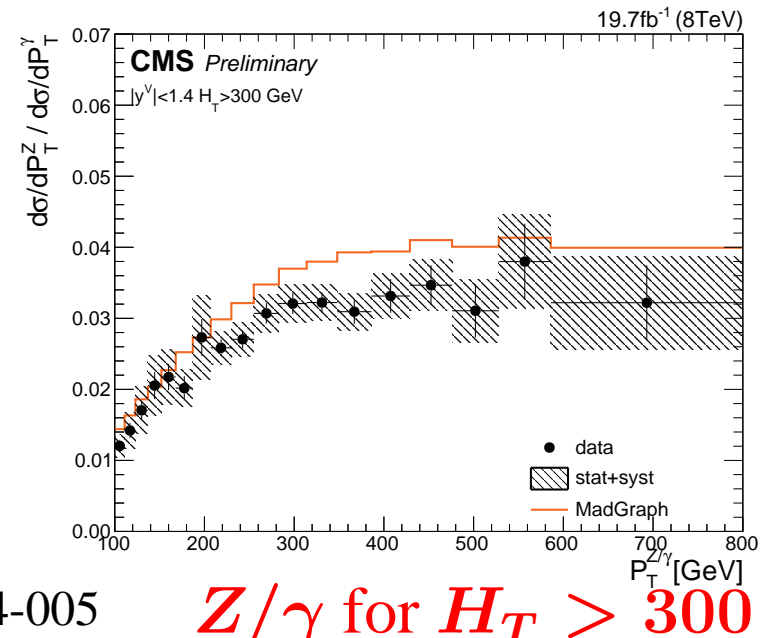
- Comparison to NLO QCD (Owens) and multi-leg MC (Sherpa, MadGraph) calculations
  - NLO QCD describes the data in all cases
  - differences in  $y_{\text{diff}}$  between MadGraph and Sherpa, but statistical precision insufficient to discriminate between them

# $\sigma(Z + \text{jets})/\sigma(\gamma + \text{jets})$ in $pp$ collisions at $\sqrt{s} = 8 \text{ TeV}$

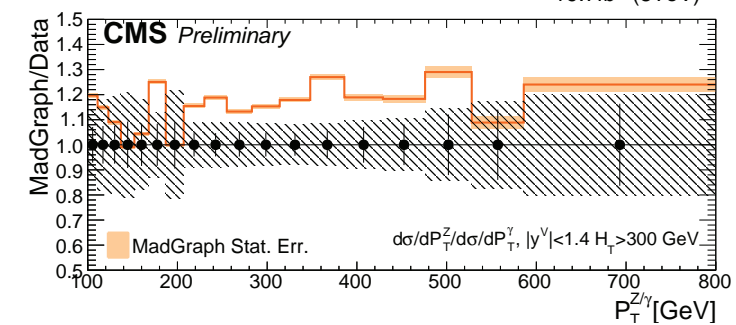
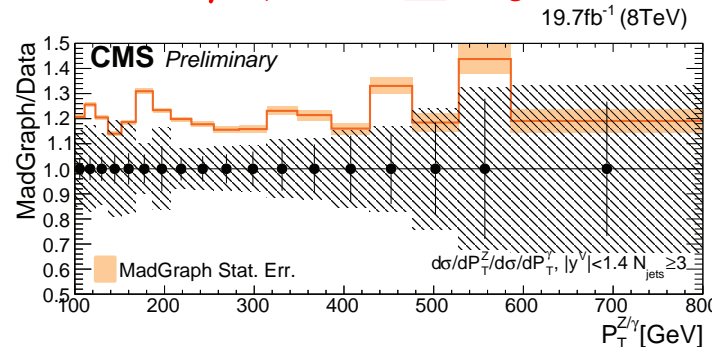


$Z/\gamma$  for  $\geq 3$  jets

CMS PAS SMP-14-005

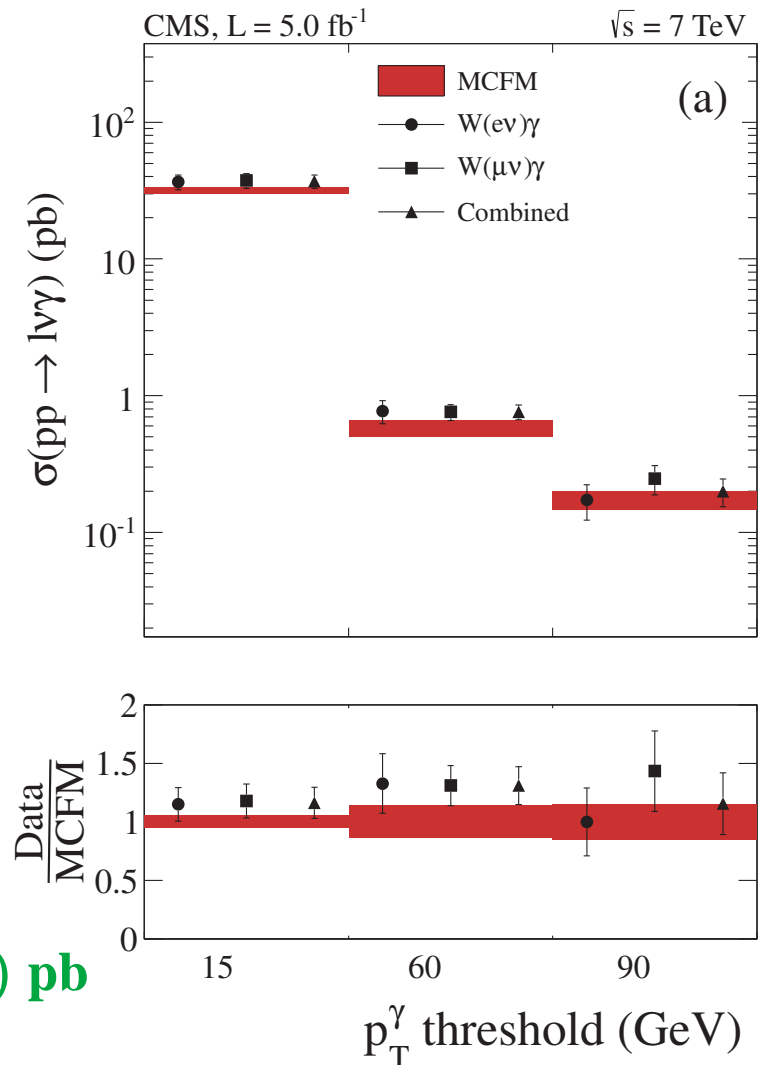
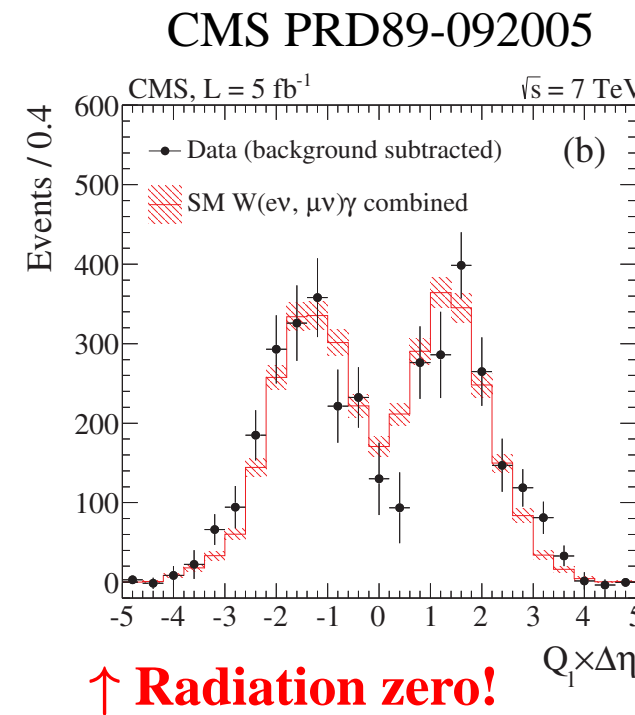
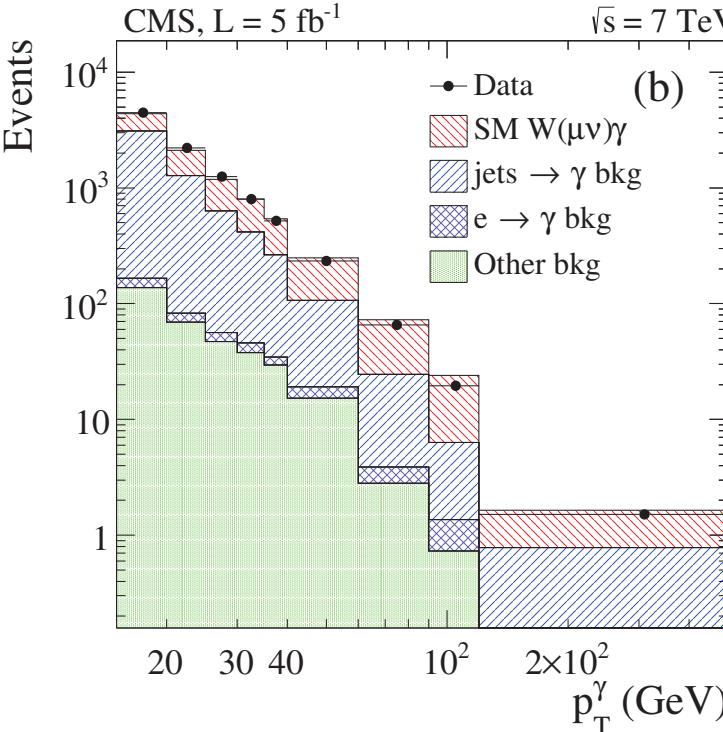


$Z/\gamma$  for  $H_T > 300 \text{ GeV}$



- Observation of a turn-on of the ratio and plateau around  $p_T \simeq 300\text{-}350 \text{ GeV}$   
 → good description of the shape by MadGraph (but  $\sim 20\%$  higher than data)  
 ⇒ These ratios are suitable to predict invisible decays of  $Z$  for searches

# $W\gamma$ production in $pp$ collisions at $\sqrt{s} = 7$ TeV using $5 \text{ fb}^{-1}$



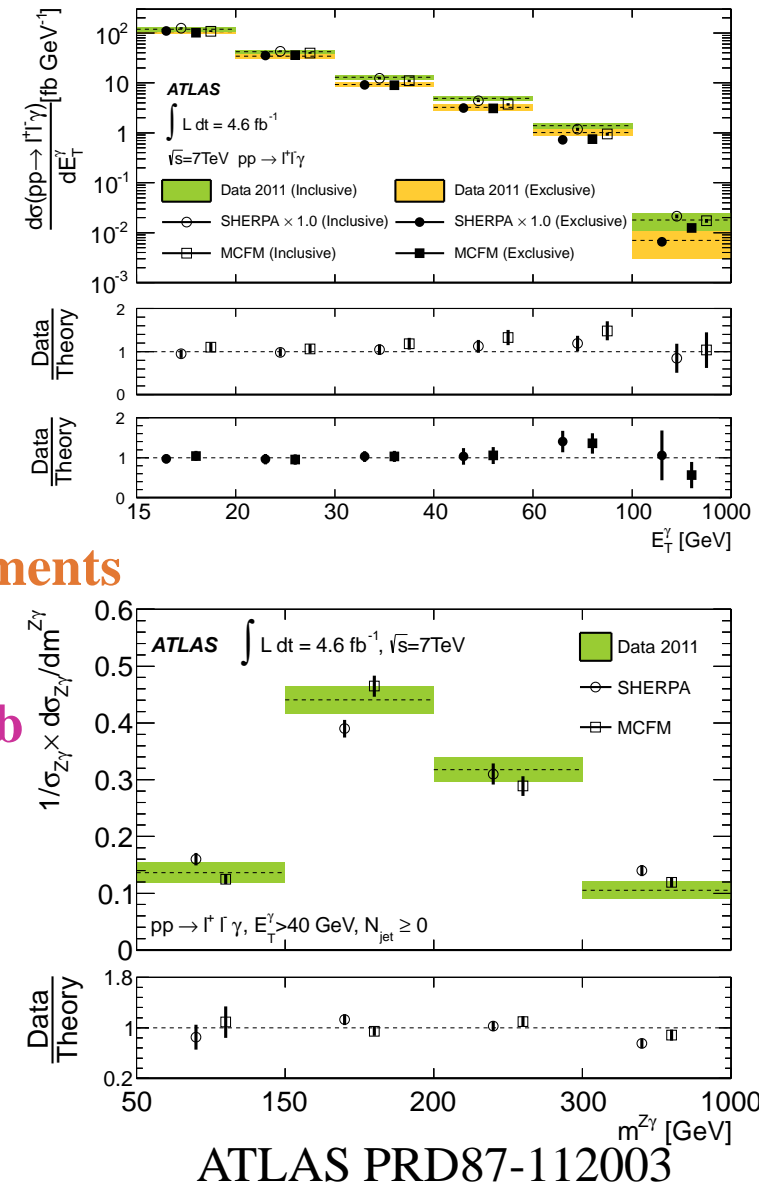
- Measurement of  $l\nu\gamma$  ( $l = e, \mu$ ) for  $p_T^\gamma > 15 \text{ GeV}$  and  $\Delta R(l, \gamma) > 0.7$

$\sigma(W\gamma) \times B(W \rightarrow l\nu) = 37.0 \pm 0.8(\text{stat}) \pm 4.1(\text{syst}) \text{ pb}$   
 NLO (MCFM)  $\sigma \times B = 31.8 \pm 1.8 \text{ pb}$

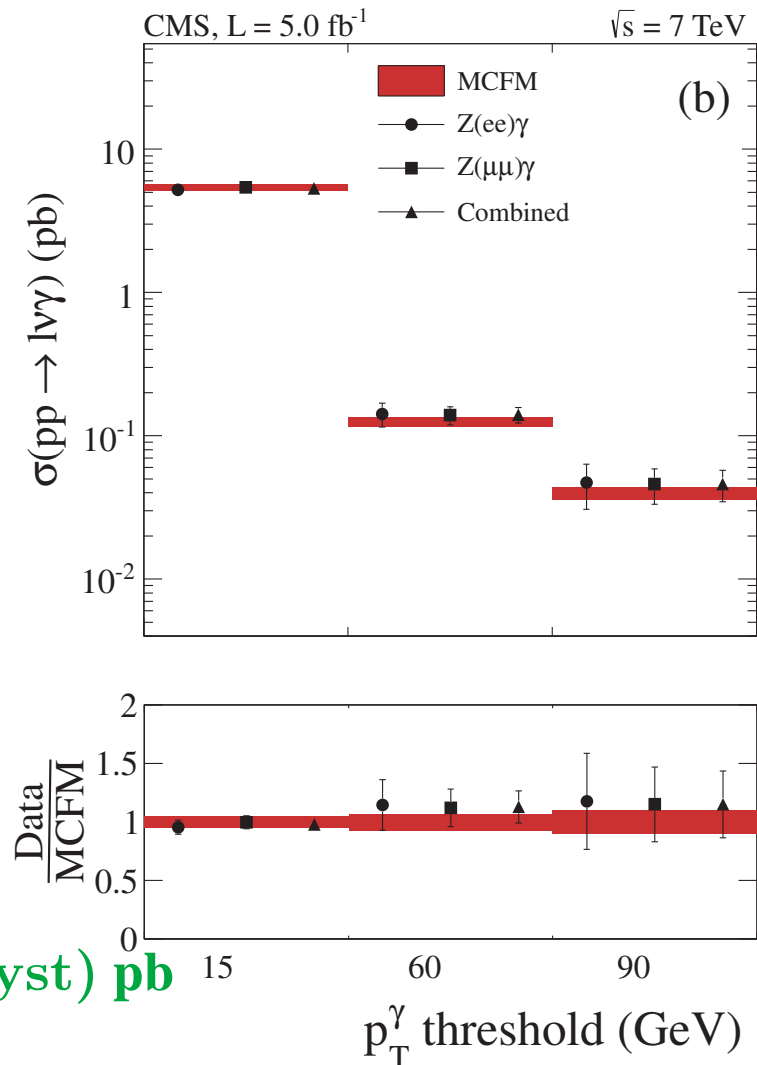
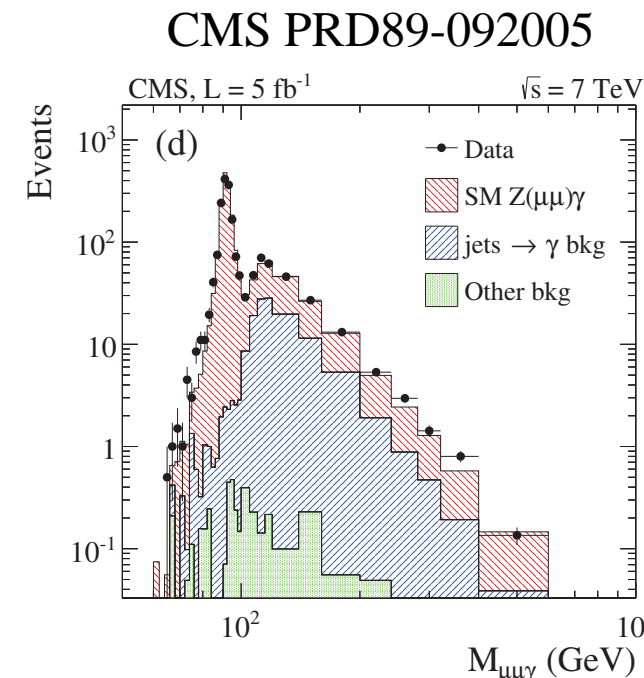
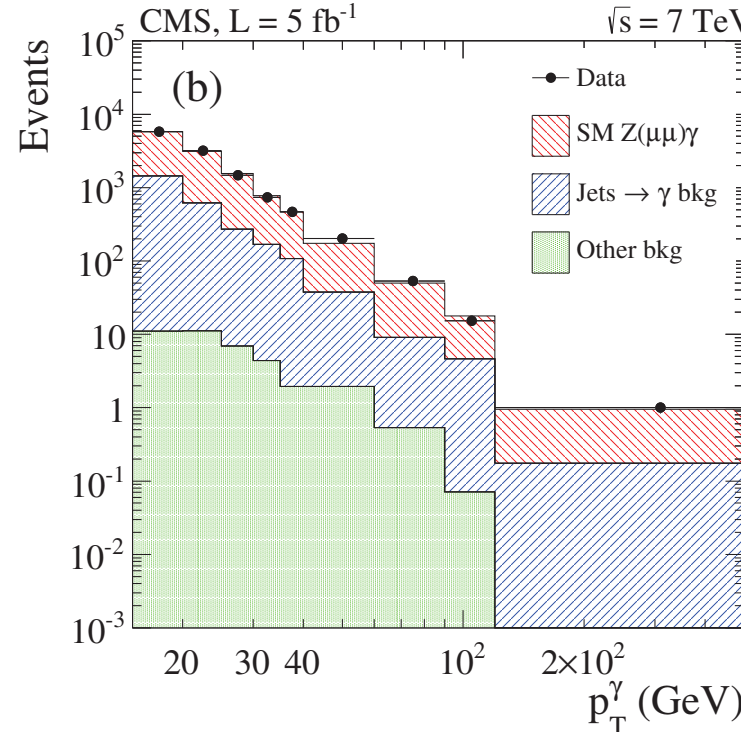
- NLO in agreement with data within uncertainties (NNLO corrections sizeable)

## $Z(l^+l^-)\gamma$ production in $pp$ collisions at $\sqrt{s} = 7$ TeV using $4.6 \text{ fb}^{-1}$

- Measurement of  $l^+l^-\gamma$  ( $l = e, \mu$ ) in the phase space
  - $\rightarrow p_T^l > 25 \text{ GeV}, |\eta_l| < 2.47, N_{l+} = N_{l-} = 1$
  - $\rightarrow m_{l+l-} > 40 \text{ GeV}$
  - $\rightarrow E_T^\gamma > 15 \text{ GeV}, |\eta^\gamma| < 2.37, \Delta R(l, \gamma) > 0.7$   
and  $\epsilon_h^p < 0.5$  (energy in cone  $R = 0.4$ /photon energy)
  - $\rightarrow$  jets: anti- $k_t$  algorithm with  $R = 0.4$
  - $E_T^{\text{jet}} > 30 \text{ GeV}, |\eta^{\text{jet}}| < 4.4, \Delta R(e/\mu/\gamma, \text{jet}) > 0.3$
- Inclusive ( $N_{\text{jet}} \geq 0$ ) and exclusive ( $N_{\text{jet}} = 0$ ) measurements
  - $\sigma_I(l^+l^-\gamma) = 1.31 \pm 0.02(\text{stat}) \pm 0.12(\text{syst}) \text{ pb}$   
NNLO (arXiv 1407.1618)  $\sigma_I(l^+l^-\gamma) = 1.327^{+0.026}_{-0.037} \text{ pb}$
  - $\sigma_E(l^+l^-\gamma) = 1.05 \pm 0.02(\text{stat}) \pm 0.11(\text{syst}) \text{ pb}$   
NNLO  $\sigma_E(l^+l^-\gamma) = 1.107^{+0.012}_{-0.018} \text{ pb}$
- NNLO corrections not so important as for  $W\gamma$ 
  - $\rightarrow$  NLO (MCFM) agrees with data over all  $E_T^\gamma$  range
- Sherpa (scaled to data) describe  $E_T^\gamma$  and  $m^{Z\gamma}$  spectra



## $Z(l^+l^-)\gamma$ production in $pp$ collisions at $\sqrt{s} = 7$ TeV using $5 \text{ fb}^{-1}$



- Measurement of  $l^+l^-\gamma$  ( $l = e, \mu$ ) for  $p_T^\gamma > 15 \text{ GeV}$ ,  $\Delta R(l, \gamma) > 0.7$  and  $m_{l^+l^-} > 50 \text{ GeV}$
- $\sigma(Z\gamma) \times B(Z \rightarrow l^+l^-) = 5.33 \pm 0.08(\text{stat}) \pm 0.28(\text{syst}) \text{ pb}$   
NLO (MCFM)  $\sigma \times B = 5.45 \pm 0.27 \text{ pb}$
- NLO in agreement with data within uncertainties

# $Z(\nu\bar{\nu})\gamma$ production in $pp$ collisions at $\sqrt{s} = 7$ TeV using $4.6 \text{ fb}^{-1}$

- Measurement of  $\nu\bar{\nu}\gamma$  in the phase space

→ no charged lepton,  $N_{l+} = N_{l-} = 0$

→  $p_T^{\nu\bar{\nu}} > 90$  GeV

→  $E_T^\gamma > 100$  GeV,  $|\eta^\gamma| < 2.37$ ,  $\Delta R(l, \gamma) > 0.7$

and  $\epsilon_h^p < 0.5$  (energy in cone  $R = 0.4$ /photon energy)

→ jets: anti- $k_t$  algorithm with  $R = 0.4$

$E_T^{\text{jet}} > 30$  GeV,  $|\eta^{\text{jet}}| < 4.4$ ,  $\Delta R(e/\mu/\gamma, \text{jet}) > 0.3$

- Inclusive ( $N_{\text{jet}} \geq 0$ ) and exclusive ( $N_{\text{jet}} = 0$ ) measurements

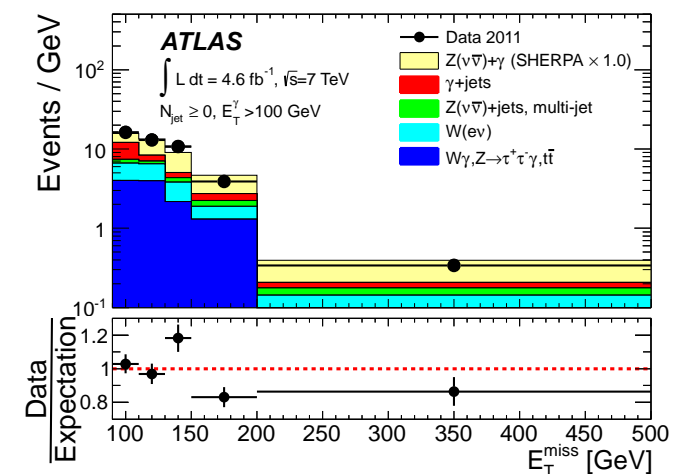
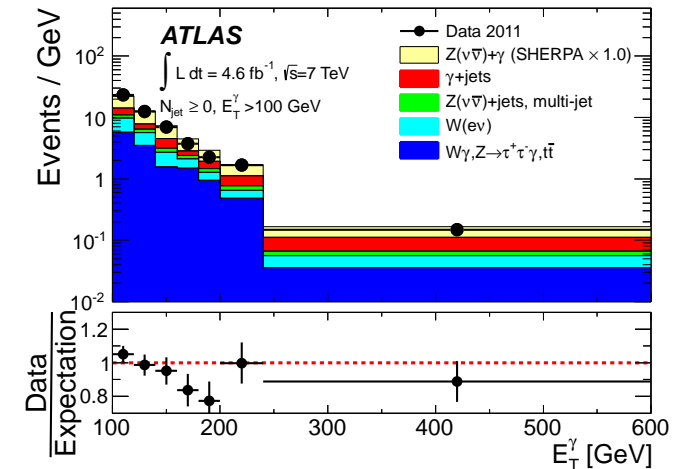
$\sigma_I(\nu\bar{\nu}\gamma) = 0.133 \pm 0.013(\text{stat}) \pm 0.021(\text{syst}) \text{ pb}$

NLO (MCFM)  $\sigma_I(\nu\bar{\nu}\gamma) = 0.156 \pm 0.012 \text{ pb}$

$\sigma_E(\nu\bar{\nu}\gamma) = 0.116 \pm 0.010(\text{stat}) \pm 0.014(\text{syst}) \text{ pb}$

NLO (MCFM)  $\sigma_E(\nu\bar{\nu}\gamma) = 0.115 \pm 0.009 \text{ pb}$

→ NLO (MCFM) agrees with data



ATLAS PRD87-112003